ADDIS ABABA UNIVERSITY

SCHOOL OF GRADUATE STUDIES

Analysis and parametric study of deep excavation with diaphragm wall using finite element based software

By

Tewodros Fekadu

June 2010

Analysis and parametric study of deep excavation with diaphragm wall using finite element based software

A thesis submitted to the school of graduate studies of Addis Ababa University in partial fulfillment of the requirements for the Degree of Masters of Science in Civil Engineering

By

Tewodros Fekadu

Advisor

Prof. Alemayehu Teferra

Addis Ababa University

School of Graduate Studies

Department of Civil Engineering

ANALYSIS AND PARAMETRIC STUDY OF DEEP EXCAVATION WITH DIAPHRAGM WALL USING FINITE ELEMENT BASED SOFTWARE

By

Tewodros Fekadu

A Thesis Submitted to School of Graduate Studies in

Partial Fulfillment of the Requirement for Degree of

Master of Science

in

Geotechnics

Approved by Board of Examiners:

Prof. Alemayehu Teferra	_____	_____
Advisor	*Signature*	*Date*
Dr. Hadush Seged	_____	_____
Internal Examiner	*Signature*	*Date*
Dr. Messele Haile	_____	_____
External Examiner	*Signature*	*Date*
Ato Biruk Melaku	_____	_____
Chair Person	*Signature*	*Date*

DECLARATION

I, the undersigned, declare that this thesis is my original work performed under the supervision of my research advisor Prof. Alemayehu Teferra and has not been presented as a thesis for a degree in any other university. All sources of materials used for this thesis have also been duly acknowledged.

Name Tewodros Fekadu

Signature _____

Place Faculty of Technology,
Addis Ababa University,
Addis Ababa.

Date June, 2010

Acknowledgements

I am grateful to my advisor Professor Alemayehu Teferra, Department of Civil Engineering, Addis Ababa University for his close supervision and constructive suggestions during my research work.

I would also like to extend my acknowledgement to my colleagues for their support. I forward my special thanks to Simeneh Abate who gave me valuable comments on this thesis. Building Design Enterprise and Saba Engineering provided me with laboratory test results, and they were very cooperative and welcoming.

The help I received from my colleagues in HEC Consult Plc. is to be acknowledged. Finally I would like to express my deepest gratitude to my family and my sister, Aster, for the fulfillment of all my interests.

Table of Contents

List of Figures

List of Tables

Abstract

Control of soil deformation is crucial for deep excavation in congested urban areas to minimize its effect on adjacent structures. Therefore, an analysis and parametric study is important to realistically represent the response of the soil to excavation and to predict the magnitude and pattern of ground movement.

This thesis presents a study of the effects of deep excavations with tie back diaphragm wall in expansive clay and red silty clay which are located in Bole Medehanealem area and Arada respectively, and also in cohesionless granular sandy soil. The objectives of this study are to investigate the effect of different parameters on the prediction of ground movement by numerical analysis and to develop a method of estimating these effects quantitatively. Extensive review of relevant literature published in the past four decades was conducted in order to understand the trends and the key developments in this area. It was revealed from the literature review that the concurrent use of the observational method and the finite element method for monitoring and controlling of ground deformations around the excavation has become a norm for deep excavation projects.

Parametric studies were carried out to identify important variables controlling the mechanisms of soil-structure interaction. The analyses focus on deep excavations supported by tie-backed diaphragm walls using techniques of top down construction. Exact site conditions and input parameters for the soil were incorporated as much as possible. The principal parameters considered in the study include soil type, depth of excavation, wall embedment depth, wall stiffness, and strut spacing. These variables were used to conduct a series of finite element analyses using simplified geometry and ground conditions for the purpose of achieving the objective of this thesis. Results of these analyses were recorded in terms horizontal displacement of the diaphragm wall, ground settlement behind the diaphragm wall, and bending moments induced in the diaphragm wall due to an adjacent deep excavation.

1. Introduction

1.1 Background

Highly urbanized cities have limited space for new development. Therefore, rising demand for commercial, residential and industrial needs has driven architects to consider underground structures in their design. Diaphragm walls have been widely used as primary structural elements for supporting deep excavations in urban areas due to their structural advantages. International experience show that diaphragm walls should be designed to have high stiffness to comply with strict specifications on the limitation of ground movements induced by excavations in congested urban areas.

Traditional empirical methods such as those suggested by Peck (1969) and Clough and O'Rourke (1990) cannot always provide reasonable prediction on the deformation pattern in complex modern construction in terms of construction sequence, tie back system and development of pore water pressure. There are many other analytical methods of prediction proposed in the literature for the complex problem but these analyses are not sensitive to the construction procedure, overall stability and movement pattern in the adjacent soil and effects on adjacent structures.

The use of finite element method for geotechnical analysis requires an accurate modeling of the soil behavior. Many constitutive models have been developed to represent the soil behavior over the past decades, for example, elastic-perfectly plastic model and hyperbolic model. The selection of the most suitable constitutive model is very crucial in insuring safe and economical design.

Thorough understandings of the parameters that control or alleviate the deformation in a soil model are essential in the modeling of excavation. Sensitivity analyses of soil and structure behavior are important that necessitate performing sanity checks on all design by alternative means.

Most commonly used constitutive models coded in geotechnical software such as FLAC, ABAQUS, CRISP and PLAXIS require different input parameters obtained from various soil testing techniques.

PLAXIS incorporates constitutive models whose parameters may be obtained directly or correlated from simple tests, e.g. SPT test. Its user friendly features have made it to be one of the popular engineering software for geotechnical engineers.

1.2 Objectives of the research

In Ethiopia, a number of high rise buildings are being constructed which need deep excavation for parking, etc. It is very important and should be a legal necessity with any construction to provide protection to the adjacent structures when excavating to any appreciable depth. Without adequate lateral support, the new excavation will almost certainly cause loss of bearing capacity, settlements, or lateral movements to existing property and these can damage buildings, streets, and utilities. Therefore, identifying and understanding the factors that affect the performance of deep excavation is an important issue for geotechnical engineers.

Thus, the objectives of this study are to investigate the effect of different parameters on the performance of deep excavation supported with diaphragm wall and to show a method of estimating these effects quantitatively using analysis and parametric study.

1.3 Methodology

The available literature in the area is examined to establish the factors that influence the proper functioning of a diaphragm wall.

A suitable finite element software is then employed to determine the different parameters that play important role in the design of diaphragm walls and parametric study is then conducted to establish the significance of each parameter.

1.4 Organization of the Thesis

The thesis consists of five chapters. The first chapter is background information on deep excavations. Literature review is presented in the second chapter. In chapter three, verification examples from literature were carried out using the finite element software PLAXIS to establish the applicability of the software.

Chapter four outlines the different parameters and results of the analysis done. Chapter five closes the whole theme of the thesis by making conclusions and recommendations. In the Appendices, relevant figures, two constitutive models of PLAXIS and different combinations of parametric study are presented.

2. Literature Review

2.1 Introduction

In recent decades, the demand for underground space, for use as underground parking, railway tunnels/stations, road tunnels, redevelopment of buildings, etc, has increased in many heavily urbanized areas. Deep excavations are required to meet the demand, and, in many cases, excavation sites are in close proximity to existing structures/facilities and problems related to deep excavations and their effects on surrounding structure are growing. Different methodologies or processes are employed to limit the impact of deep excavation on surrounding structures. The objective of this literature review is to assess the progress made in this area in terms of research as well as in the technological developments.

Performance of deep excavation is related to both stability and deformation. Deep excavations are designed to be stable and to limit deformations to acceptable levels. A stable deep excavation is an excavation whose walls do not collapse, and whose base does not heave uncontrollably. Ground deformations around excavations can damage adjacent buildings, streets, and utilities. The severity and extent of damage depends on the magnitude and pattern of ground movements around the excavation.

Stability and deformation are related. Thus, prediction of deep excavation performance involves analysis of both stability and deformation. Experience has shown that stability can be evaluated with sufficient accuracy using simple limit equilibrium calculations. Deformations, however, are significantly more difficult to predict, and finite element analyses are often used for this purpose when ground movements are particularly important.

The excavation of soil from a deep excavation has two main effects. The first is that the removal of the weight of the excavated soil results in a decrease in the vertical stress in the soil beneath the excavation. The second is that the removal of the soil in the excavation results in a loss of lateral support for the soil around the excavation.

The purpose of a deep excavation support system is to provide lateral support for the soil around an excavation and to limit movement of the surrounding soil. Support systems for deep excavation consist of two main components. The first is a retaining structure. The second component is the support provided for the retaining structure. Many types of supports have been used in deep excavations. The principal types of supports are diaphragm wall (structural slurry), sheet pile, soldier piles, tangent piles, and contiguous piles. The principal types of supports are struts (braces), rakers, and tieback anchors.

The literature review is divided into the following categories:

- Approaches to design and analysis of excavation support walls
- Earlier Works
- Analytical studies of deep excavations.
- Field performance studies of deep excavations.

2.2 Approaches to design and analysis of excavation support walls

There are three major approaches to design and analyze excavation support walls exist: (a) the classical approach; (b) the beam–column approach; and (c) the finite element approach. The major characteristics of the classical approach are quoted from A. Teferra and M. Leikun (1999) and A. Teferra (1992). Some of the major characteristics of the beam–column approach are presented from the design manual for excavation support by C. J. Rutherford (2004) and its details can be found in literature and beam–column program manuals (e.g. Briaud and Kim, 1998 and Matlock et al., 1981 respectively).

2.2.1 The Classical Approach

The classical method for diaphragm walls bases its calculations on the Rankine failure criteria. With regard to their structural functions, walls are categorized into two types. Namely, cantilever walls and anchored walls.

2.2.1.1 Cantilever Retaining Walls

Cantilever retaining walls are normally used when the depth of excavation is small. The walls derive their support from the passive resistance developed in the soil below the excavation level in front of the wall (Figure 2.1). The wall must penetrate to a sufficient embedment. The minimum embedment depth d for equilibrium can be determined by solving simultaneously two equations in which x and d are the unknowns, ∑H=0 and ∑MD=0.

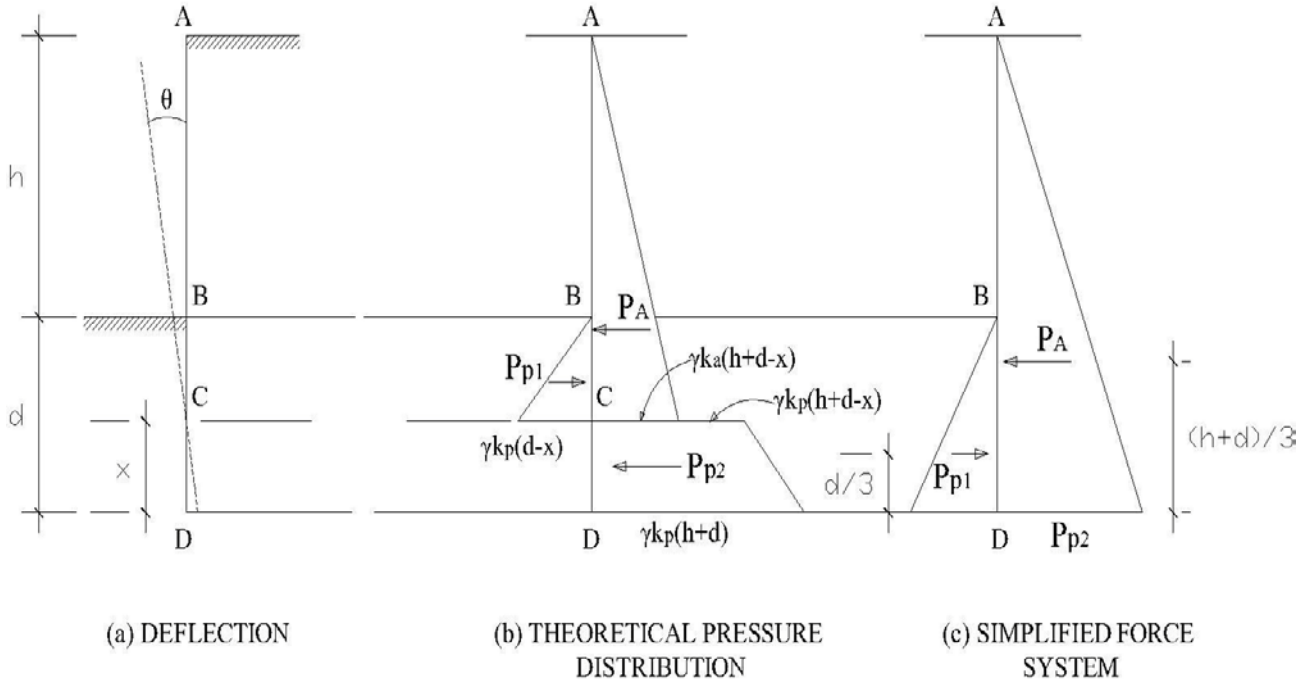

Figure 2. 1 Cantilever retaining wall

$$P_A = \frac{1}{2} K_a \gamma (h+d)^2 \quad \text{----------Eq.2.1a}$$

$$K_p d^3 - K_a \gamma (h+d)^3 = 0 \quad \text{----------Eq.2.1b}$$

The solution of Eq. (2.1) gives the guide to the embedment depth required and the calculated depth is increased by 20% to allow extra length for the development of the passive force P_{p2} (A. Teferra and M. Leikun, 1999).

2.2.1.2 Anchored Retaining Walls

Anchored retaining walls are held in tact by tie-rods anchored into the soil. The principal methods of analyzing the equilibrium of anchored wall are based on two assumption related to the method of support of the driven end. These are known as the *free earth support method* and the *fixed earth support method*. Here, a single supported wall is considered.

2.2.1.2.1 Free earth support method

In this method, the wall is assumed to rotate freely about its base and freely supported above the ground by the anchorage forces and below the ground level by passive resistance.

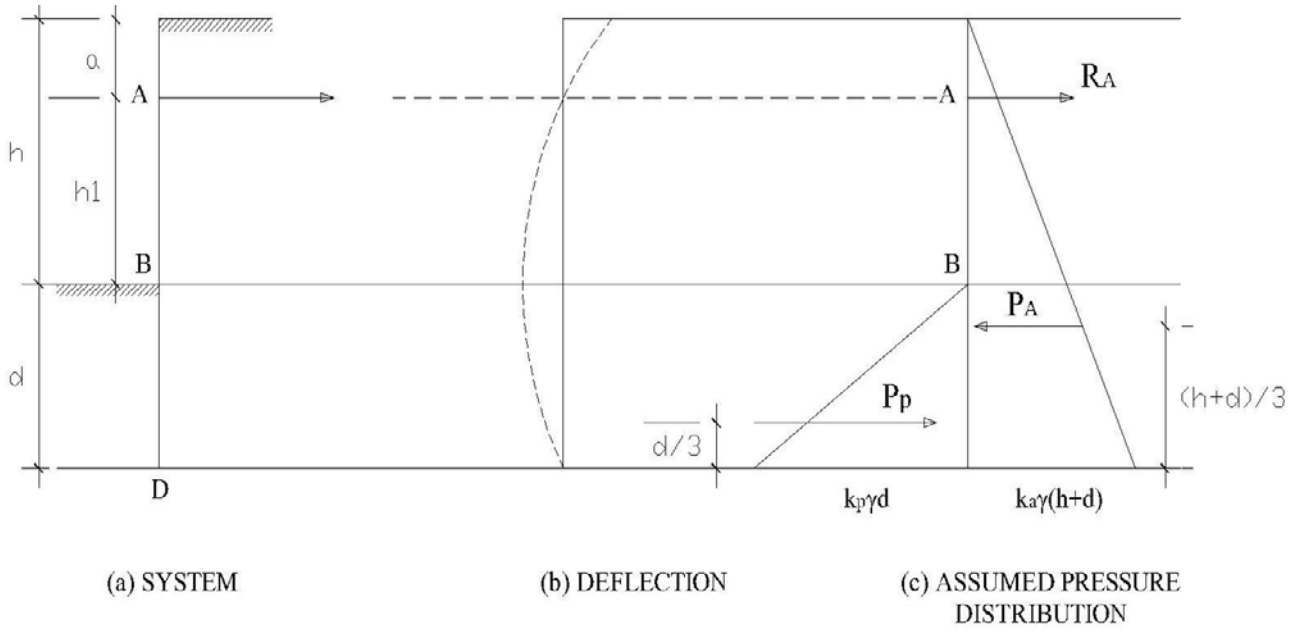

Figure 2. 2 The free earth support methods

The minimum driving depth, d required for stability is obtained by taking moments about A,

$$\frac{1}{2}K_p d^2(h_1+\tfrac{2}{3}d)=\frac{1}{2}K_a\gamma(h+d)^2(\tfrac{2}{3}d-\tfrac{1}{3}h+h_1)-----Eq.2.2$$

The above cubic equation is solved by assigning trial values of d and then the calculated minimum depth of embedment is increased by 20% for safety factor.

2.2.1.2.2 Fixed earth support method

In this method, the end of the retaining wall is assumed fixed and as a result the elastic line will be as indicated in Figure 2.3.

Point C is considered as a hinge transmitting shear only and the moment at this point is zero. Using the method of the equivalent beam method, the structures may be regarded as two separate beams, AC and DC, with force R_C as reaction at the hinge.

The procedure of the analysis is as follows:

a) The position of C is estimated from the relationship that exists between the angle of internal friction Φ and the distance y as indicated in Table 2.1.

Table 2. 1 Relationship between Φ and y (A. Teferra and M. Leikun, 1999).

Φ(°)	y	
20	0.25h	For normal frictional soils, it is sufficient to use y = o.1h
25	0.15h	
30	0.08h	
35	0.035h	
40	-0.006h	

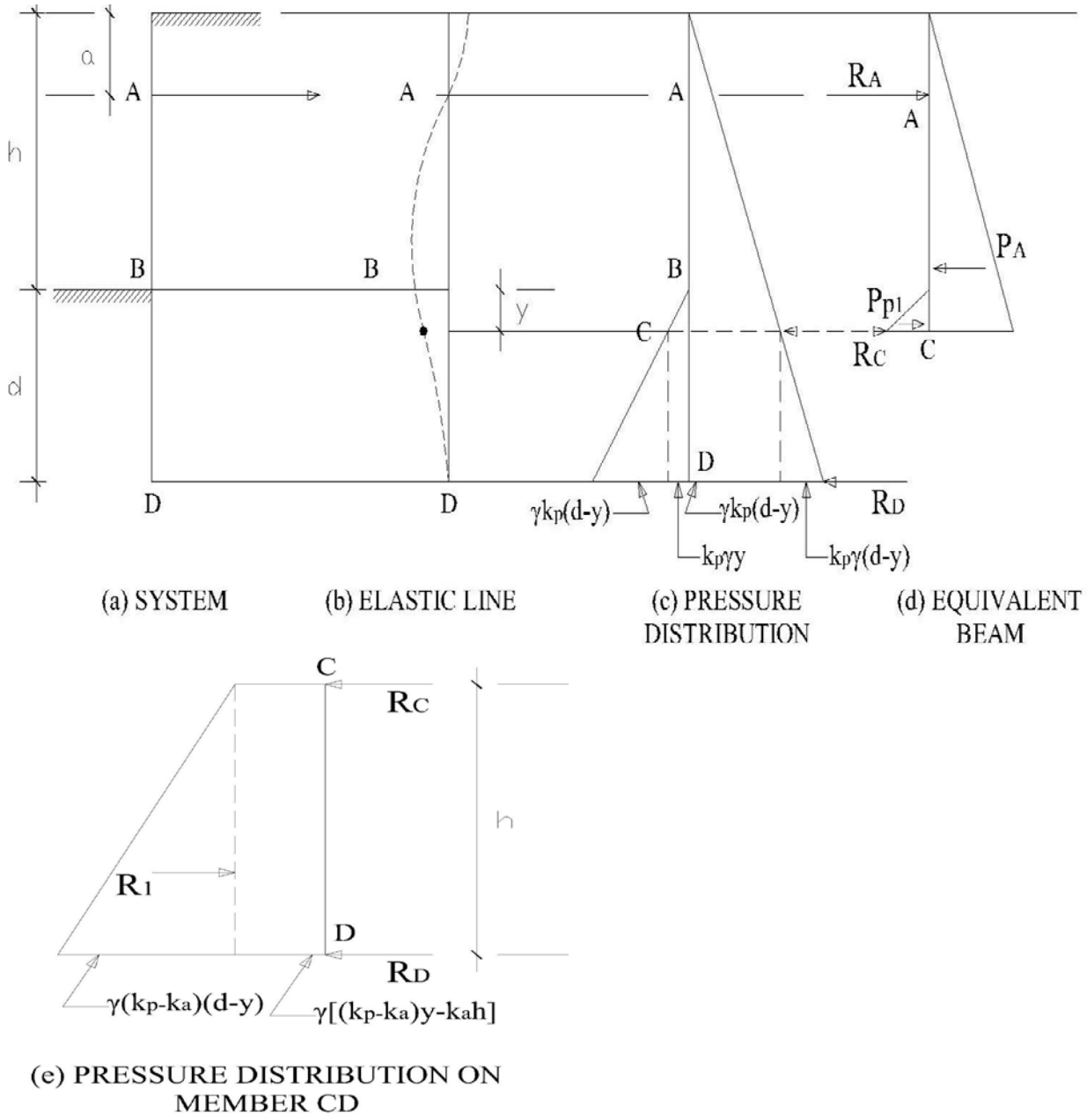

Figure 2. 3 Anchored retaining wall for fixed earth support

b) The forces on the upper beam AC are calculated from the active and passive pressures.

$$P_A = \frac{1}{2} K_a \gamma (h + y), and$$

$$P_P = \frac{1}{2} K_p \gamma y^2 \quad ---------- \quad Eq.2.3$$

c) The reaction R_C at the hinge C is found by taking moments of force about A.

$$R_C = \frac{\frac{1}{2}K_a\gamma(h+y)^2\left[\frac{2}{3}(h+y)-a\right]-\frac{1}{2}K_p\gamma^2(h-a+\frac{2}{3}y)\gamma}{(h+y-a)} --Eq.2.4a$$

The anchor force R_A is found either by taking moment about C or from

$\sum R_A+P_A+P_P+R_C=0$----------*Eq. 2.4b*

d) For loads on the beam CD; taking the moments about D, re-arranging terms and solving a quadratic in (d-y), one obtains

$$d = \frac{3}{2}\left(\frac{K_a}{K_p-K_a}\right)h - \frac{y}{2} + \sqrt{\frac{9}{4}\left(y-\frac{K_a h}{K_p-K_a}\right)^2 + \frac{6Rc}{\gamma(K_p-K_c)}} --Eq.2.5a$$

The first term under the root in Eq. 2.5a is very small compared with the second and may be neglected. Hence,

$$d = \frac{3}{2}\left(\frac{K_a}{K_p-K_a}\right)h - \frac{y}{2} + \sqrt{\frac{6Rc}{\gamma(K_p-K_c)}} ----------- Eq.2.5b$$

As in the previous cases, the calculated minimum embedment depth should be increased by 20% to allow for the fact that the lower passive resisting force R_D is not a knife-edge reaction as assumed in the simplified calculation.

2.2.2 Beam-Column Method

The boundary element method, BEM (Figure 2.4), consists of modeling the wall as a set of vertical elements Δ_Z long with a bending stiffness, EI, and an axial stiffness, AE. The soil is represented by a series of vertical and horizontal springs placed along the wall. Spring models for tieback walls have been recommended by Briaud and Kim (1998). Typical programs include BMCOL and TBWALL. A typical input for the BEM is the length of the wall, the length of the wall elements, and the wall stiffness.

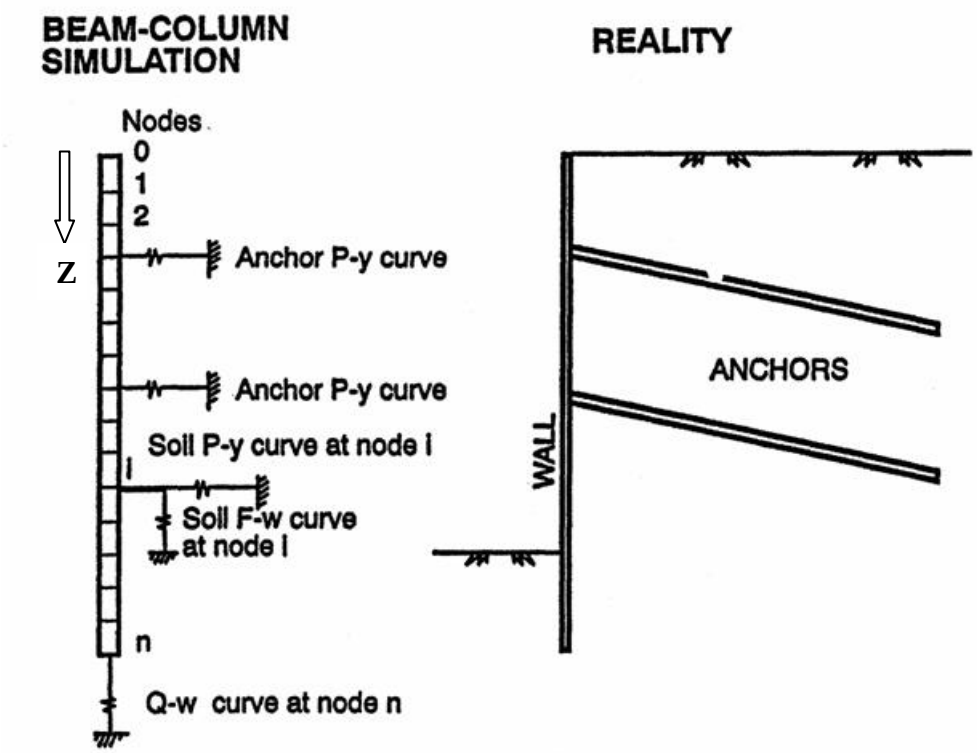

Figure 2. 4 Boundary Element Model of Repeatable Section of Wall (After Briaud and Kim, 1998)

The beam-column method for tieback walls deals with the analysis of the wall as a structural element interacting with the soil and the anchors (Briaud and Kim, 1998). An element of wall is considered and horizontal equilibrium of this element together with the constitutive law for the wall in bending (M=EI d2y/dz2) and the constitutive law for the soil [P = P(y, z)] leads to one of the governing differential equations (Matlock et al., 1981).

$$EI\frac{d^4y}{dz^4}+Q\frac{d^2y}{dz^2}-P(y,z)=0 \quad\text{---------- Eq.2.6}$$

where:

E = wall modulus

I = wall moment of inertia

y = wall horizontal deflection at depth z

Q = axial load in the wall at depth z

P = horizontal soil reaction for a wall deflection y at a depth z.

The soil reaction P is a load per unit height of wall (kN/m, for example).

Vertical equilibrium of the same element together with the constitutive law for the wall in compression (Q=AE dw/dz) and the constitutive law for the soil [F = F(w, z)] lead to second governing differential equation (Matlock et al., 1981).

$$AE\frac{d^2w}{dz^2} + F(w,z) = 0 \quad \text{---------- Eq.2.7}$$

where:

E = wall modulus

A = wall cross section

w = wall vertical deflection at a depth z

F = vertical soil reaction for a wall deflection w at a depth z.

The soil reaction F is a load per unit height of wall.

Eq. 2.6 and Eq. 2.7 are solved by the finite difference technique by considering that the wall is made of n elements having n + 1 horizontal deflections y_i, and n + 1 vertical deflections w_i. Once the deflections y_i and w_i are known, the bending M, the shear V, the soil reaction P, and the axial-load W can be obtained through their relation to y and w.

2.2.3 Finite Element Method

The finite element method, FEM, consists of modeling the wall and the soil as made of small elements and assigning to the elements properties which control their behavior. Beam elements are usually chosen to represent the wall while brick elements are used for the soil. A typical input for the FEM is the mesh description including the geometry of the elements for the wall, the anchors, the soil, the models for the wall material and water, boundary conditions, and the boundary loads. Typical programs include PLAXIS, FLAC and ABAQUS.

2.2.4 Comparison of Design Methods

Although classical methods are quick and simple, computer aided analysis may be required for complex soil and site conditions. Computer aided analysis is growing in use and represents the future trend. The comparison of the design methods are presented in Table 2.2.

Table 2. 2 Comparison of Design Methods

Method	Data Required	Advantages	Disadvantages
Classical	c, φ, S_u, k, EI, f_{max}	Simple. Quick. No computer necessary.	Many assumptions made. Limited application.
Beam–Column	c, φ, S_u, k, y_a, y_p, EI, k_{anchor}, f_{max}	Better bending moment and reaction predictions. Multilayer soils. Relatively simple.	No seepage condition. Limited precision on movement. Requires computer and program.
Finite Element	c, φ, S_u, k, E_{soil}, EI, f_{max}, k_{anchor}	Simulates construction sequence. Good bending moment predictions. Good movement predictions. Unlimited geometry. Multilayer. Any loading. Simulate construction sequence.	Difficult and time consuming to use properly. Requires computer and program.

2.3 Earlier Works

2.3.1 Review of Peck (1969)

Peck, (1969) developed the first empirical method to predict the wall movement based on actual ground deformation data collected from temporary braced sheet pile and soldier pile walls with tie back support as shown in Figure 2.5.

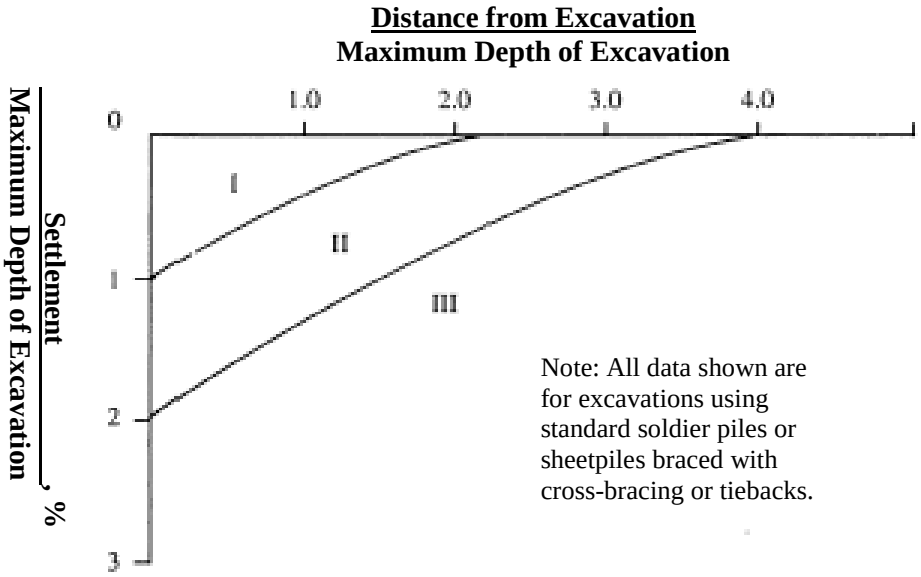

Zone I Sand and Soft to Hard Clay average workmanship

Zone II
a) Very Soft to Soft Clay
(1) Limited depth of clay below bottom of excavation
(2) Significant depth of clay below bottom of excavation but $N_b < N_{cb}$

b) Settlements affected by construction difficulties

Zone III Very soft to soft clay to a significant depth below bottom of excavation and with $N_b > N_{cb}$

Figure 2. 5 Summary of Settlements adjacent to open cuts in various soils as a function of distance from edge of excavation [Peck, 1969]

Figure 2.5 gives the settlements, divided by the maximum excavation depth *H*, and plotted against the distance from the walls also divided by the depth *H*. Three categories of behavior were defined according to soil types: 1) sand and soft to hard

clay, (zone I), 2) very soft to soft clay (a) limited depth of clay below the bottom of excavation. (b) Significant depth of clay below the bottom of excavation but $N_b < N_{cb}$, (zone II); and 3) very soft to soft clay to a significant depth below the bottom of excavation and with $N_b > N_{cb}$ (zone III).

The stability number N_b is defined as $\gamma H / S_{ub}$, where γ is the unit weight of the soil above the base of excavation, S_{ub} is the undrained shear strength below the base of excavation, and N_{cb} is the critical stability number for basal heave. The factor of safety against basal heave was defined by Terzaghi (1943) as follows in Figure 2.6.

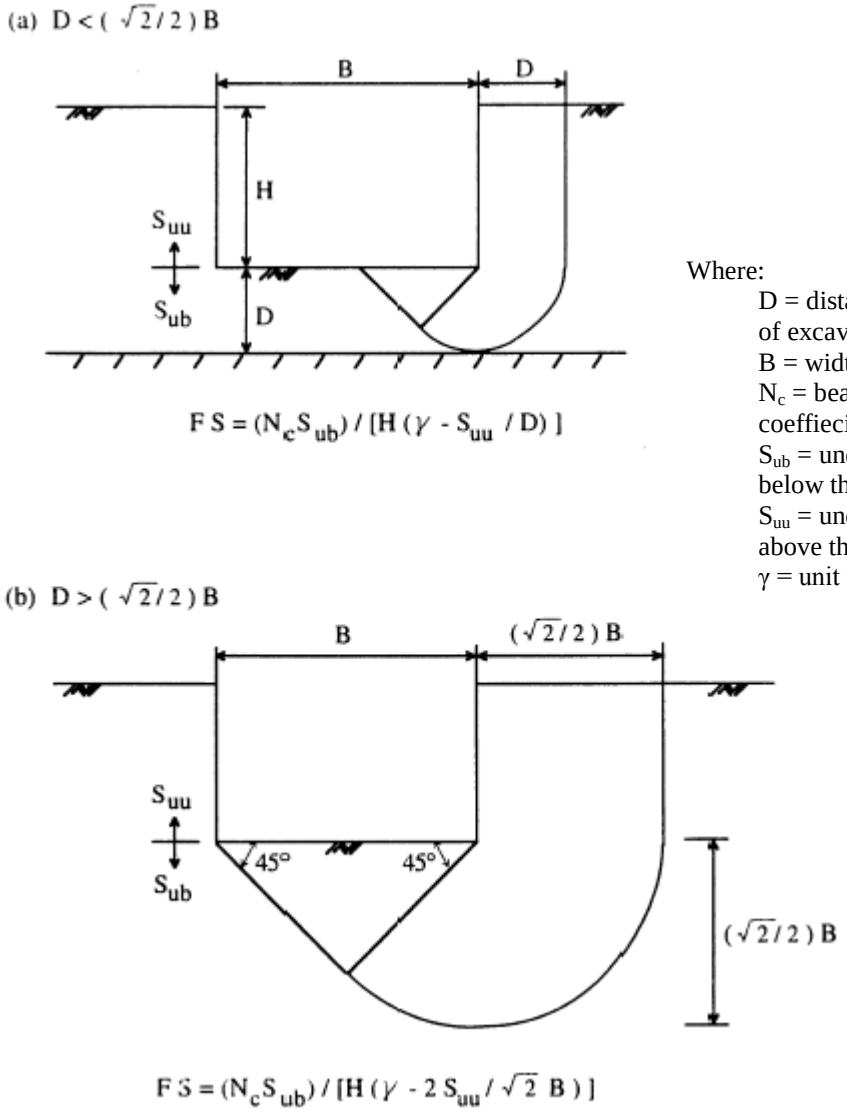

Where:

D = distance between the base of excavation and hard stratum
B = width of excavation
N_c = bearing capacity coeffiecient
S_{ub} = undrained shear strength below the base of excavation
S_{uu} = undrained shear strength above the base of excavation
γ = unit weight of soil

Figure 2. 6 Excavation Geometry and Soil Strength Parameters for Factor Safety Against Basal Heave [Terzaghi, 1943]

The chart, Figure 2.5, can be used to predict the ground deformation which can extend up to four times the excavated depth from the wall. However, since it is based on data collected from excavations less than about 15 meters depth with relatively flexible retaining walls, there would be uncertainties in extrapolating these observations to much deeper excavations supported by diaphragm walls.

2.3.2 Review of Clough and O'Rourke (1990)

Clough and O'Rourke (1990) presented the current state-of-the-art of empirical observations for estimating the lateral wall deflections and surface settlements in excavations.

Clough and O'Rourke (1990) conduct a finite element parametric study on excavation in sands, stiff clays, and residual soils supported by soldier piles, sheet piles, diaphragm walls, soil nail walls, drilled pier walls, and soil cement walls. Figure 2.7 and Figure 2.8 were prepared to show the maximum lateral wall deflections, δ_{Hm} vs. excavation depth, H; and the maximum surface settlements, Δ_{max} vs. excavation depth, H, respectively

From the cluser of points in Figure 2.7 and Figure 2.8 one observes that:

1) The maximum lateral wall deflections and maximum surface settlements were usually less than 0.5%H.

2) The maximum lateral wall deflections tended to average about 0.2%H.

3) The maximum surface settlements tended to average about 0.15%H.

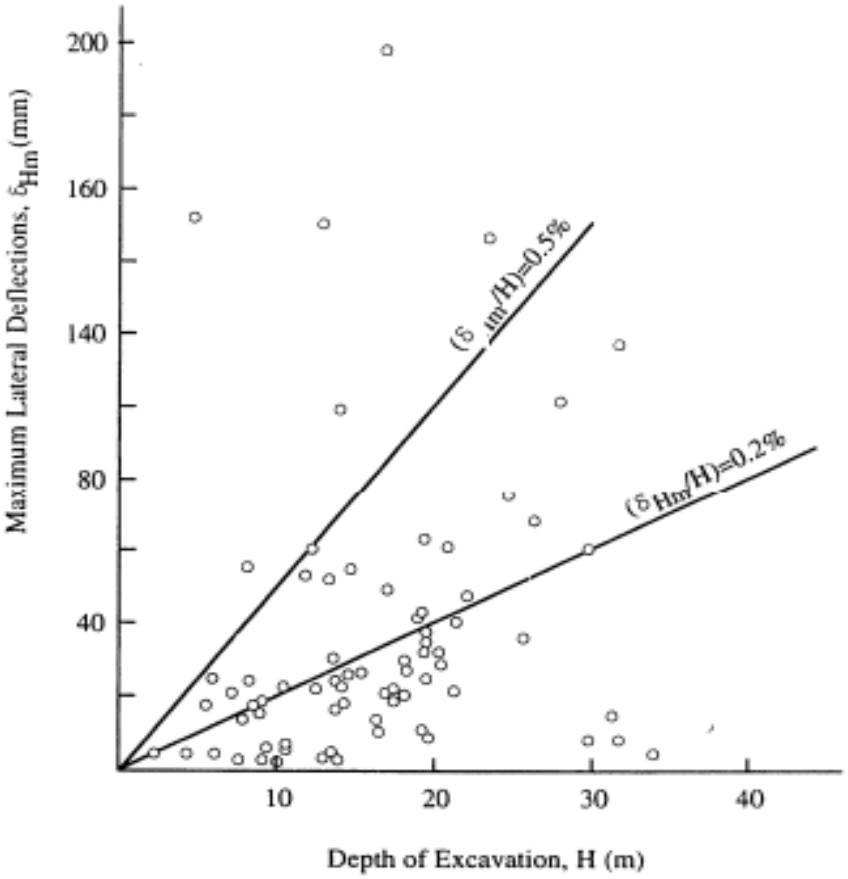

Note: Type of walls are soldier piles, sheet piles, diaphragm walls, soil nail walls, drilled pier walls, and soil cement walls.

Figure 2. 7 Maximum Lateral Wall Deflections in Sands, Stiff Clays, and Residual Soils [Clough and O'Rourke, 1990]

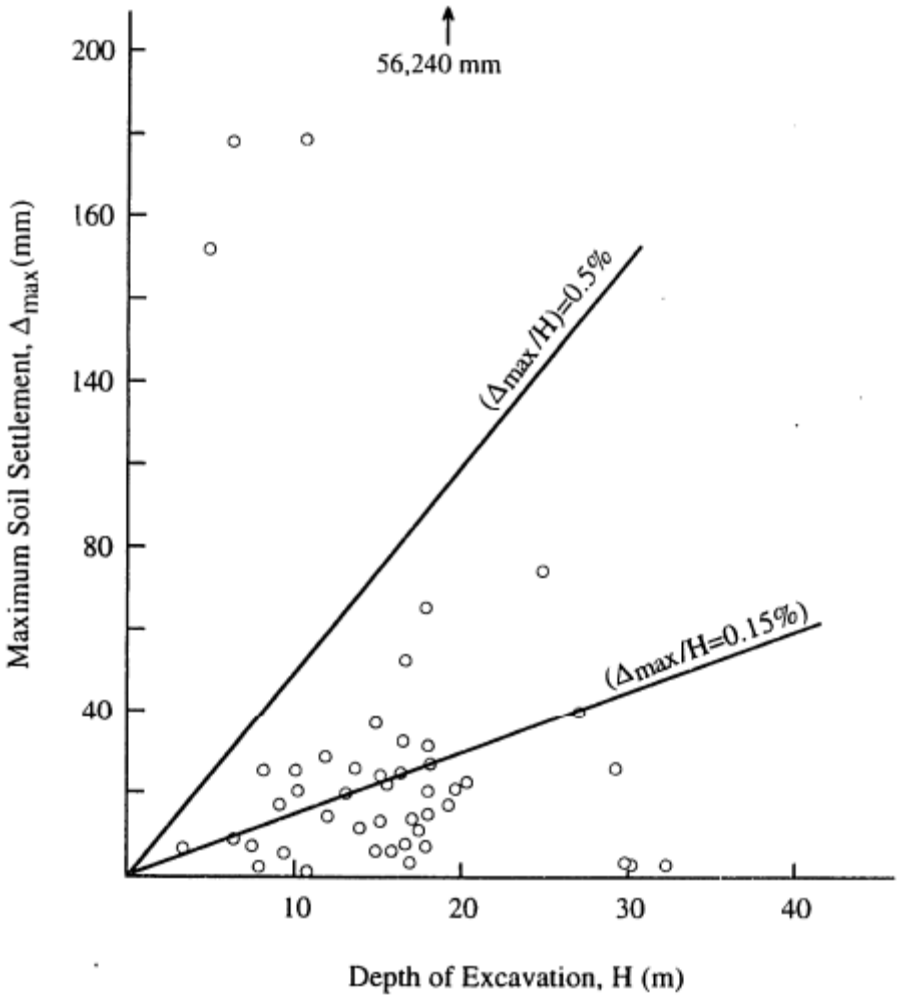

Note: Type of walls are soldier piles, sheet piles, diaphragm walls, and drilled pier walls.

Figure 2. 8 Maximum Surface Settlements in Sands, Stiff Clays, and Residual Soils [Clough and O'Rourke, 1990]

Clough and O'Rourke (1990) have developed a semi-empirical method for estimating excavation deformation in soft clays whereby the maximum lateral deformations induced by excavation are dependent on the system stiffness, S, and the factor of safety against basal heave. The maximum lateral wall deflection is expressed in terms of an effective stiffness of the system as shown in Figure 2.9. In this method, the system stiffness is defined as follows:

$$S = \frac{EI}{H^4 \gamma} \text{----------} \textit{Eq. 2.8}$$

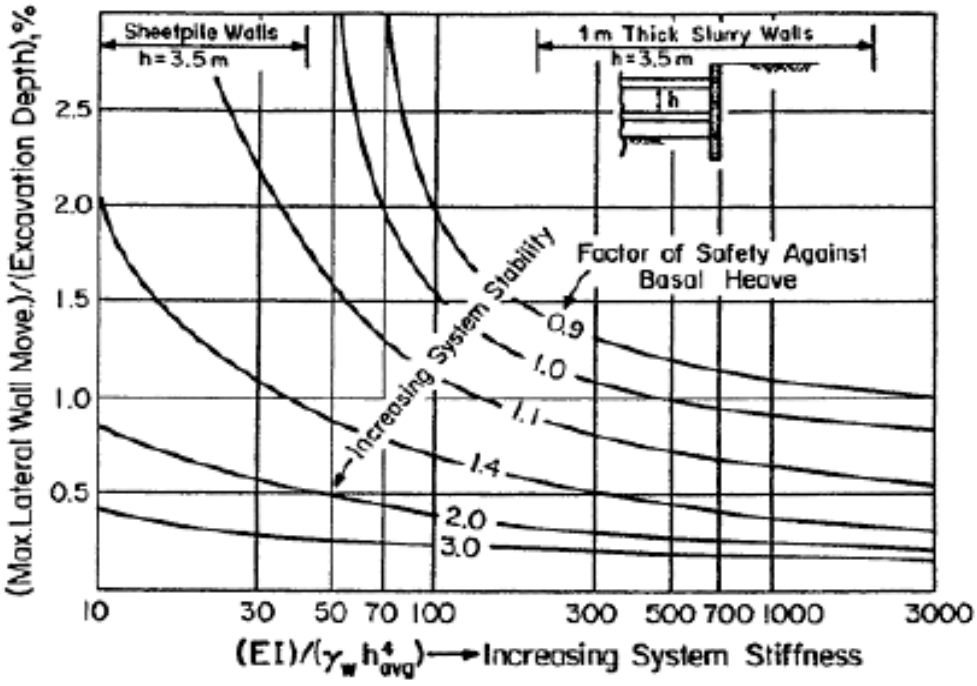

Figure 2. 9 Correlation for Maximum Lateral Wall Deflection with Factor of safety Against Basal Heave and System Stiffness [Clough and O'Rourke, 1990]

The Figure 2.9 is characterized by the following:

1) The system stiffness ((EI) / (γ_w h_{avg}^4)) combines the effect of the average struts spacing h_{avg} and the flexural stiffness of wall EI. The maximum lateral wall deflections depend on the average struts spacing raised to the fourth power.

2) The lateral wall deflections depend on the factor of safety against basal heave defined by Terzaghi (1943). Lines of equal factor of safety against basal heave represent lines of equal excavation depth.

3) The figure is divided into two main regions, one for excavations supported by sheetpile walls and another for excavations supported by concrete diaphragm walls (slurry walls). The maximum lateral wall deflections in the excavations supported by sheetpile walls are greater than those supported by concrete diaphragm walls in the case of an equal factor of safety against basal heave.

4) The maximum lateral wall deflections increase rapidly, as the factor of safety against basal heave falls below 1.5.

5) The maximum lateral wall deflections decrease below 0.5%H, as the factor safety against basal heave falls below 1.5.

6) The lateral wall deflections can exceed 1%H even with increasing system stiffness if the factor of safety against basal heave is close to unity.

Clough and O'Rourke (1990) presented a dimensionless settlement profile as shown in Figure 2.10 to Figure 2.12 for sand, stiff to very hard clays, and soft to medium clays to further support these findings. Based on the figures below, the settlement influence zone is 3H for excavations in stiff to very hard clays and 2H for excavations in sands and soft to medium clays. Nevertheless, other settlement associated activities, such as dewatering, deep foundation removal or construction, and wall installation as practiced in modern day construction of diaphragm wall are not taken into consideration and it should be used as a conservative settlement prediction method.

Clough and O'Rourke (1990) also concluded from Figure 2.10 to Figure 2.12 as follows:

- If the deep lateral wall deflections were the predominant mode, which would be the case with deep excavations in soft clay, the surface settlement would tend to have a trapezoidal distribution.

- If the cantilever mode predominated, which would be the case for excavations in sand and stiff to hard clay, the surface settlements would tend to be a triangular distribution.

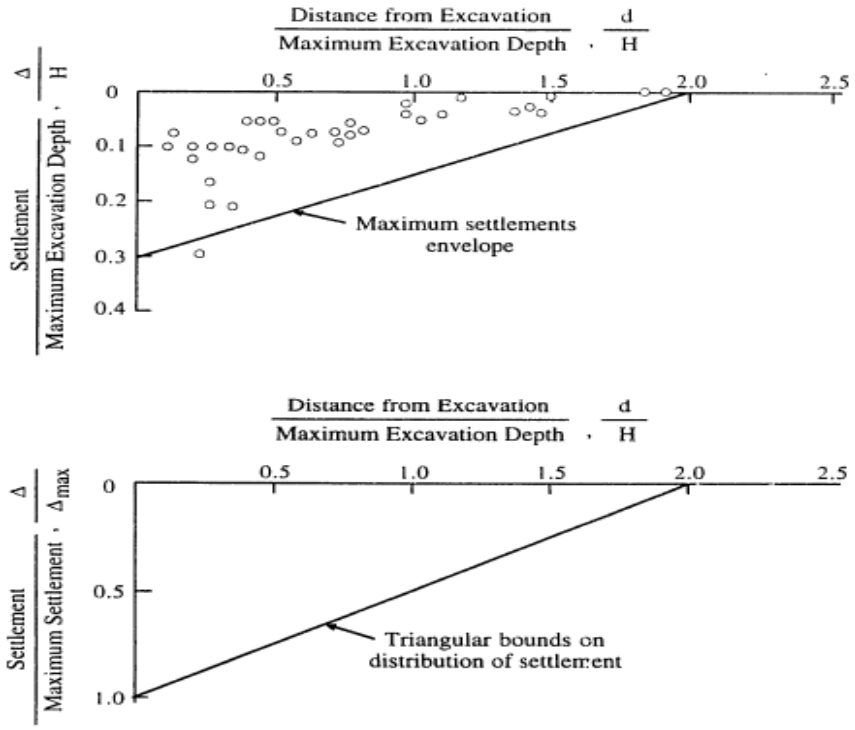

Figure 2. 10 Surface Settlements Adjacent to Excavations in Sand [Clough and O'Rourke, 1990]

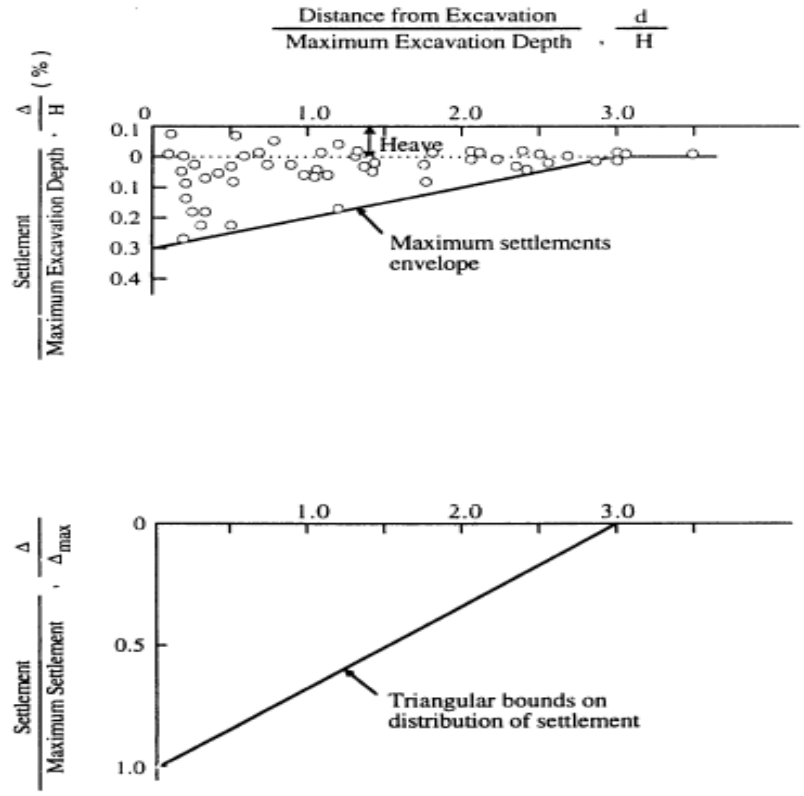

Figure 2. 11 Surface Settlements Adjacent to Excavations in Stiff to Hard Clay [Clough and O'Rourke, 1990]

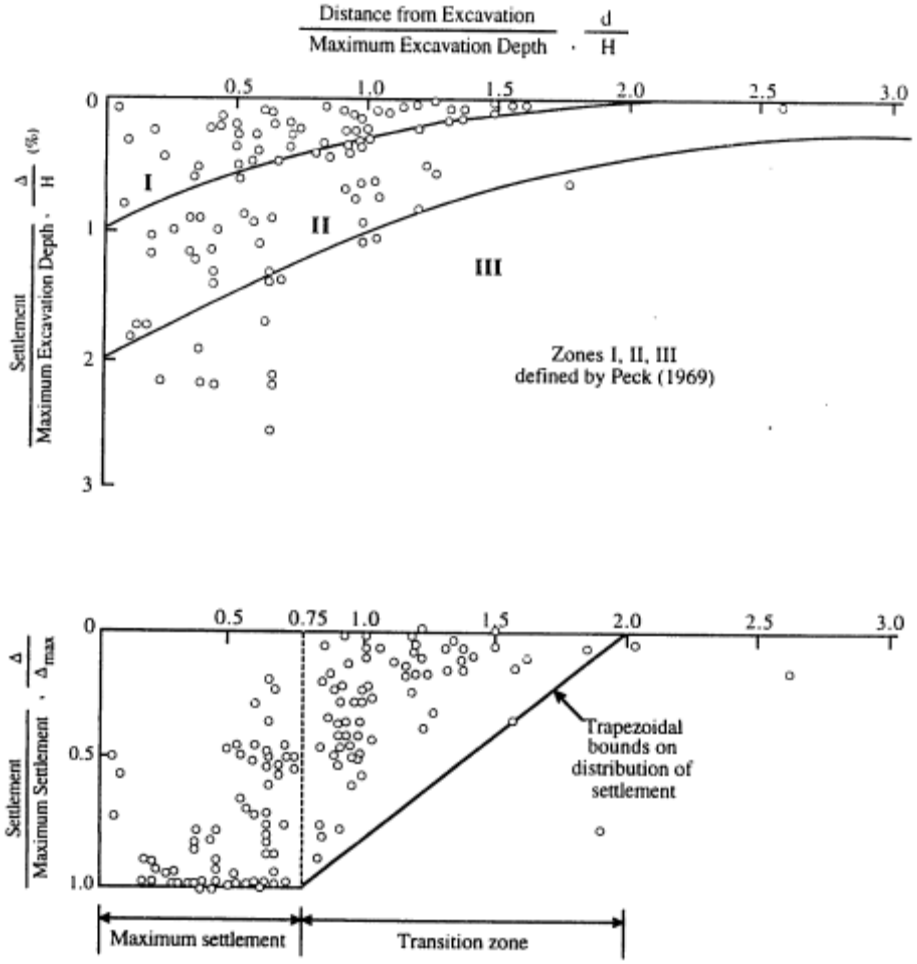

Figure 2. 12 Surface Settlements Adjacent to Excavations in Soft to Medium Clay [Clough and O'Rourke, 1990]

2.3.3 Review of Hashash (1992)

Hashash (1992) developed a new capability to model deep excavations supported by diaphragm walls in soft clay deposits using accurate numerical techniques and an advanced soil model. Hashash (1992) was motivated by the practical problem of predicting the performance of deep excavations (excavation depth up to 30m) in soft clays associated with the construction of the Central Artery/Tunnel project in Boston and the Taipei Rapid Transit system in Taiwan. In these situations, accurate predictions of lateral wall deflections and surface settlements are important design criteria to avoid damages to adjacent structures/facilities.

The study is divided into three main sections:

1) The development of numerical procedures to integrate advanced constitutive soil models (Modified Cam Clay, MCC, and MIT-E3, effective stress soil model develop at MIT) in the finite element method, FEM, and numerical procedures to model excavation activities including soil removal and support installation are studied.

2) The fundamental mechanisms of the short term (undrained) performance of deep excavations are studied. Principal parameters are the soil model, stress history profile, wall length and vertical strut spacing. The study interprets soil response at the element level, as well as global performance such as lateral wall deflections and ground surface settlements.

3) The top-down construction of a seven-story (23m deep) underground parking garage at post Office Square in Boston is studied. The predictions are evaluated through comparisons with field measurements during construction. The predictive capabilities and limitations in analyzing the complex construction sequence are demonstrated.

Hashash (1992) carried out analyses for L = 12.5m, 20.0m, 40.0m and 60.0m long walls. The results show two distinct failure mechanisms. For short walls (L = 12.5m and 20.0m) there is a basal failure of the soil beneath with the embedded length of the walls deflects in a cantilever mode with the largest deflections occurring at the toe ("kick-out" mode). For long walls (L = 40.0m and 60.0m), the failure mechanism is constrained by bending of the embedded wall length ("bulging mode") and the failure may initiate with the formation of a plastic hinge in the wall.

From the results of the numerical study concerned with the lateral wall deflections in excavations supported with diaphragm walls, Figure 2.13 is presented to summarize the numerical predictions of maximum lateral wall deflections δ_{Hm} for excavations in normally consolidated Boston Blue clay, BBC, as a function of the excavation depth

H and strut spacing h (note it is assumed that the excavation width B is B = 40m and the diaphragm wall thickness t is t = 0.9m, which are typical conditions expected for the CA/T project). The figure includes loci of failure conditions obtained for walls of different lengths L ranging from 12.5m to 60m.

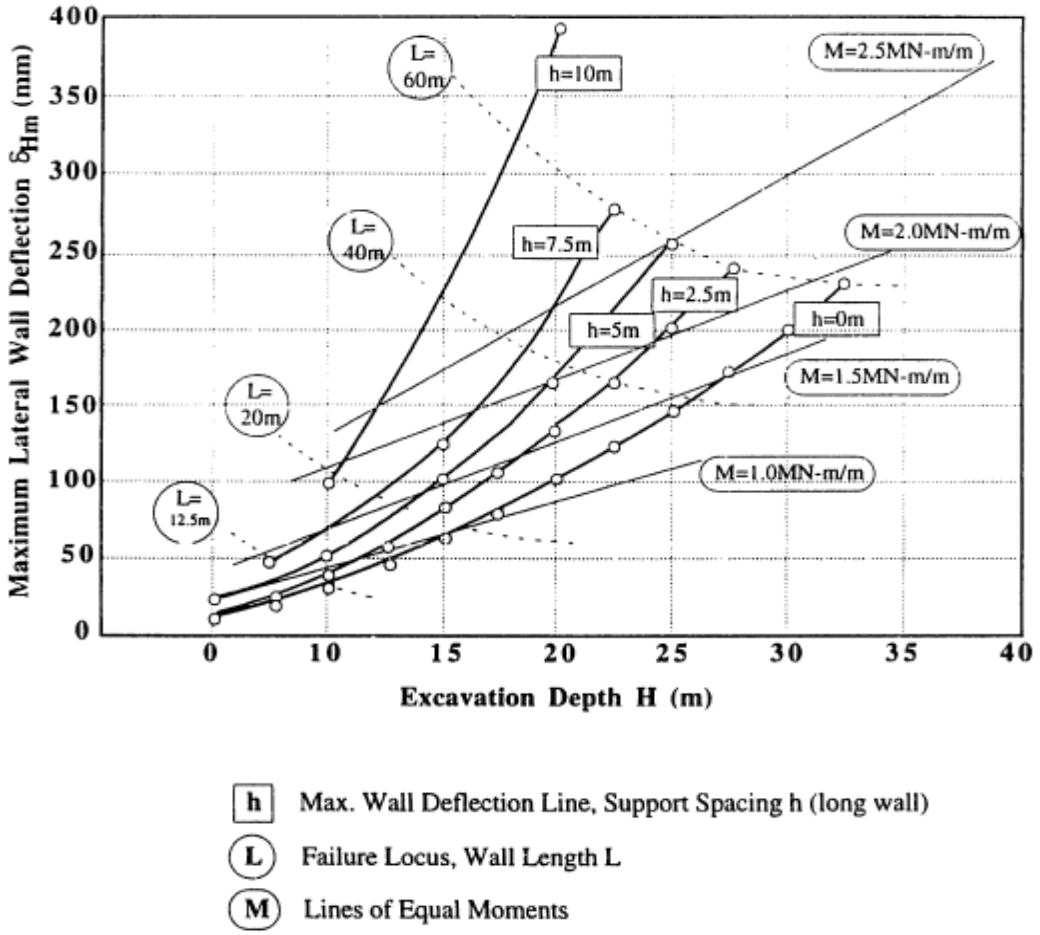

Note: Examples of the ratio of maximum lateral wall deflection δ_{Hm} to excavation

$H_{(m)}$	$\delta_{Hm\ (mm)}$	$\delta_{Hm\ /\ H}$ (%)
22.5	40	0.18
	120	0.53
	160	0.71
	280	1.24
	400	1.78

Figure 2. 13 Numerical Predictions of Maximum Lateral Wall Deflections, N.C. Boston Blue Clay [Hashash, 1992]

Figure 2.13 illustrates the following points:

1) For excavations which are perfectly supported (i.e., h = 0m) the ratio of the maximum wall deflections to the excavation depth is (δH_m / H) ≥ 0.5%.

2) For minimally supported wall (i.e., h = 10m) this ratio increases to (δH_m / H) ≥ 1.5 to 2.0%.

3) The predictions of maximum wall deflections can be summarized as functions of the excavation depth and support spacing.

2.4 Numerical studies of deep excavations

Clough, G.W. and Tsui, Y. (1974) compared the performance of tied-back walls and braced walls using finite element analysis and examined the effects of pre-stressing, anchor stiffness, anchor spacing, wall rigidity, and excavation depth on tied-back walls with parametric finite element studies. The analyses are performed assuming that plane strain condition exists. The soil model employed is a nonlinear elastic model similar to that described by Duncan and Chang in which the soil behavior is assumed to consist of a nonlinear portion for primary loading and a linear response for unloading and reloading. They concluded that tied-back walls are not inherently better than braced walls; pre-stressing and increasing wall and anchor stiffness can reduce soil movements with tied-back walls; widely spaced tiebacks can cause large concentrations in earth pressure at the anchor levels. They also concluded that two significant factors that cause settlement behind tied-back walls to be smaller than those for braced walls would appear to be that the tied-back wall is usually prestressed and the braced wall is not, and that over-excavation often occurs during construction of braced wall can easily double movements.

Goh, A. T. C. (1990) performed parametric studies using the finite element method to assess the effects of the wall properties, depth of competent soil, excavation width, and wall embedment on deep excavation stability in clay. The parametric studies

showed that thickness of the clay layer beneath the excavation, embedment depth of wall, and the stiffness of the wall are important factors affecting basal stability.

Powrie, W. and Li, E.S.F. (1991) investigated the behavior of cantilever structural slurry walls forming permanent retaining wall system for a depressed highway, the soil and a continuous slab propped at a formation level of 9-m-deep excavation in stiff over-consolidated boulder clay. Parametric finite element studies were carried out to study the effects of soil, wall, and prop slab stiffness, and coefficient of lateral earth pressure (K_0). They found soil stiffness, the value of K_0, and structural connection between the roadway slab and the wall were important factors in the behavior of the walls. It was found that computed deformations were governed by assumed stiffness of the soil rather than the flexural rigidity of the wall. Bending moments in the wall were influenced significantly by the assumed pre-excavation lateral earth pressures and, to a lesser extent, by the nature of the structural connection between the wall and the permanent prop slab.

Hoe, N. H. (2007) carried out a parametric study using finite element method to investigate the effects of soil stiffness, the initial coefficient of lateral earth pressure and rock socket length. He also investigated the suitability of constitutive models (Hardening Soil model and Mohr-Coulomb model) by comparison with field monitored measured data. He used PLAXIS V-8 employing plain strain assumption and wished-in-place diaphragm wall. From the study he concluded that wall deflection is very sensitive to change in soil stiffness and coefficient of lateral earth pressure. Through comparison with measured field monitored data, it was observed that Hardening Soil model can predict ground deformation more precisely than Mohr-Coulomb model.

Hsieh, P.G. and Ou, C.Y. (1997) extended Duncan and Chang's hyperbolic model with plasticity theory for the $\Phi=0$ condition and studied a case history of an excavation using a finite element analysis and the modified hyperbolic model. From the study they concluded that finite element analysis using modified hyperbolic model gave reasonable agreement with observed wall and soil behavior.

Balasubramaniam, A. S. et al (1994) analyzed the performance of six deep excavations with different support systems and construction methods in Bangkok subsoils. Parametric finite element studies of the effects of pre-loading, barrette pile and foundation pile and foundation pile installation, embedment depth, and surcharge are also presented. Analytical results agreed in general with the observed behavior and they concluded that the stiffness of the retaining wall and bracing element control deformations. They also found that diaphragm walls performed better (smaller movements) than sheet pile walls and wall embedment depth was a more significant performance factor with sheet pile walls than diaphragm walls.

2.5 Field performance studies of deep excavations

Lings, M. L. et al (1991) presented and compared the performance of a deep excavation constructed by top-down methods in Gault Clay to design predictions. Earth pressures, heave, and pore pressures were measured. They found diaphragm wall construction caused a significant decrease in lateral stresses and also deflections, prop forces, and bending moments were substantially lower than predicted.

Garvin, R. and Boward, J. (1992) described the cut-and-cover construction of a five level underground parking structure in Pittsburgh. A diaphragm wall with tiebacks was used to support the 7-m to 8-m excavation. Movements and groundwater levels were monitored during construction. Slurry wall system performed well and permitted dewatering within the excavation within a minimum influence on groundwater levels outside excavation. Maximum lateral movements for the excavation were between 10 and 20 mm. An adjacent 80 year old sandstone structure experienced no distress.

Gifford, D. and Wheeler, J. (1992) described the performance of a structural slurry wall used to support an excavation for a 5-level underground parking garage in Baltimore. The use of a slurry wall simplified construction operations. The slurry wall was relatively watertight and movements were acceptable. Most of the settlement was caused by pretrenching operation. Excessive grouting pressures during tieback installation caused 1/2 inch of wall movement towards excavation.

Schoenwolf, D. A.et al (1992) described the performance of a structural slurry wall used in the top-down construction of the seven-level (24.4 m deep excavation) garage for the Post Office Square project in downtown Boston. The authors compared measured movements predicted with finite element analyses. Movements during diaphragm wall construction were less than 8 mm and small rebound of ground during concreting of panels was noted. Shrinkage and creep related movements of structural garage floor slabs were noted. Large temperature drop during initial stages of construction caused inward movement of walls. Stiffness of bedrock and its resistance to movement of the toe of the wall was underestimated in design.

Winter, E. et al (1992) described the performance of a 10-m deep excavation supported by a structural slurry wall with tiebacks adjacent to the church of the Epiphany in Washington, D.C.. Movements measured during wall installation next to the church were 3 mm or less. Very minor displacements were recorded during excavation. Maximum horizontal displacement of wall was 0.15% H.

Ou, C. Y. et al (1993) studied the characteristics of ground surface settlement during excavation by examining data from ten case histories of deep excavations in Tapei. They examined maximum wall deflection and the relationship between wall deflection and ground settlement. Maximum lateral wall deflection often occurs near the bottom of an excavation. Upper limit on maximum ground settlement is the maximum lateral wall deflection; in general ground settlement is about 50% to 70% of the maximum wall deflection. Maximum wall deflections were usually between 0.2% and 0.5% of the excavation depth.

Wong, I. H. et al (1996) presented the performance of deep excavations for the Central Expressway (CTE) Phase II project in Singapore. They examined lateral wall deflections, soil settlements, and prop loads for the different support systems used and soil conditions encountered. They found that maximum wall movements were typically less than 0.005 H for excavations with a combined thickness of soft soil layers of 0.9 H overlying stiff soils, maximum wall movements were typically less than 0.0035 H for excavations with a combined thickness of soft soil layers of 0.6 H

overlying stiff soils and concluded that placing the first layer of struts near the top of braced walls is effective in reducing movements for walls embedded in stiff soil.

3. Verification Examples from Literature

On this part of the thesis, it will be examined whether the software PLAXIS is applicable to analyze diaphragm wall. For this purpose two examples are picked from literature that have detailed input and output data.

3.1 Finite element software PLAXIS

PLAXIS is a finite element package intended for analysis of deformation, stability and groundwater flow problems in geotechnical engineering (Brinkgreve et al. 2004). It is widely used in practice because of its simplicity, user-friendliness and reliability.

PLAXIS is equipped with features to deal with deep excavation supported with diaphragm wall. A brief summary of some important features of PLAXIS is given below:

- The input parameters and the boundary conditions of the geometry can be drawn based on computer-aided drawing (CAD) procedures. A 2-D finite element mesh can also be generated easily.
- It allows automatic generation of unstructured triangular 2-D finite element meshes with options for global and local mesh refinements.
- 6-node and 15-node triangular elements are available to model stresses and deformations in the soil.
- Special beam elements (designated as plates) are used to model structural elements such as diaphragm walls, tunnel linings, shells, and other slender structures.
- Elastoplastic spring elements are used to model anchors and struts.
- The presence of geosynthetic reinforcements (e.g. a geotextile or a geogrid) can be simulated by the use of special tension elements.
- Steady-state pore pressure can be generated using either phreatic levels or groundwater flow calculation. Excess pore pressures are computed during plastic calculations when undrained soil layers are subjected to loads.

- Automatic load stepping avoids the need for the user to select suitable load increments for plastic calculations, thus ensuring an efficient and robust calculation process.
- Stage construction feature enables a realistic simulation of construction and excavation processes by activating and deactivating clusters of elements, application of loads, changing of water tables, etc.
- The change in excess pore pressures with time can be computed using a consolidation analysis. It incorporates simple linear, isotropic Mohr-Coulomb Soil model as well as more complex and non-linear models such as Hardening Soil model, Jointed Rock model, Soft-Soil-Creep model, Soft Soil model and Modified Cam-Clay model.

In major deep excavation projects, the Mohr-Coulomb (MC) model and the Hardening Soil (HS) model are mostly used to simulate soil behavior. The details of the Mohr-Coulomb model can be found in any geotechnical engineering text (e.g. Budhu 2000). A comprehensive description of the Hardening Soil model can be found in Schanz et al. (1999). The essential features of the Mohr-Coulomb model and Hardening Soil model are provided in Appendix 1.

3.2 Modeling for a tunnel entrance pit

Raithel, M. et al (2005) have given design and numerical investigations of a deep excavation for a tunnel entrance pit in Germany. This new shield tunnel is constructed to replace the existing bridge for the crossing of the trave river in Lübeck, Germany. The paper studied the construction and design of the retaining structures together with the 12.5 m high cofferdam using FE-program PLAXIS 8.2. This section presents the calculation result of Raithel M. et al and measurements for verification purpose.

Site Description

The excavation is partly supported by a fourfold anchored, 27 m deep and 80 cm thick diaphragm wall which has a free height of about 12.5 m. At a distance of 8 m behind the wall, a 15 m wide and 12.5 m high (reference: diaphragm wall head) cofferdam made of tied back soldier piles was constructed before the beginning of the excavation on which the federal highway temporarily runs.

The underground is characterized by a succession of sand, basin silt and boulder clay. In general, the layers have a sufficient load bearing capacity. The basin silt, however, exhibits unfavorable bearing and deformation behavior compared to the overlying and underlying layers. The essential soil parameters of the governing soil layers are given in Table 3.1. The elastic modulus in Table 3.1 is at a reference pressure of p_{ref} = 100 kN/m². The groundwater is characterized by two different aquifers which are independent from each other.

Table 3. 1 Soil parameters at the excavation pit

Soil layer	Unit weight γ/γ' [kN/m³]	Friction angle Φ' [°]	Cohesion c' [kN/m²]	Elastic modulus Es [MN/m²]
Sand fill	19/11	37.5°	0	50
Upper sand	19/11	37.5°	0	50
Basin silt	19/20	25.0°	20	20-25
Boulder clay	22/22	30.0°	20	30
Lower sand	19/21	37.5°	0	50

Excavation Pit

The part of the retaining structure presented here consisted in the original design a 0.8 m thick diaphragm wall supported at four positions with ground anchors. The anchors were prestressed to about 85% of the service load. Also the wall was assumed to be supported by bottom concrete slab placed under water and has a thickness of 0.8m. The governing load on the wall comes from the nearby 12.5 m high cofferdam beside

to the 12.5 m deep excavation. The construction was done by gradual lowering of the groundwater followed by dry excavation.

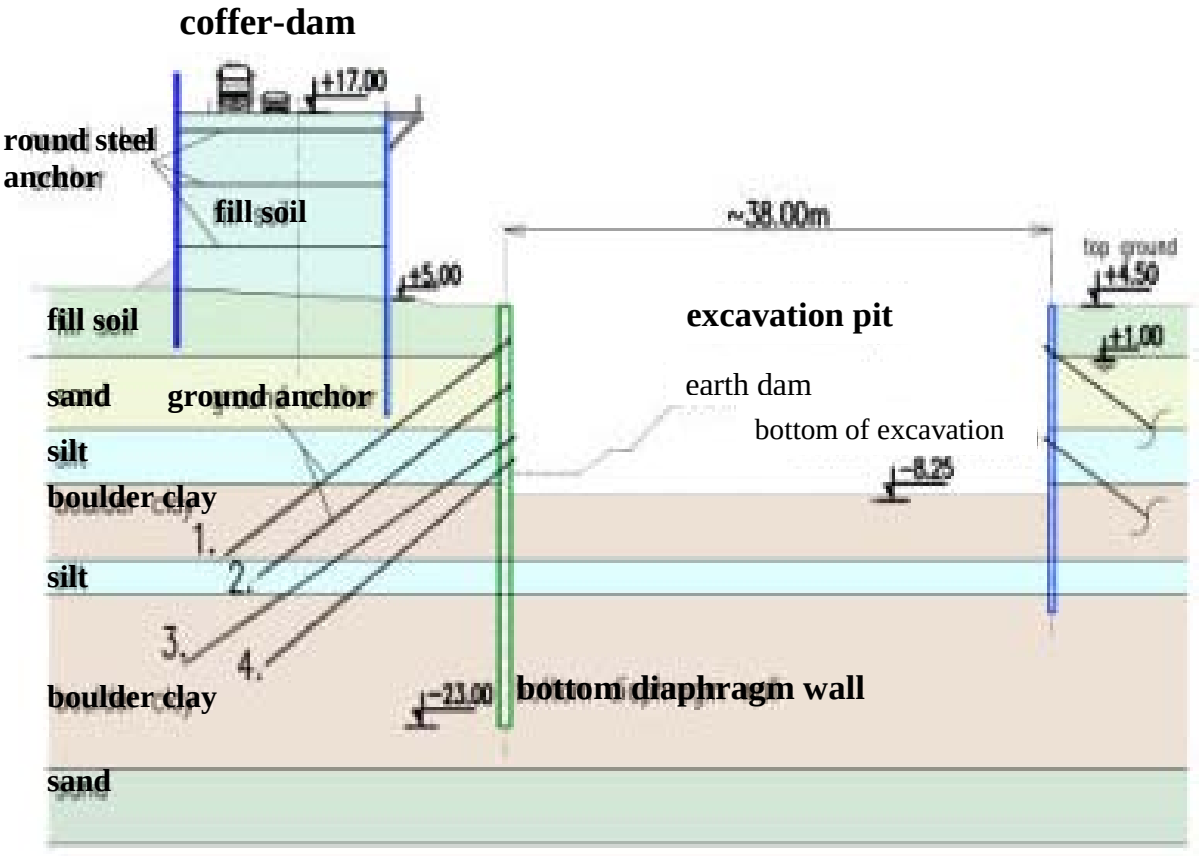

Figure 3. 1 Cross section of the excavation pit [Raithel, M. et al, 2005]

Numerical Analysis

The numerical analysis of the excavation was performed with the FE-program "PLAXIS" and a 15 node triangular element was used to generate the model mesh. An advanced constitutive soil model known as the hardening soil model (HSM) was used to simulate the soil behavior under excavation. The FE-computations were carried out for the different construction stages. The groundwater table in the upper aquifer is taken to be at a depth of 3.5 m below the surface and the lower confined aquifer at 4.5 m below the surface.

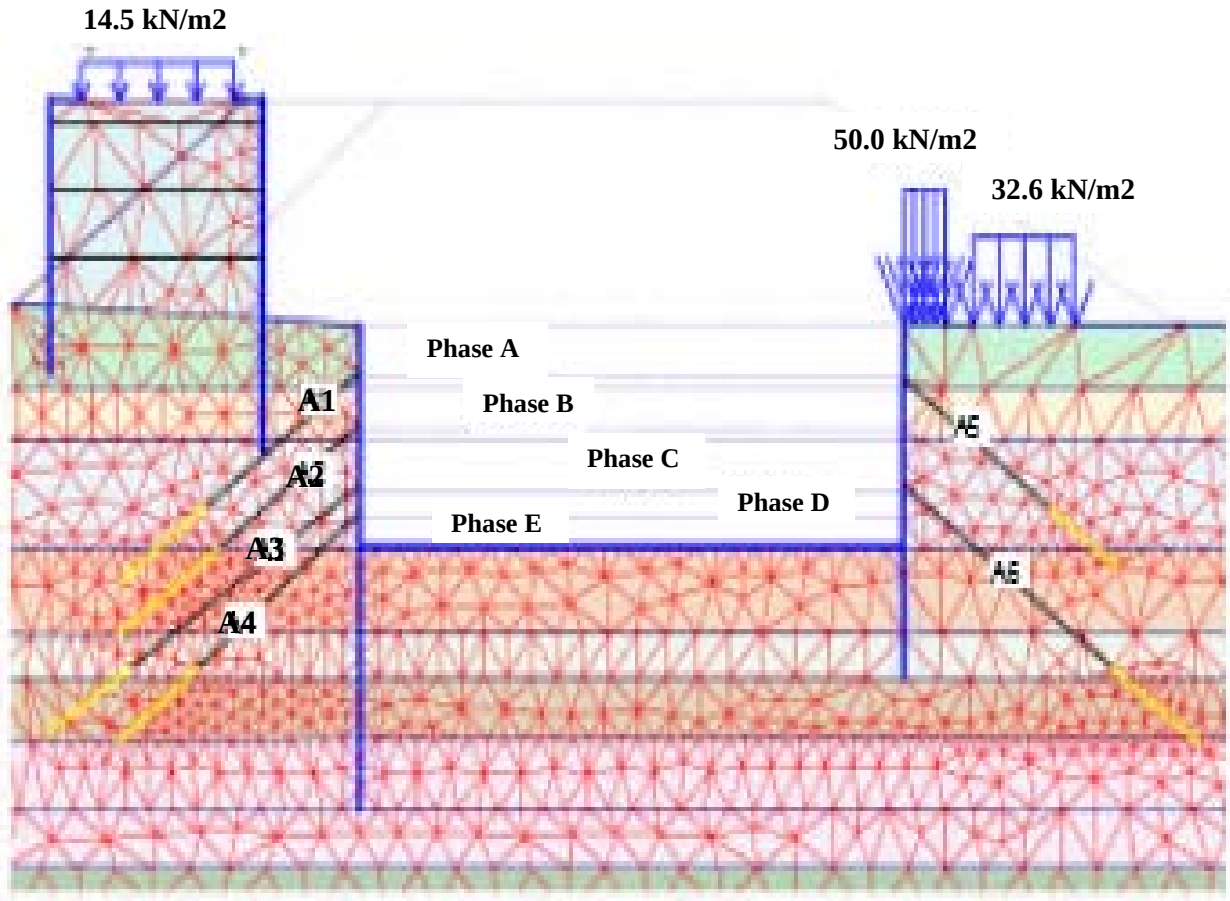

Figure 3. 2 Finite element model and construction stages [Raithel, M. et al, 2005]

Computation results

The computed and measured values are presented in Figure 3.3.

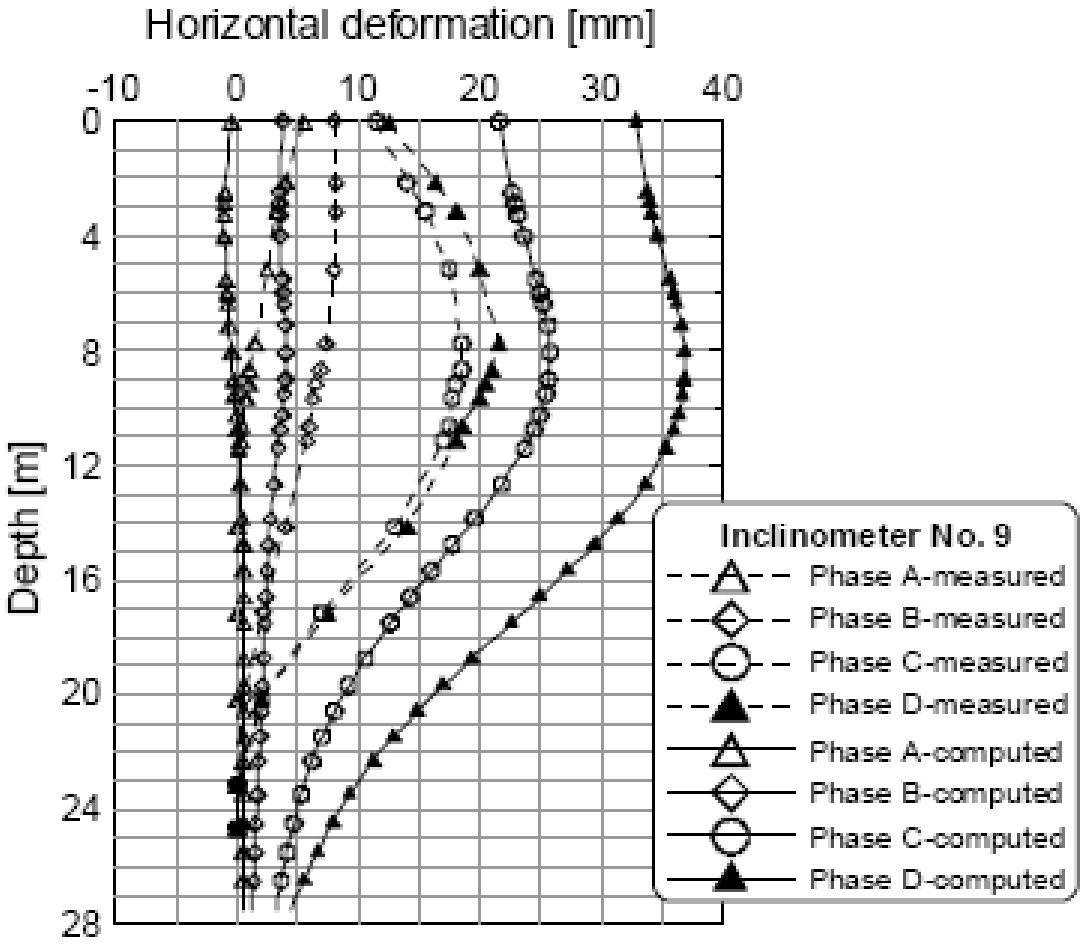

Figure 3. 3 Comparison of the measured and computed deformations [Raithel, M. et al, 2005]

During comparison of the measured and computed values in the evaluation of the inclinometer data, the assumption should be taken into consideration that the toe of the wall is fixed. In reality, however, there always exists a horizontal movement of the toe of the wall in-situ, which is also shown by the FEM-results. Therefore, the additional toe displacement of about 5 mm in (Phase C) should be taken into account in the evaluation of the inclinometer result. In respect to the excavation phase C, a deformation increment of about 20 mm was calculated up to the end of the excavation.

Generally, the numerical results show a good agreement with the measured values, especially when the additional in-situ wall toe displacement is taken into consideration in the analysis of the inclinometer measurements. The reason for the relatively small measured deformation in comparison to the computed values may lie on the favorable geometrical in-situ situation, the possibility of an uncompleted consolidation process (excess pore pressure might still exist in some layers at the end of the excavation) and the necessary approximation of some input parameters.

3.3 Modeling for Dana Research Tower

Konstantakos, D. C. et al (2004) have done back analyses on an excavation up to 23m deep for the Dana Farber research tower in the Longwood medical area of Boston (Figure 3.4), which was supported by a permanent perimeter diaphragm wall using finite element software, PLAXIS 8.2. This paper summarizes the performance of the lateral earth support system based on field monitoring data measured during excavation of the basement and details of back analyses used to evaluate and interpret the wall and ground movements. In this paper, unlike the paper in previous example, contains almost full inputs data for both soil and support systems. This section presents the computed results of Konstantakos D. C. et al and field measurements for verification purpose.

Site Description

During the site investigation, there was a very limited program of laboratory tests (index properties, water content and UU strength testing in the clay, and particle size distributions for the granular layers) while permeability properties were reported from borehole falling head tests. The subsurface profile comprises 20m - 27m of post-glacial sediments overlying the Roxbury conglomerate bedrock. The bedrock was described as medium to hard, slightly weathered gray to purple, coarse-grained conglomerate with closely spaced dipping joints and RQD = 28% - 40%. The surface of the rock is quite irregular and dips from north to south across the site (Figure 3.5). The overlying soils can be sub-divided into four main units: 1) top fill (up to 5m thick at the southern edge of the site), 2) low plasticity (I_P = 10—15%) marine clay (Boston

Blue Clay) ranging in consistency and coloration and ranging in thickness from 10m – 17m (the upper clay contains discontinuous pockets of sand), 3) deposits of underlying sands and silts which taper to the north and south of the site but appear more continuous in the east-west plane; and 4) a drape of glacial till (0.3m – 3.0m thick) comprising very dense sand with silt and gravel.

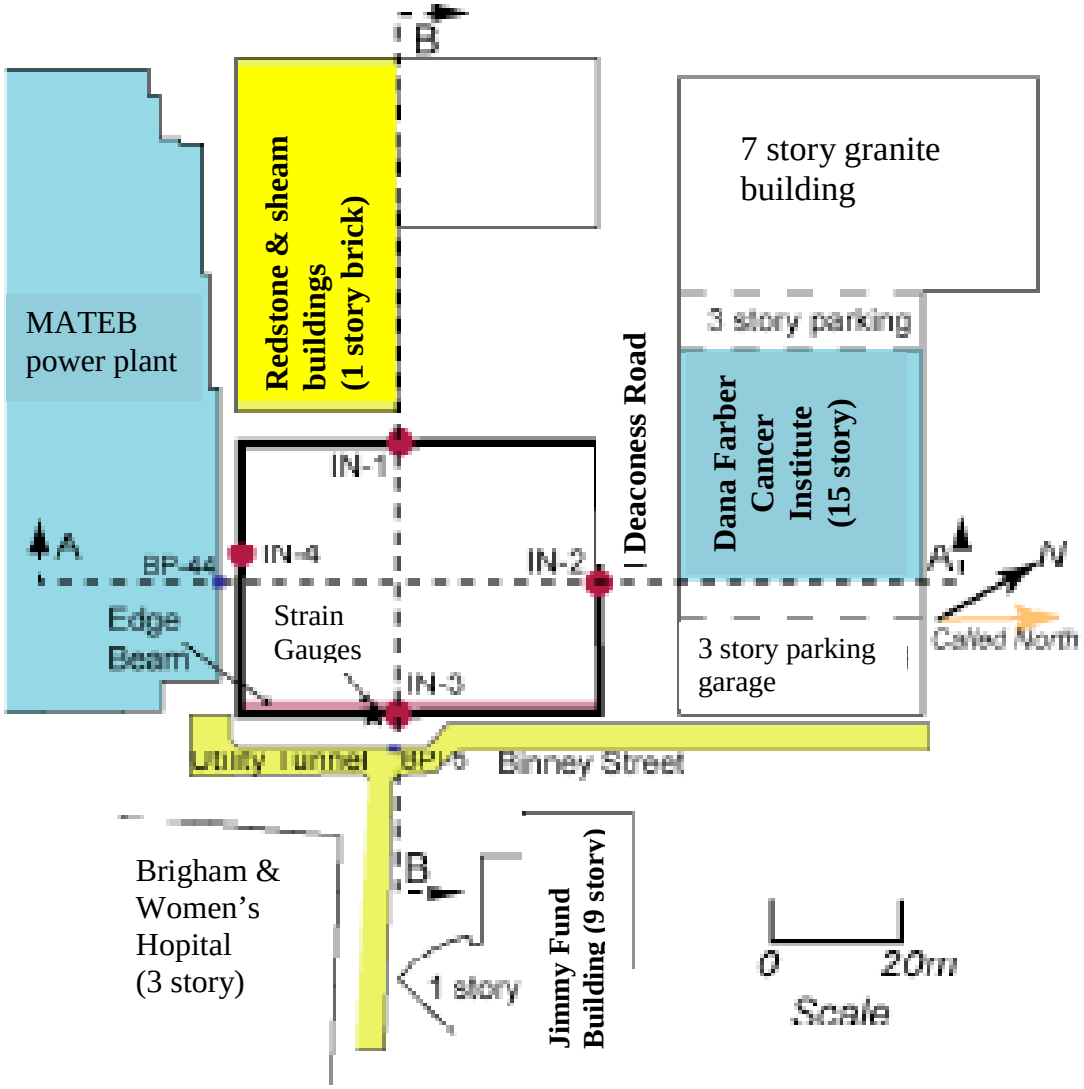

Figure 3. 4 Dana Farber research tower site plan [Konstantakos, D. C. et al, 2004]

The clay deposits range in consistency from a very stiff, oxidized crust (yellow coloration) to stiff (with gray coloration), and corresponding undrained shear strengths from UU tests, S_u = 90kPa, 60kPa, respectively. The clays are clearly overconsolidated, but no consolidation tests were performed for this project. The underlying silts, sands and till layers were found to have relatively high permeability

in the range, k = 0.3 – 3.0m/day. The silty fine sand and glacial till layers were classified as very dense layers based on SPT data. In some locations (Figure 3.5), there are looser deposits of 'silt with sand' (N = 12 – 37bpf) directly beneath the marine clay There is a perched groundwater table in the overlying fill which is typically 1m - 2m below the ground surface.

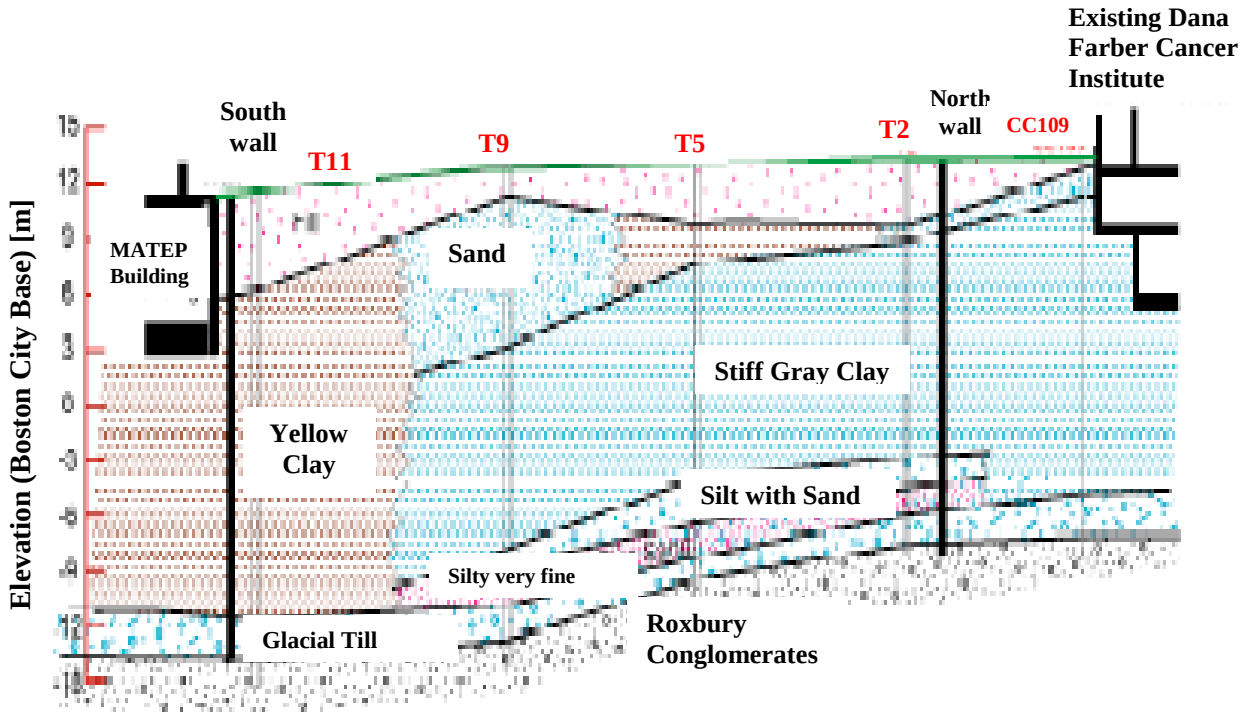

Figure 3. 5 Interpreted stratigraphy and location of adjacent structures [Konstantakos, D. C. et al, 2004]

Lateral Earth Support System

The permanent lateral earth support system comprising a 0.9m thick perimeter slurry wall extending a minimum of 0.6m into the underlying Roxbury conglomerate. The tieback anchors were installed through steel sleeves cast into the slurry wall. Each anchor was inclined at 45° with minimum fixed anchor lengthsof 6m in the bedrock. Horizontal spacing of the anchors ranged from 1.65m to 3.2m and each tendon comprised from 9 to 16 strands of 1.5cm diameter high tensile strength steel.

Finite Element Simulation

A series of finite element simulations have been carried out to obtain better insight into the performance of the excavation support system for the Dana Farber research tower. The calculations have been carried out using the Plaxis finite element code (2002), plane strain models. Each of the soil layers has been simulated using the Hardening Soil (HS) model as it enables a realistic description of the stiffness of the retained soil relative to the excavated material with minimal additional parameters. The perimeter slurry wall was modeled using elastic beam elements (with axial and bending stiffnesses; EA = 2.52x107kN/m and EI = 1.7x106kNm2/m, respectively), while elastic properties and prestress loads for the rock anchors are EA = $1.0x10^5$ kN/m.

Computation results

Figures 3.6 and 3.7 compare the measured wall deflections and surface settlements at the South and North walls (i.e., section A-A, Figure 3.4, Figure 3.5) at selected stages of the excavation. The results show a small (5mm) inward cantilever deflection of the North wall (Stage L1, Figure 3.6b). However, subsequent excavation and prestressing of anchors causes a reversal in wall deflections such that there is a small net outward movement (up to 6mm at El. 5m) at the end of the excavation (stage L7, Figure 3.7b). The toe of the wall rotates but shows no net displacement. The behavior of the South wall is strongly influenced by the proximity of the MATEP foundation mat. There is no space for the P1 and P2 anchors. However, the inward cantilever deflections (6mm) at L3 are similar in magnitude to those found for the North wall at L1. This behavior can be attributed to the stiffening effects from grouting that was carried out to mitigate shallow soil cave-ins that occurred during installation of the South wall. Prestressing of anchors P3 – P6 is able to control subsequent inward wall deflections to less than 18mm. The proximal edge of the MATEP power plant settled a similar amount (approx. 15mm) and there is less than 10mm of differential settlement across of the foundation mat. Settlements up to 20mm occurred behind the North wall, but movements of the Dana Farber Cancer Institute were less than 10mm.

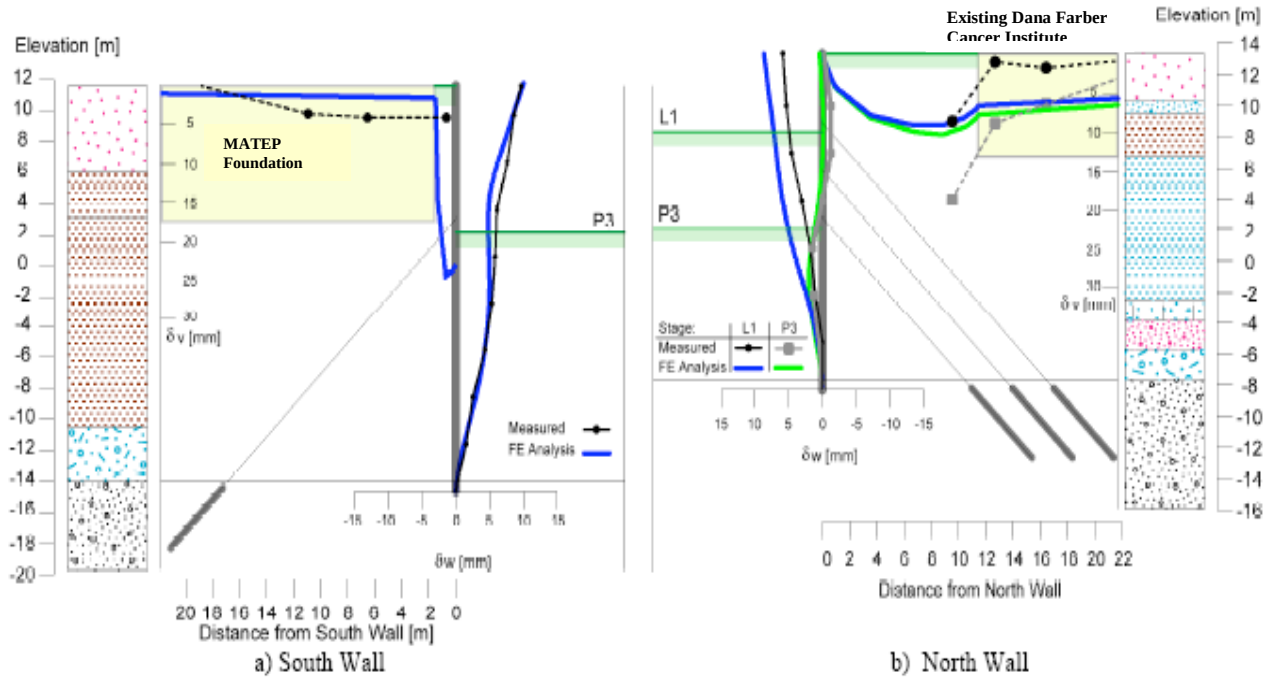

Figure 3. 6 Measured and predicted behavior of Section A-A walls at early stages of excavation [Konstantakos, D. C. et al, 2004]

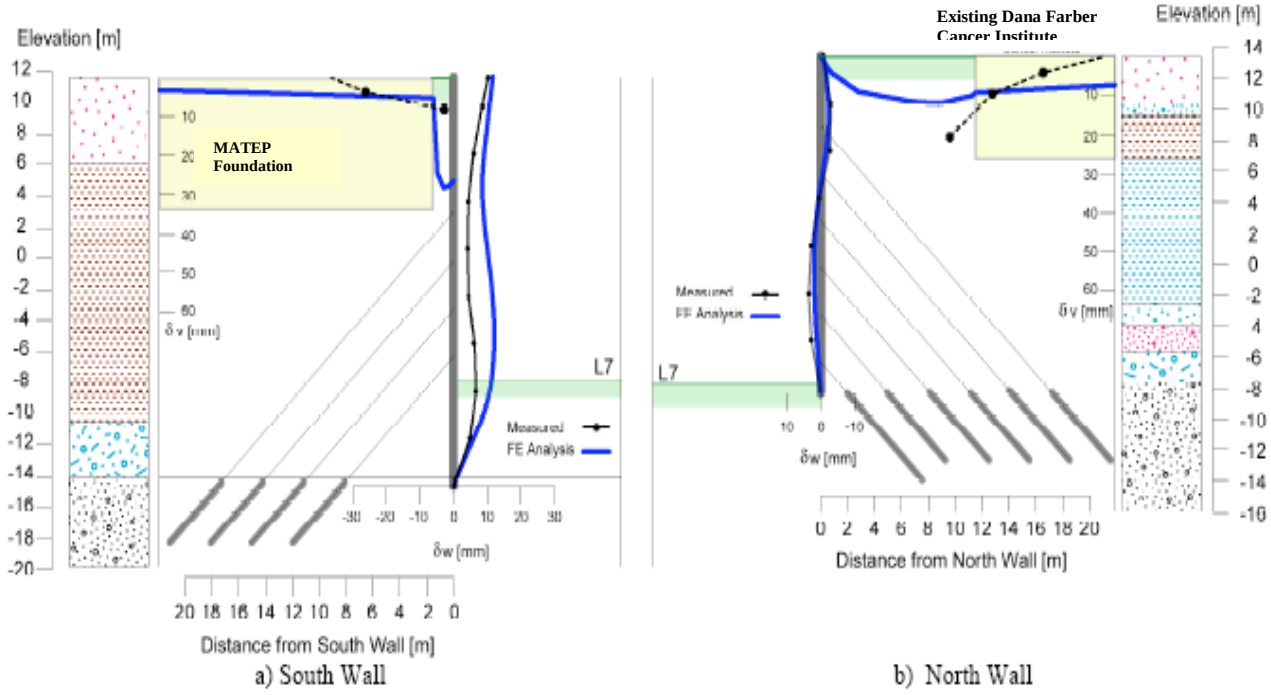

Figure 3. 7 Measured and predicted behavior of Section A-A walls at end of excavation [Konstantakos, D. C. et al, 2004]

Back-analyses of the excavation performance using PLAXIS 2-D finite element analyses were able to give consistent estimates of the measured wall deflections on each sides of the excavation.

4. Analysis and Parametric Study

4.1 Parameter Identification

In the previous chapter of this thesis, two verification examples from literature were presented which were analyzed using PLAXIS Finite Element Code For Soil And Rock Analyses software and the results were compared with measured values. From the comparison made, the results from PLAXIS give reliable values. Thus for the parametric study, PLAXIS shall be used.

There are a number of parameters to be considered if one is interested in conducting a comprehesive parametric study. But as reported by earlier investigators (e.g. Goh, A.T.C.,1990), some of the variables have little or no effect in the performance of deep excavation supported by diaphragm wall. In this paper, variables that have practical importance and reported to have significant influence in the perofrmance of deep excavations are considered.

From the verification made in Chapter 3 and reports from earlier investigators (e.g. Hoe, N. H., 2007), Hardening Soil model gives precise prediction of ground deformation for deep excavations. This model is an updated version of the well known Duncan-Chang model (Duncan et al., 1980), formulated using elasto-plasticity in which the non-linear shear-stress behavior in loading is represented by a hyperbolic function. The details of the model are presented in Appendix 1. In this paper, each of the soil types are simulated using the Hardening Soil (HS) model.

Previously reviewed papers show that soil type is a key factor in performance of deep excavations. Soil type is important because the performance of deep excavations is governed by the interaction between the soil and the support system. Support systems for deep excavation consist of two main components. The first is a retaining structure. The second component is the support provided for the retaining structure. The stiffness of the support system is governed by individual stiffness of the components. Thus, parameters are identified accordingly.

Soil type, depth of excavation, wall embedment depth, wall stiffness and anchor spacing are the variables considered in the parametric study. When one of the above parameters is varied, the rest are kept constant. The issue of heave is not addressed in this parametric study as PLAXIS does not include this parameter in the calculation.

The soil types considered for the parametric study are expansive clay from Bole-Medhanealem area, red silty clay(non expansive) from Arada area and for the sake of comparison a typical sandy soil. Ground water level is assumed to be 3.0 meters below existing ground level.

The appropriate input parameters for expansive clay and red silty clay are incorporated from laboratory reports obtained from Saba Engineering Plc and Construction Design Share Company (CDSCo.) for Bole-Medhanealem and Arada areas respectively. Relevant parameters for sand is taken from litrature which are assumed to be typical for fine grained granular soil as shown later in Table 4.2.

The soil parameters for the expansive soil are obtained from CDSCo geotechnical reports for W/o Fozia Hassen B+G+7 multipurpose building located in Bole-Medehanealem area and also confirmed by different investigation conducted by Saba Engineering Plc for Aschalew Belay Hotel near Bole-Medehanealem church.

The following engineering design parameters are considered to represent the expansive clay:-

Total Unit Weight	= 16.3kN/m3
Cohesion (Total stress)	= 27kN/m2
Angle of Friction (Total stress)	= 13°
Modulus of Elasticity	= 20MPa
Poisson’s Ratio	= 0.3
Specific Gravity	= 2.5
Free Swell	= 130%
Compressive Index	= 0.303
Initial Void Ratio	=0.760

The soil parameters for the red silty clay are obtained from CDSCo geotechnical reports for G+4 Health Centre and G+3 Youth Centre located in Arada area. According to the reports, the red silty clay is considered to have the following engineering design parameters.

Total Unit Weight	= 16.5kN/m3
Angle of Friction (Total stress)	= 20°
Cohesion (Total stress)	= 21kN/m2
Modulus of Elasticity	= 25MPa
Poisson's Ratio	= 0.3
Specific Gravity	= 2.65
Liquid Limit	= 48.5 %
Plastic Limit	= 29.7%
Plasticity Index	= 18.8%
Moisture Content	= 29.4%

Table 4.1 to Table 4.6 which show the soil type, the relevant soil properties, the diaphragm wall parameters, the tie-back wall parameters, the depth of excavation and the depth of embedment used for the base model are presented below.

Table 4. 1 Soil type for base model

Description	Type	Area
Soil 1	Expansive Clay	Bole
Soil 2	Red Silty Clay	Arada
Soil 3	Sand	-

Table 4. 2 Soil parameters for base model

Parameters	Unit	Soil S1	Soil S2	Soil S3
Model*	--	HS(U)	HS	HS
Bulk unit weight (saturated)	γ_{sat} (kNm^{-3})	19.0	17.0	20.0
Total unit weight	γ (kNm^{-3})	16.3	16.5	19.0
Permeability	K (m/day)	0.0001	0.001	0.1
Poisson's ratio	ν (-)	0.3	0.3	0.35
Secant modulus at 50%**	E_{50}^{ref} (kNm^{-2})	20,000	25,000	30,000
Oedometer modulus	E_{oed}^{ref} (kNm^{-2})	20,000	25,000	30,000
Unloading reference Young's modulus	E_{ur}^{ref} (kNm^{-2})	60,000	75,000	90,000
Cohesion	C (kNm^{-2})	27	21	-
Friction	Φ (^{0})	13	20	34
Coefficient of lateral earth pressure***	K_0^{nc}	0.770	0.658	0.441

Notes: * - HS – Hardening soil; (U) – 'undrained' capability to develop excess pore pressures
Default parameters used: $E_{oed}^{ref} = E_{50}^{ref}$, $E_{ur}^{ref} = 3\,E_{50}^{ref}$, $R_f = 0.9$

** - Stiffness parameters assumed to be at reference pressure, P_{ref} = 100KPa

*** - nc: normally consolidated

Table 4. 3 Diaphragm wall parameters for the base model

Parameters	Unit	Dpgm1	Dpgm2	Dpgm3	Dpgm4	Dpgm5
Type	-	Elastic	Elastic	Elastic	Elastic	Elastic
EA*	kN/m	9.00E+06	1.35E+07	1.80E+07	2.25E+07	2.70E+07
EI	kNm	6.75E+04	2.28E+05	5.40E+05	1.05E+06	1.82E+06
Thickness	m	0.3	0.45	0.6	0.75	0.9

Notes: * - EA and EI are per unit length of diaphragm wall

EA = Et, t = thickness of diaphragm wall

$EI = Et^3/12$

Table 4. 4 Strut parameters for the base model

Parameters	Unit	St1	St2	St3
Type	-	Elastic	Elastic	Elastic
EA	kN/m	1.00E+05	1.00E+05	1.00E+05
Ls (Strut spacing)	m	2	3	4
Fmax (Prestressed Load)	KN	150	150	150

Table 4. 5 Depth of excavation for the base model

Parameters	Unit	$D_{ex}1$	$D_{ex}2$	$D_{ex}3$
Depth of excava.	m	8	12	16

Table 4. 6 Depth of embedment for the base model

Parameters	Unit	$D_{em}1$	$D_{em}2$	$D_{em}3$
Depth of embed.	m	5	7.5	10

4.2 Base model generation

A typical base model geometry and general dimensions for the study is shown in Figure 4.1. The model is simulated as a symmetrical plain strain finite element employing 15-noded triangular elements and half of the geometry with a width of 100 meters and depth of 50 meters.

The relevant soil properties used for the base model is listed in Table 4.2. Because of its low permeability, undrained material model is used for expansive soil. The effect of drained and undrained material model on the performance of excavation is presented in appendice 2.

The diaphragm wall is modeled as elastic beam elements in which the unloading of the ground during the installation of diaphragm wall is not considered. The Young's modulus, Es = 30000 Mpa, of the diaphragm wall is kept constant for all the analyses, a change in thickness of the diaphragm wall represents a change in both the bending

stiffness and the axial stiffness of the diaphragm wall. In addition to that, interface elements are also taken into consideration to model the soil-structure behavior (Table 4.3).

The tieback anchors are installed into the diaphragm wall. Each anchor is inclined at 45° with horizontal spacing ranged from 2m to 4m. The anchors assumed to have tensile strength, EA, of 1.00E+05 KN/m and prestressed load of 150KN. At the end of tieback anchors, ground anchors of 5.65m length are installed. Ground anchors, which have no bending stiffness but axial stiffness only, allow a continuous load transfer from the tieback anchors to the ground along its entire length (Table 4.4).

The values of depth of excavation and depth of embedment considered in the parametric study are shown in Table 4.5 and Table 4.6.

The figure below gives representative model in PLAXIS

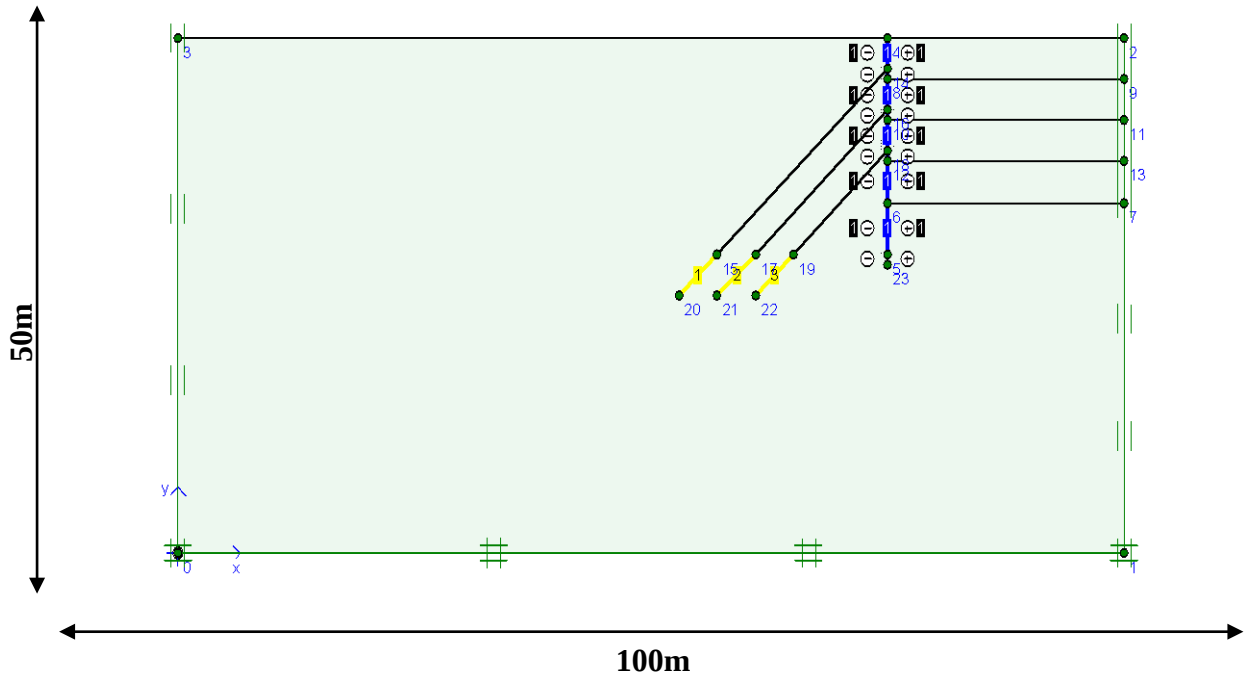

Figure 4. 1 Typical finite element model in PLAXIS for a deep excavation.

The typical phases in staged construction which are assumed to be carriedout an interval of 4m are:

Initial Phase

Phase 1: Installation of diaphragm wall

Phase 2: Excavation to first level RL-4.00m

Phase 3: Installation of strut at RL-3.00m

Phase 4: Excavation to second level RL-8.00m

Phase 5: Installation of strut at RL-7.00m

Phase 6: Excavation to final level RL-12.00m

4.3 Analysis Results and Discussion

In this section, the details and the results of a total of 125 parametric studies are presented. The parametric study conducted included a number of alternative arrangements of variables under consideration (Appendix 3). Accordingly, the effect of varying a parameter is manifested by obtaining the variation in the following three quantities:

- Maximum horizontal displacement of the diaphragm wall [δh_{max}]
- Maximum ground settlement behind the diaphragm wall [δv_{max}]
- Maximum bending moment in the diaphragm wall [BMmax]

1. Effect of Change in Soil Type

In this part of analysis, the paper concentrates on how change in soil type affects the performance of deep excavations supported by diaphragm wall for each of 8m, 12m and 16m depth of excavation. The output of this analysis is presented for each soil for varying thickness of diaphragm wall as follows.

For all the analyses conducted in this section of parametric study, the following quantities or features are kept the same:

- All the parameters for the soil types, i.e. expansive clay, red silty clay and sandy soil.
- Tieback anchor strut spacing (L_s = 2 m)
- Depth of embedment (D_{em} = 5 m)
- Construction sequences (as described at the end of section 4.2)

Figure 4.2 – Figure 4.10 show the effect of soil properties (soil type) on the maximum horizontal displacement of the diaphragm wall, maximum ground settlement behind the diaphragm wall, maximum bending moment induced in the diaphragm wall due to deep excavations.

- ***Case 1. Depth of excavation, D_{ex} = 8 m***

In this section, the effect of change in soil type on the performance of deep excavations supported by diaphragm wall for 8 m depth of excavation is presented.

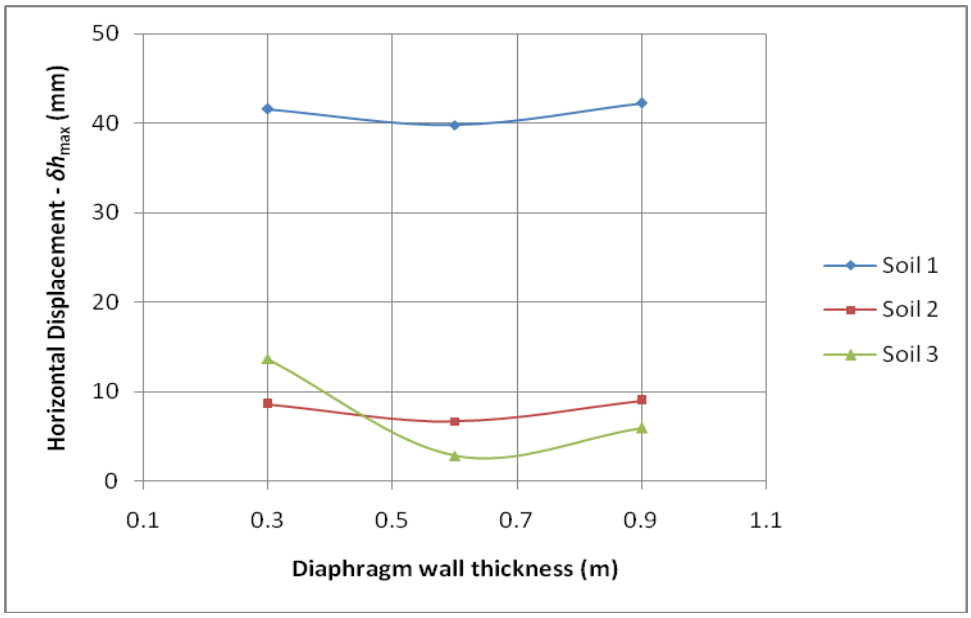

Figure 4. 2 Maximum horizontal displacement of the diaphragm wall with diaphragm wall thickness (Case 1)

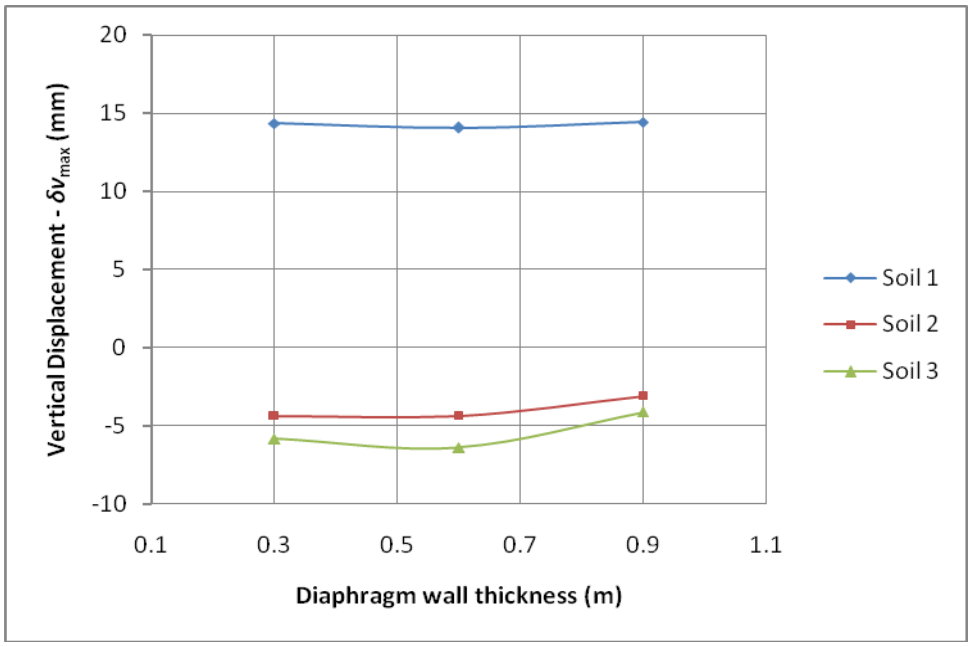

Figure 4. 3 Maximum ground settlement behind the diaphragm wall with diaphragm wall thickness (Case 1).

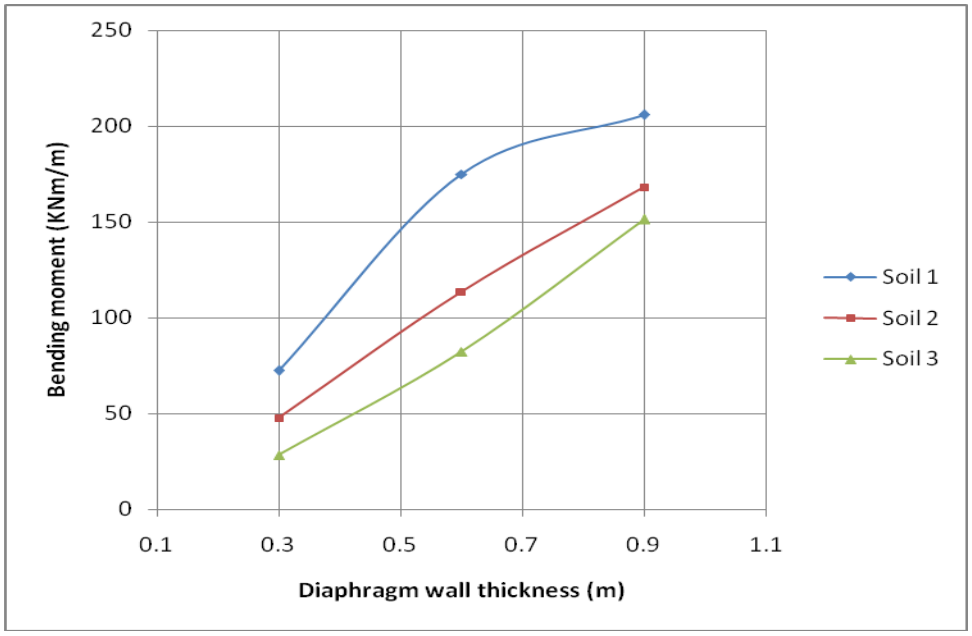

Figure 4. 4 Maximum bending moment in the diaphragm wall with diaphragm wall thickness (Case 1)

- ***Case 2. Depth of excavation, D_{ex} = 12 m***

In this section, the effect of change in soil type on the performance of deep excavations supported by diaphragm wall for 12 m depth of excavation is presented.

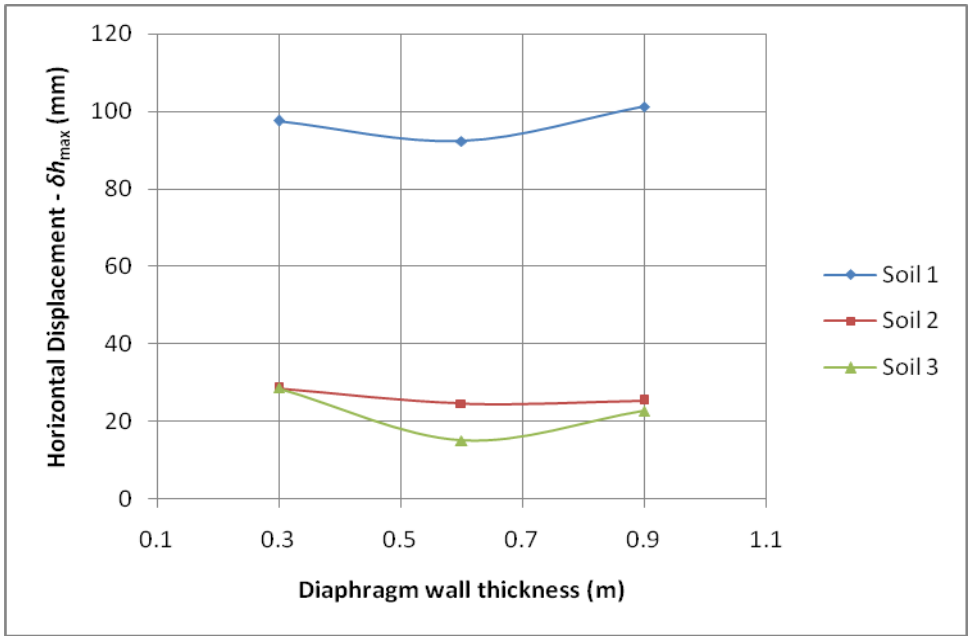

Figure 4. 5 Maximum horizontal displacement of the diaphragm wall with diaphragm wall thickness (Case 2)

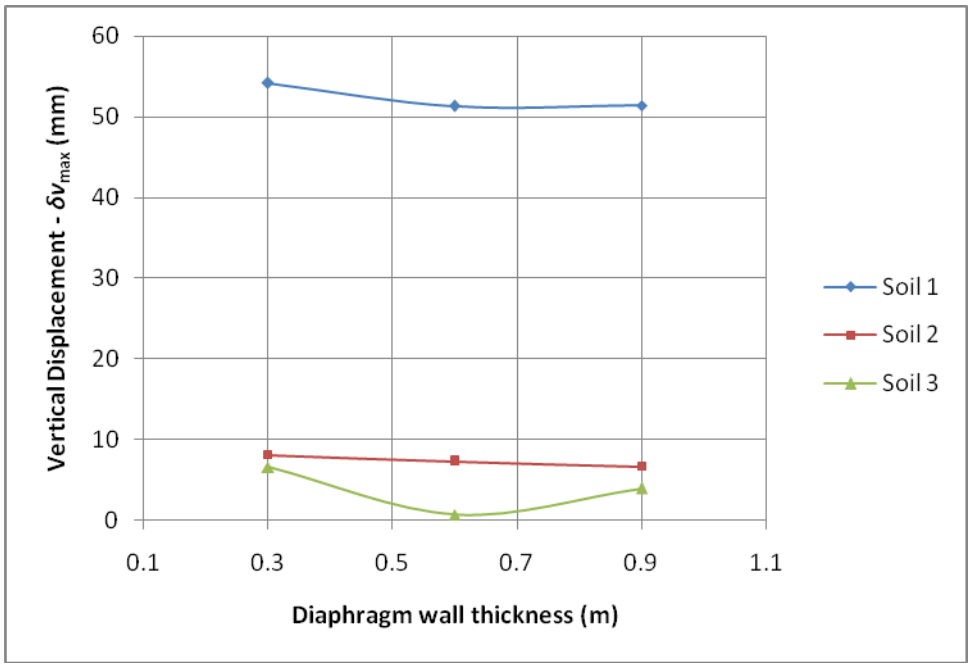

Figure 4. 6 Maximum ground settlement behind the diaphragm wall with diaphragm wall thickness (Case 2)

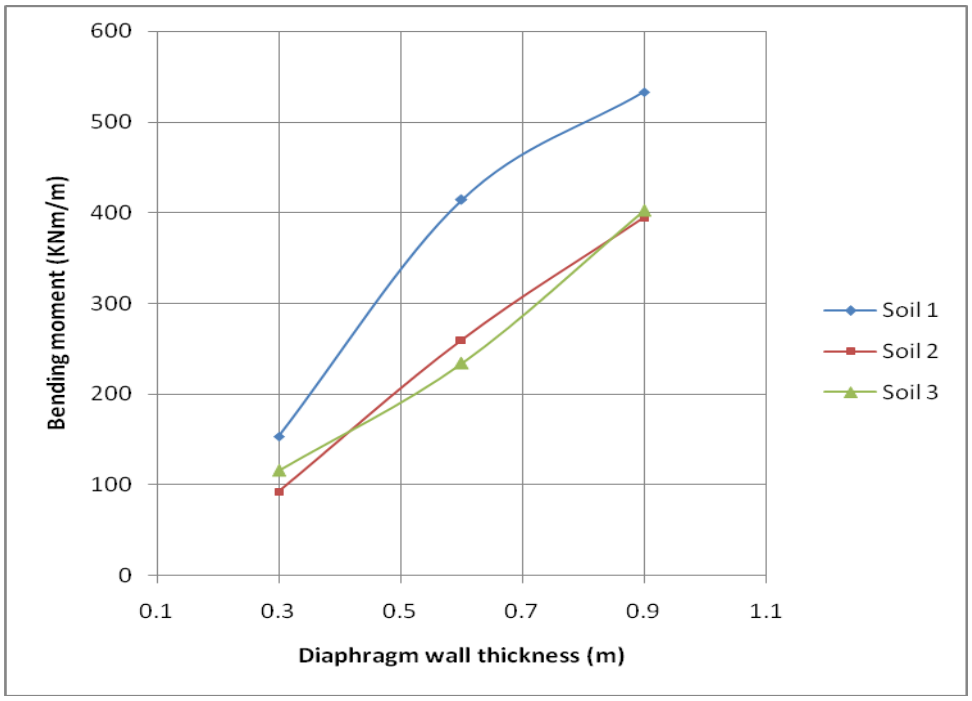

Figure 4. 7 Maximum bending moment in the diaphragm wall with diaphragm wall thickness (Case 2)

- ***Case 3. Depth of excavation, D_{ex} = 16 m***

In this section, the effect of change in soil type on the performance of deep excavations supported by diaphragm wall for 16 m depth of excavation is presented.

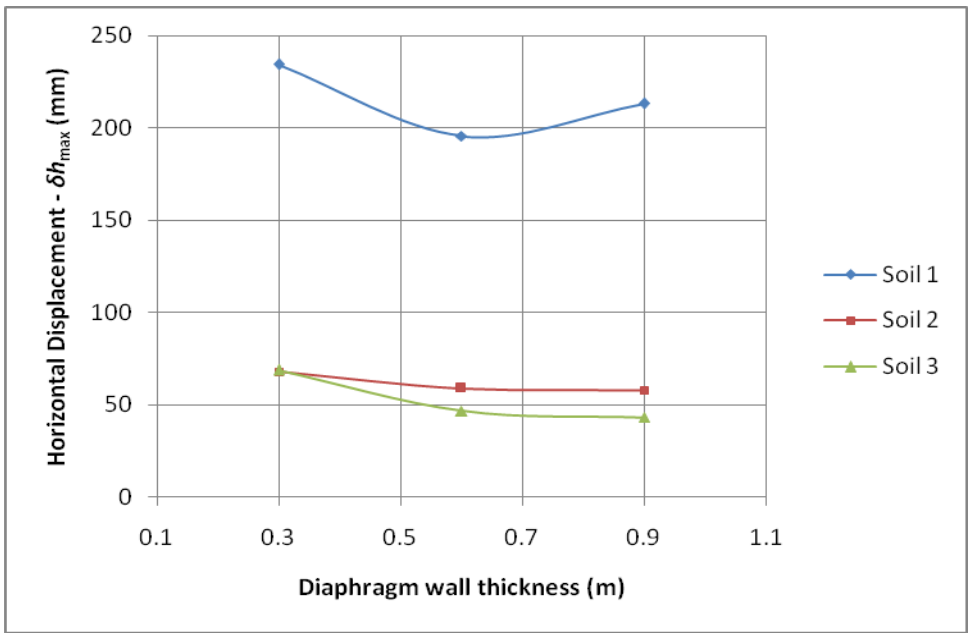

Figure 4. 8 Maximum horizontal displacement of the diaphragm wall with diaphragm wall thickness (Case 3)

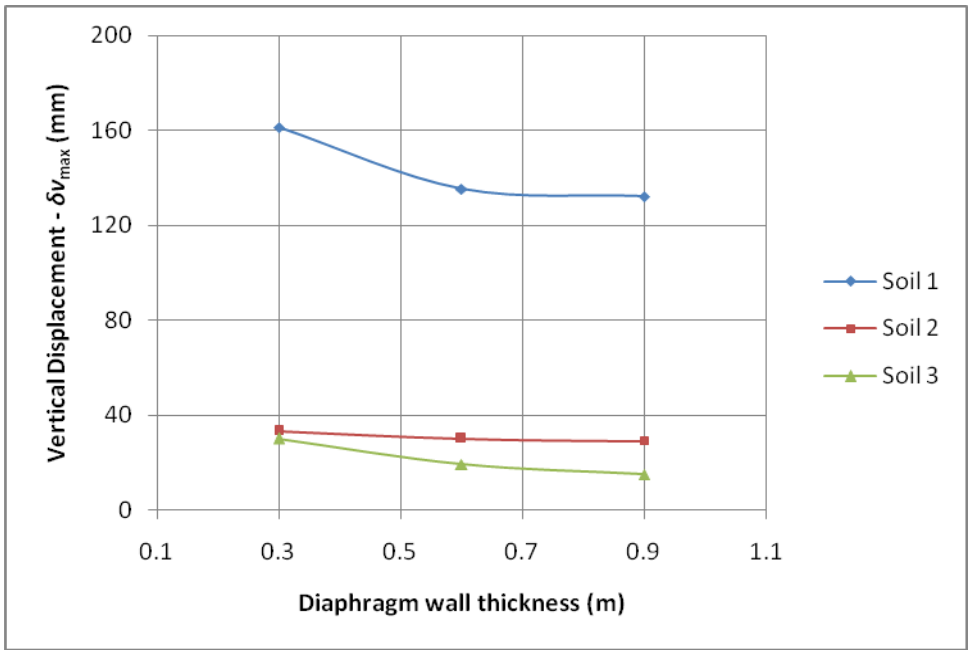

Figure 4. 9 Maximum ground settlement behind the diaphragm wall with diaphragm wall thickness (Case 3)

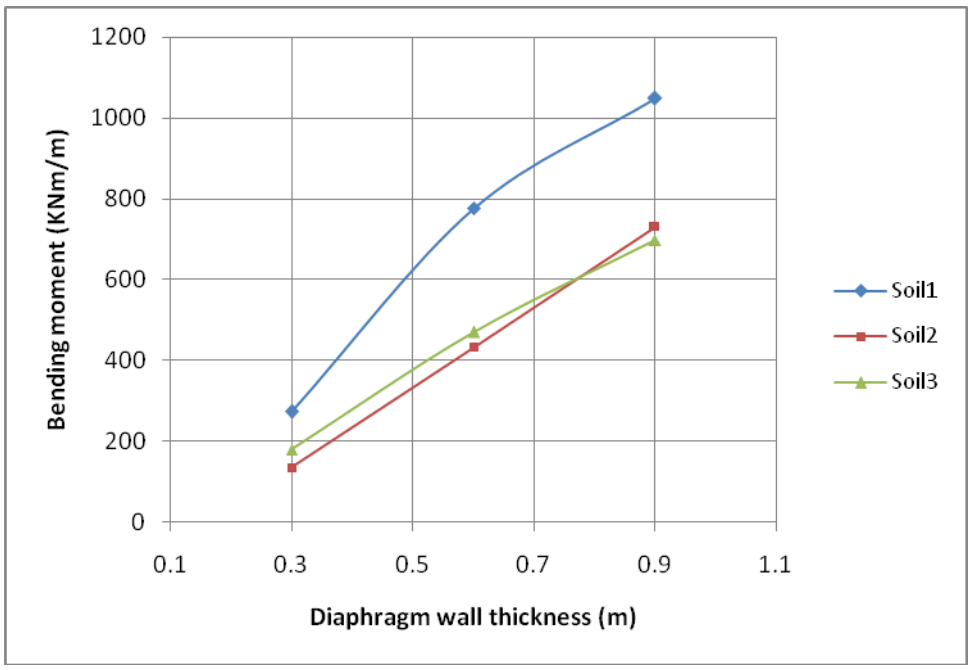

Figure 4. 10 Maximum bending moment in the diaphragm wall with diaphragm wall thickness (Case 3)

A significant increase in the ground deformation around the deep excavation is observed for black cotton soil when compared to sand and red silty clay soil. When we consider a 12m deep excavation supported by 0.6m thick diaphragm wall thickness, it has a horizontal displacement of 92.4mm in expansive clay which is

67.8mm and 77.3mm more than that is observed for red silty and sand soils respectively. From figures, it can be observed that expansive clay has much more vertical settlement than the others and vertical settlement increases with horizontal displacement. The maximum bending moment in the diaphragm wall also increases in response to increase in the ground deformation; however, the increase in maximum bending moment is less than the increase in horizontal displacement or ground settlement. The main parameters responsible for higher deformation in soil from Bole area are relative low modulus of elasticity, E and angle of internal friction, Φ.

2. Effect of Change in Depth of Excavation

As depth of excavation is one of a key factor influencing performance of deep excavation, this section will concentrate on it. The output of this analysis is presented from Figure 4.11 – Figure 4.13 as follows.

For all the analyses conducted in this section of parametric study, the following quantities or features were kept the same:

- All the parameters for the soil types, i.e. expansive clay, red silty clay and sandy soil.
- Thickness of diaphragm wall (t = 0.6 m)
- Tieback anchor strut spacing (Ls = 2 m)
- Depth of embedment (Dem = 5 m)
- Construction sequences (as described at the end of section 4.2)

Figure 4.11 – Figure 4.13 show the effect of change in depth of excavation on the maximum horizontal displacement of the diaphragm wall, maximum ground settlement behind the diaphragm wall, maximum bending moment induced in the diaphragm wall due to deep excavations.

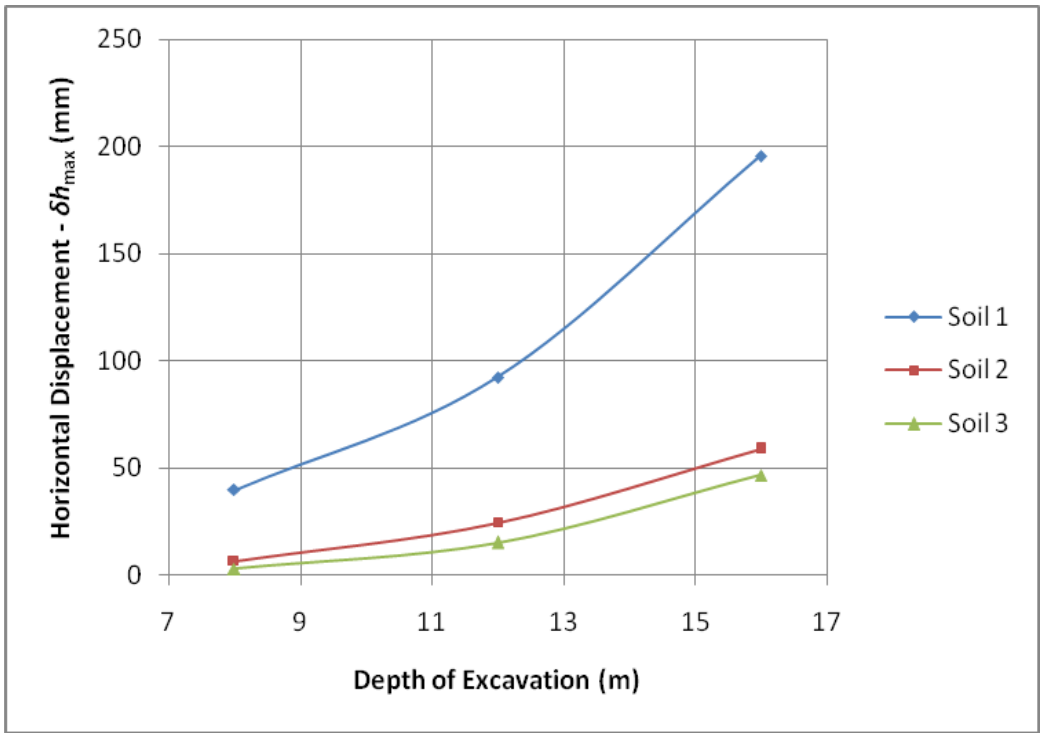

Figure 4. 11 Maximum horizontal displacement of the diaphragm wall with depth of excavation

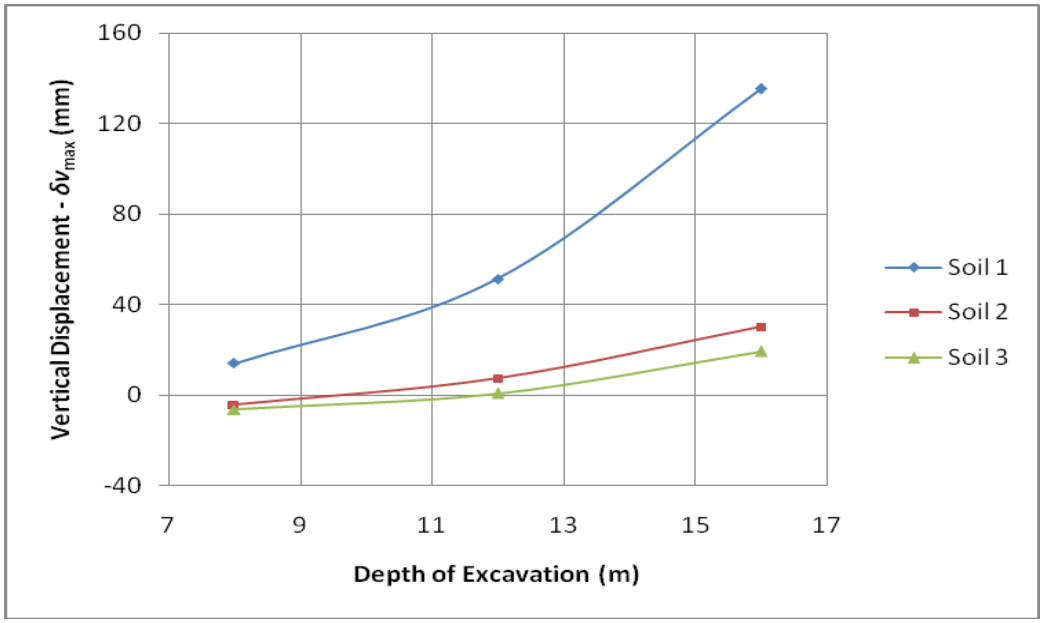

Figure 4. 12 Maximum ground settlement behind the diaphragm wall with depth of excavation

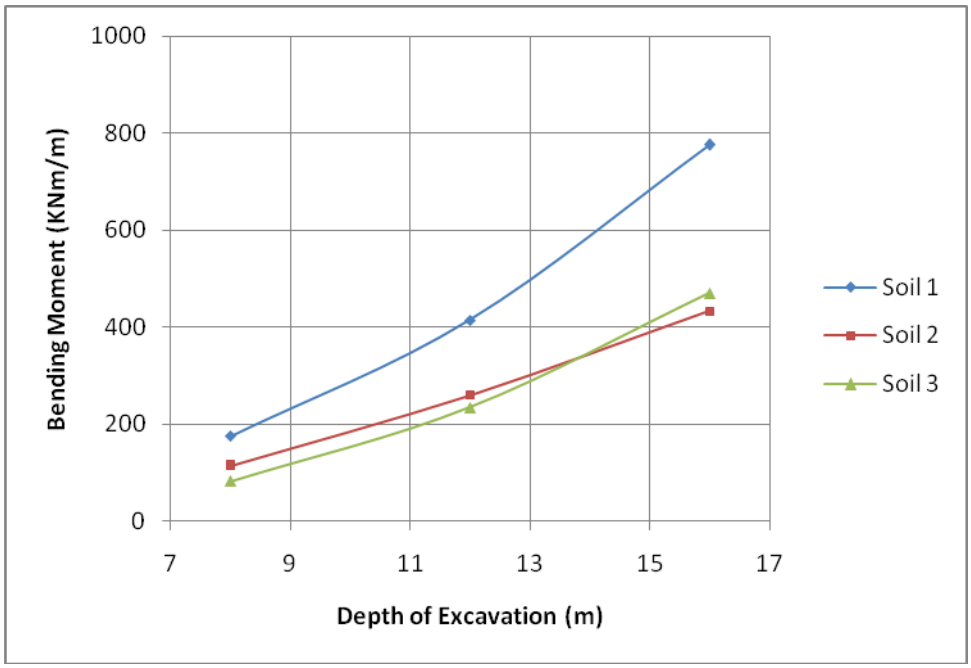

Figure 4. 13 Maximum bending moment in the diaphragm wall with depth of excavation

A radical change on the performance of deep excavation is observed for all soil types when the depth of excavation increases. For the change of 8m to 12m depth of excavation, it is shown that a 132%, 269%, and 428% change in maximum horizontal displacement from the original value for expansive clay, red silty clay and sand soils respectively. It has also shown that a 112%, 139%, and 210% change in maximum horizontal displacement from the original value for each soil respectively for a change in depth of excavation from 12m to 16m.

For the change of 8m to 12m depth of excavation, it is observed that 265%, 267%, and 112% change in vertical settlement from the original value for expansive clay, red silty clay and sand soils respectively. Vertical settlement increases with increasing of horizontal displacement.

The maximum bending moment in the diaphragm wall also increases in response to increase in depth of excavation in the same manner as the horizontal displacement. For the change of 8m to 12m depth of excavation, it is shown that a 137%, 128%, and 184% change in maximum bending moment from the original value for expansive clay, red silty clay and sand soils respectively. It has also shown that an 87%, 66%,

and 101% change in maximum bending moment from the original value for each soil respectively for a change in depth of excavation from 12m to 16m.

3. Effect of Change in Wall Embedment Depth

In this section, the effect of change in wall embedment depth on the performance of deep excavation supported by diaphragm wall will be studied into two cases. One is for stiffer wall, thickness = 0.9m, and the other is less stiff wall, thickness = 0.3m, for both 12m and 16m depth of deep excavation. The output from this analysis is given below.

For all the analyses conducted in this section of parametric study, the following quantities or features are kept the same:

- All the parameters for the soil types, i.e. expansive clay, red silty clay and sandy soil.
- Tieback anchor strut spacing (L_s = 3 m)
- Construction sequences (as described at the end of section 4.2)

Case 1: Stiffer wall, t = 0.9 m

Figure 4.14 – Figure 4.19 show the effect of change in depth of wall embedment on the maximum horizontal displacement of the diaphragm wall, maximum ground settlement behind the diaphragm wall, maximum bending moment induced in the diaphragm wall due to deep excavations for stiffer wall.

❖ *Depth of excavation, D_{ex} = 12 m*

In this section, the effect of change in depth of wall embedment on the performance of deep excavations supported by stiffer diaphragm wall for 12m depth of excavation is presented.

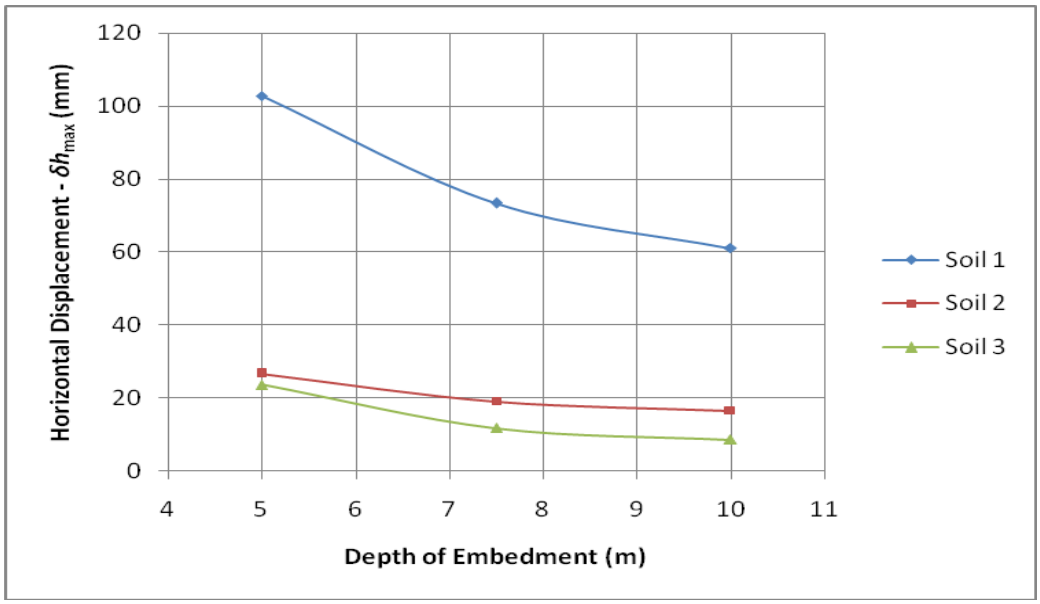

Figure 4. 14 Maximum horizontal displacement of the diaphragm wall with depth of embedment (D_{ex} = 12m, Case 1)

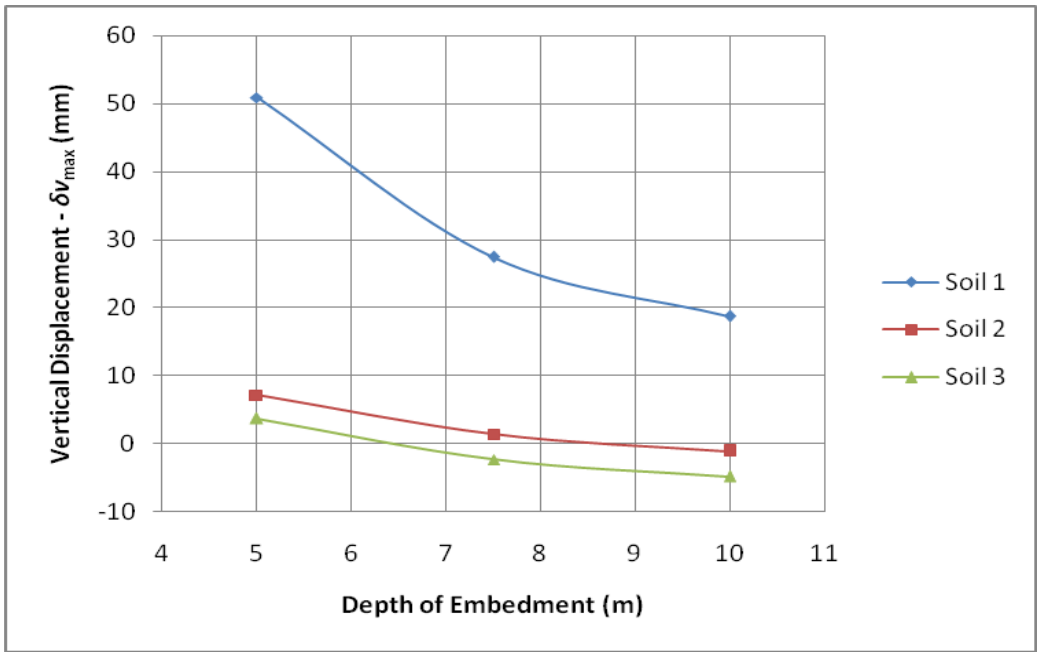

Figure 4. 15 Maximum ground settlement behind the diaphragm wall with depth of embedment (D_{ex} = 12m, Case 1)

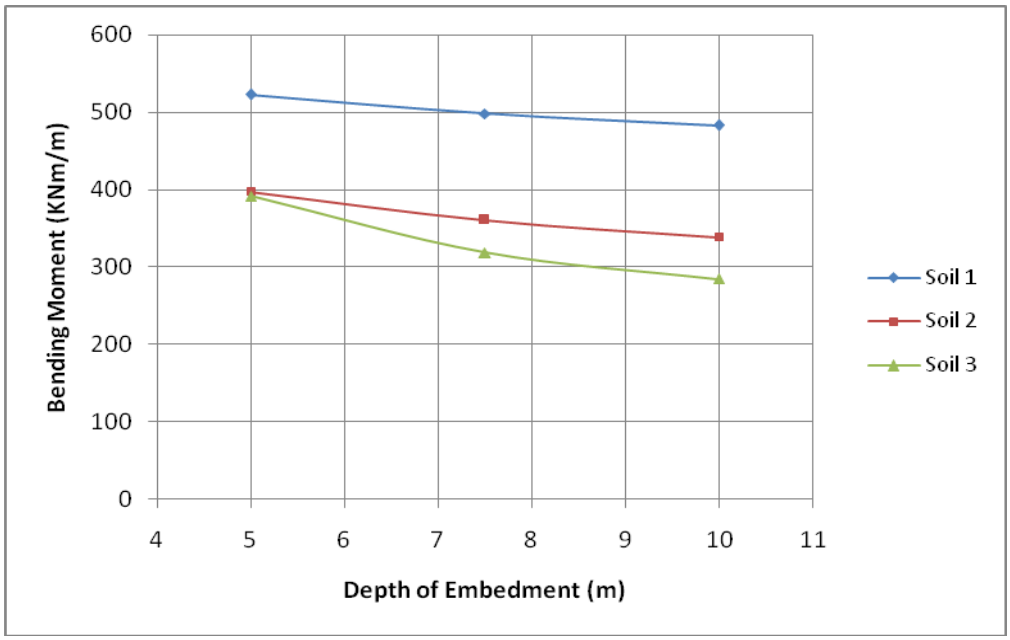

Figure 4. 16 Maximum bending moment in the diaphragm wall with depth of embedment (D_{ex} = 12m, Case 1)

- ***Depth of excavation, D_{ex} = 16 m***

In this section, the effect of change in depth of wall embedment on the performance of deep excavations supported by stiffer diaphragm wall for 16m depth of excavation is presented.

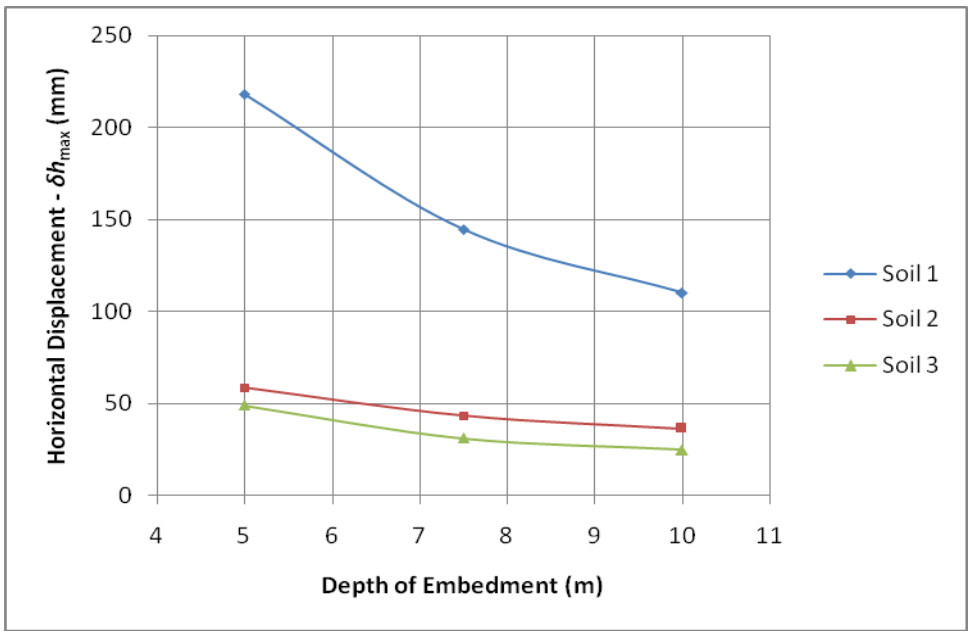

Figure 4. 17 Maximum horizontal displacement of the diaphragm wall with depth of embedment (D_{ex} = 16m, Case 1)

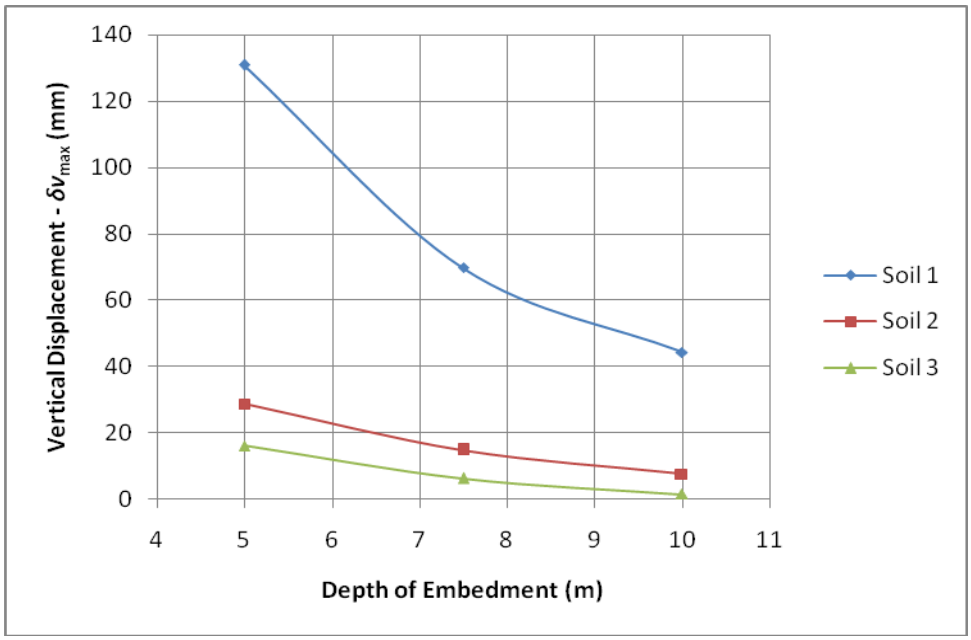

Figure 4. 18 Maximum ground settlement behind the diaphragm wall with depth of embedment (D_{ex} = 16m, Case 1)

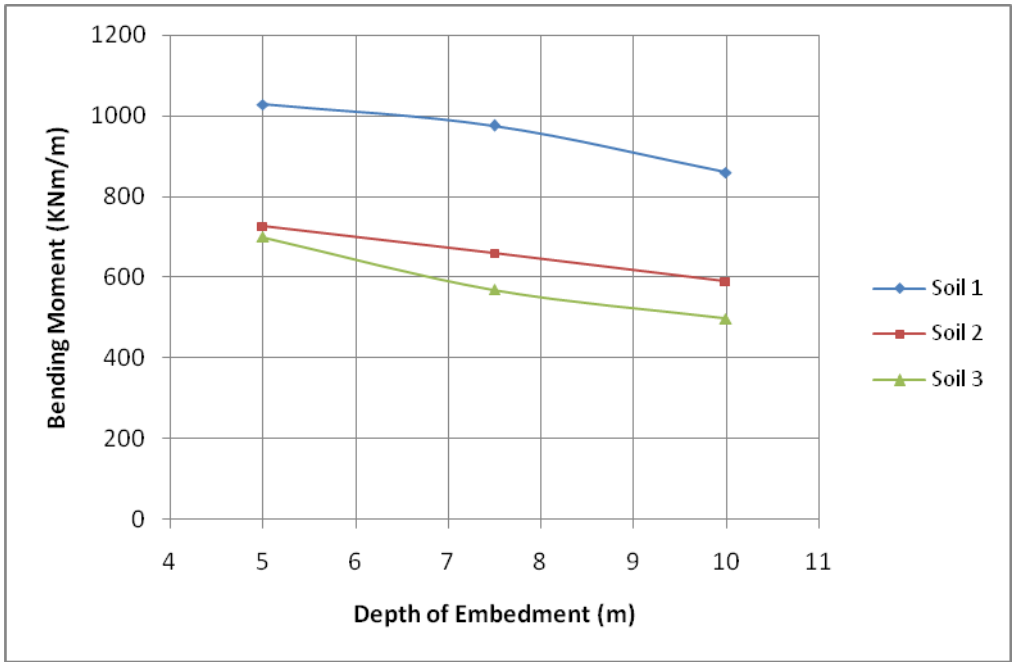

Figure 4. 19 Maximum bending moment in the diaphragm wall with depth of embedment (D_{ex} = 16m, Case 1)

A significant decrease in the ground deformation around the deep excavation is observed for all soil types when the depth of wall embedment increases. For the change of 5m to 7.5m depth of wall embedment, it is shown that a -29%, -28%, and -50% change in maximum horizontal displacement from the original value for 12m

deep excavation and -34%, -26% and -37% for 16m deep excavation for expansive clay, red silty clay and sand soils respectively. It has also shown that a -17%, -14%, and -27% change in maximum horizontal displacement from the original value for 12m deep excavation and -24%, -16% and -20% for 16m deep excavation for each soil respectively for a change in depth of wall embedment from 7.5m to 10m.

For the change of 5m to 7.5m depth of wall embedment, it is shown that a -46%, -81%, and -163% change in maximum vertical settlement from the original value for 12m deep excavation and -47%, -49% and -61% for 16m deep excavation for expansive clay, red silty clay and sand soils respectively. It has also shown that a -32%, -182%, and -104% change in maximum vertical settlement from the original value for 12m deep excavation and -36%, -48% and -76% for 16m deep excavation for each soil respectively for a change in depth of wall embedment from 7.5m to 10m. The maximum bending moment in the diaphragm wall also decreases in response to increase in depth of wall embedment in the same manner as the horizontal displacement. For the change of 5m to 7.5m depth of wall embedment, it is shown that a -5%, -9%, and -19% change in maximum bending moment from the original value for 12m deep excavation and -5%, -9% and -19% for 16m deep excavation for expansive clay, red silty clay and sand soils respectively. It has also shown that an -3%, -6%, and -11% change in maximum bending moment from the original value for 12m deep excavation and -12%, -11% and -13% for 16m deep excavation for each soil respectively for a change in depth of excavation from 7.5m to 10m.

- ***Case 2: Less stiffer wall, t = 0.3 m***

Figure 4.20 – Figure 4.25 show the effect of change in depth of wall embedment on the maximum horizontal displacement of the diaphragm wall, maximum ground settlement behind the diaphragm wall, maximum bending moment induced in the diaphragm wall due to deep excavations for less stiffer walls.

❖ ***Depth of excavation, D_{ex} = 12 m***

In this section, the effect of change in depth of wall embedment on the performance of deep excavations supported by less stiff diaphragm wall for 12m depth of excavation is presented.

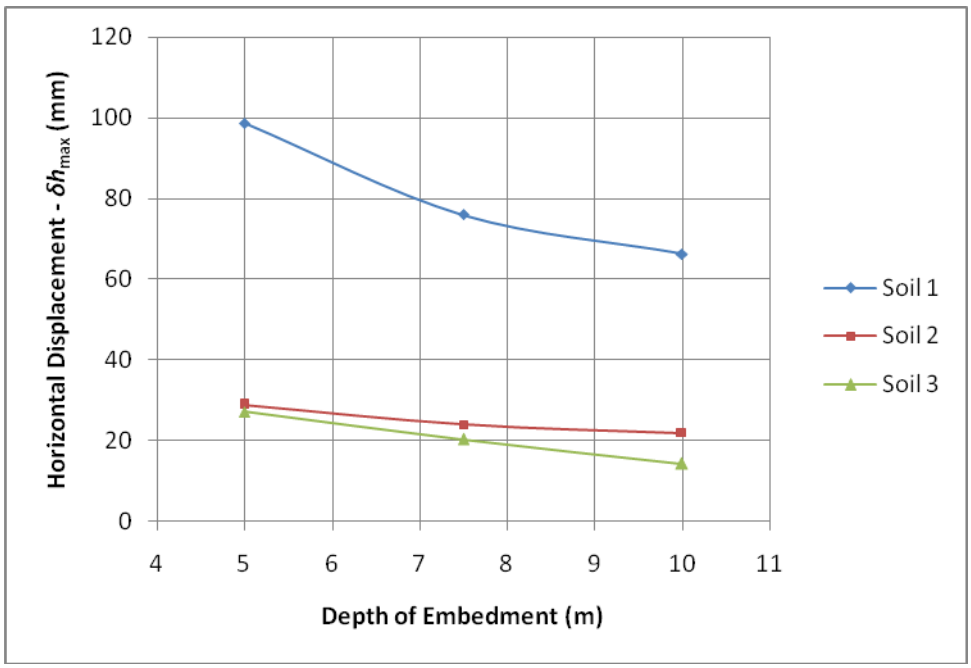

Figure 4. 20 Maximum horizontal displacement of the diaphragm wall with depth of embedment (D_{ex} = 12m, Case 2)

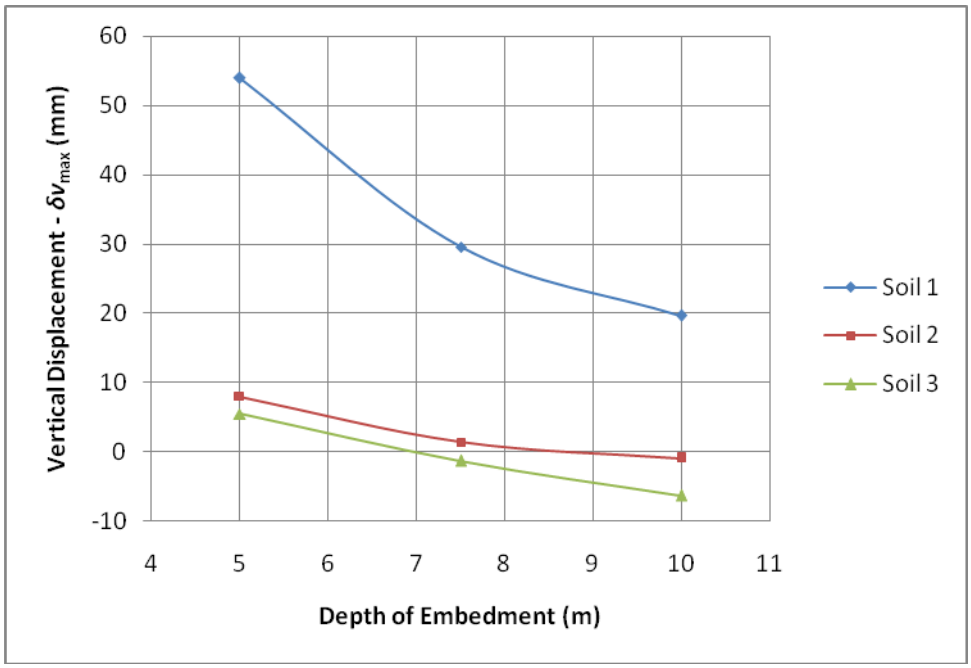

Figure 4. 21 Maximum ground settlement behind the diaphragm wall with depth of embedment (D_{ex} = 12m, Case 2)

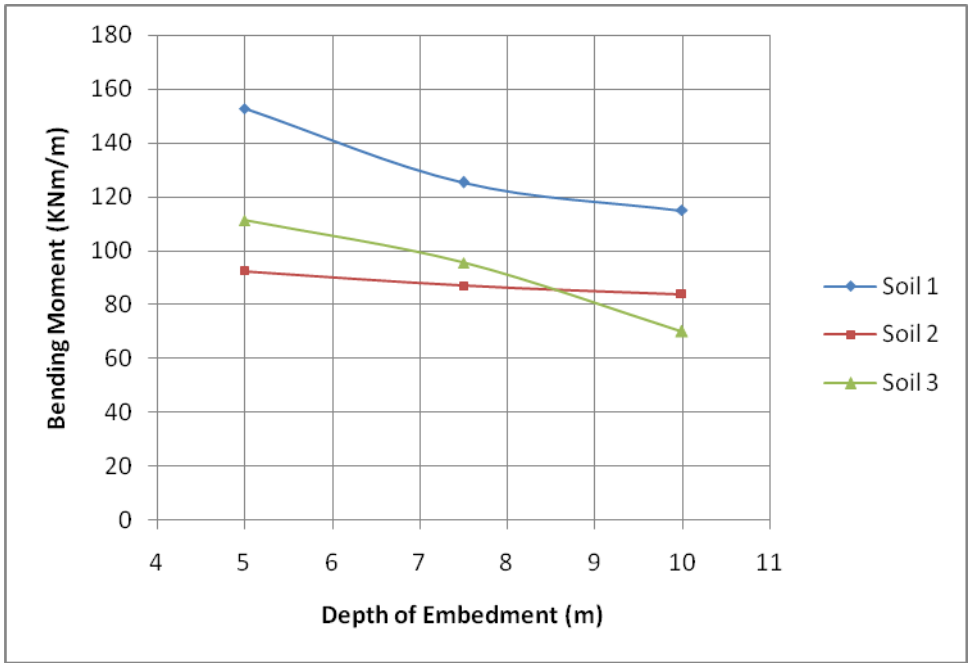

Figure 4. 22 Maximum bending moment in the diaphragm wall with depth of embedment (D_{ex} = 12m, Case 2)

❖ ***Depth of excavation, D_{ex} = 16 m***

In this section, the effect of change in depth of wall embedment on the performance of deep excavations supported by less stiff diaphragm wall for 16m depth of excavation is presented.

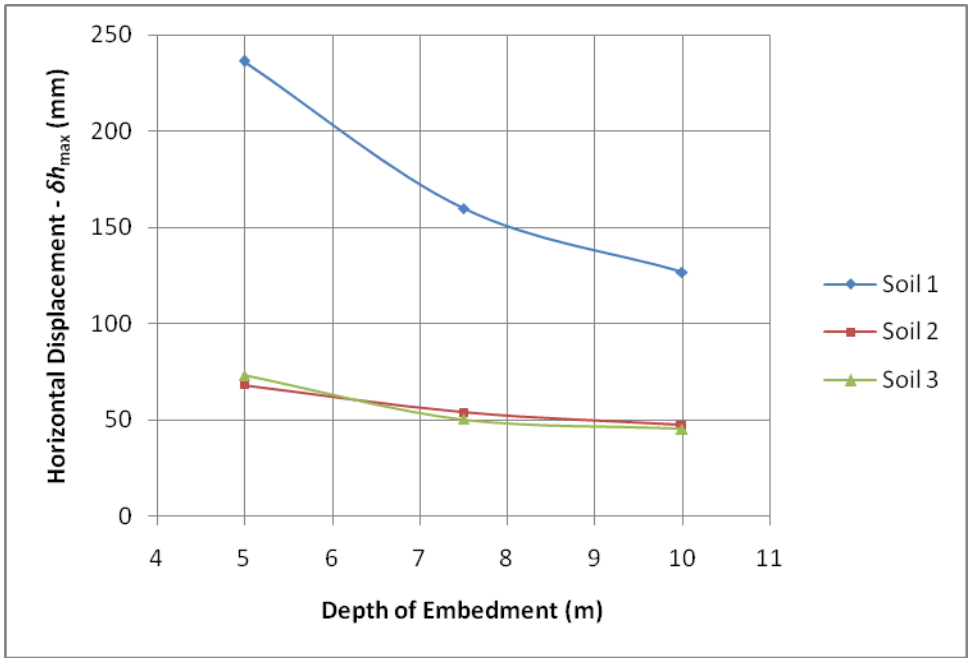

Figure 4. 23 Maximum horizontal displacement of the diaphragm wall with depth of embedment (D_{ex} = 16m, Case 2)

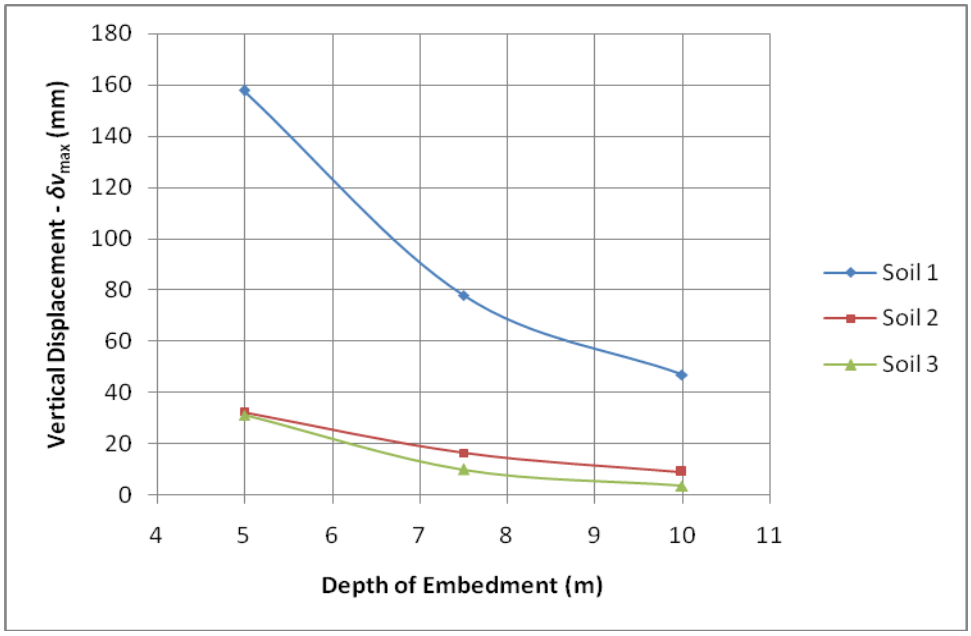

Figure 4. 24 Maximum ground settlement behind the diaphragm wall with depth of embedment (D_{ex} = 16m, Case 2)

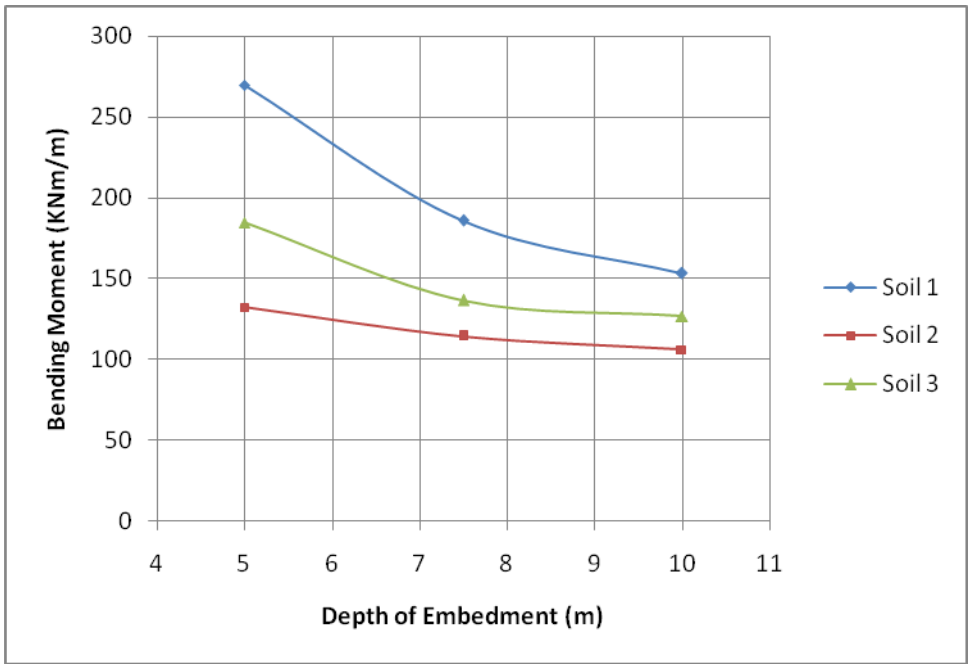

Figure 4. 25 Maximum bending moment in the diaphragm wall with depth of embedment (D_{ex} = 16m, Case 2)

A significant decrease in the ground deformation around the deep excavation is observed for all soil types when the depth of wall embedment increases. For the change of 5m to 7.5m depth of wall embedment, it is shown that a -23%, -17%, and -25% change in maximum horizontal displacement from the original value for 12m deep excavation and -32%, -21% and -32% for 16m deep excavation for expansive clay, red silty clay and sand soils respectively. It has also shown that a -13%, -9%, and -30% change in maximum horizontal displacement from the original value for 12m deep excavation and -21%, -12% and -10% for 16m deep excavation for each soil respectively for a change in depth of wall embedment from 7.5m to 10m.

For the change of 5m to 7.5m depth of wall embedment, it is shown that a -45%, -82%, and -124% change in maximum vertical settlement from the original value for 12m deep excavation and -51%, -49% and -68% for 16m deep excavation for expansive clay, red silty clay and sand soils respectively. It has also shown that a -34%, -167%, and -379% change in maximum vertical settlement from the original value for 12m deep excavation and -40%, -46% and -64% for 16m deep excavation for each soil respectively for a change in depth of wall embedment from 7.5m to 10m.

The maximum bending moment in the diaphragm wall also decreases in response to increase in depth of wall embedment in the same manner as the horizontal displacement. For the change of 5m to 7.5m depth of wall embedment, it is shown that a -18%, -6%, and -14% change in maximum bending moment from the original value for 12m deep excavation and -31%, -14% and -26% for 16m deep excavation for expansive clay, red silty clay and sand soils respectively. It has also shown that an -8%, -4%, and -27% change in maximum bending moment from the original value for 12m deep excavation and -18%, -7% and -7% for 16m deep excavation for each soil respectively for a change in depth of excavation from 7.5m to 10m.

4. Effect of Change in Stiffness of the Diaphragm Wall

In this part of the analysis, the paper concentrates on how change in stiffness of diaphragm wall affects the performance of deep excavation. The output from this analysis is presented below.

Table 4.3 gives the range of values for the thickness of diaphragm wall used in the parametric study. Since the young's modulus of the diaphragm wall was kept unchanged for all the analyses, a change in thickness of the diaphragm wall represents a change in both the bending stiffness and the axial stiffness of the diaphragm wall.

For all the analyses conducted in this section of parametric study, the following quantities or features are kept the same:

- All the parameters for the soil types, i.e. expansive clay, red silty clay and sandy soil.
- Depth of excavation (H = 16 m)
- Tieback anchor strut spacing (L_s = 3 m)
- Depth of embedment (D_{em} = 16 m)
- Construction sequences (as described at the end of section 4.2)

Figure 4.26 – Figure 4.28 show the effect of change in thickness of the diaphragm wall on the maximum horizontal displacement of the diaphragm wall, maximum ground settlement behind the diaphragm wall and the maximum bending moment induced in the diaphragm wall due to deep excavations.

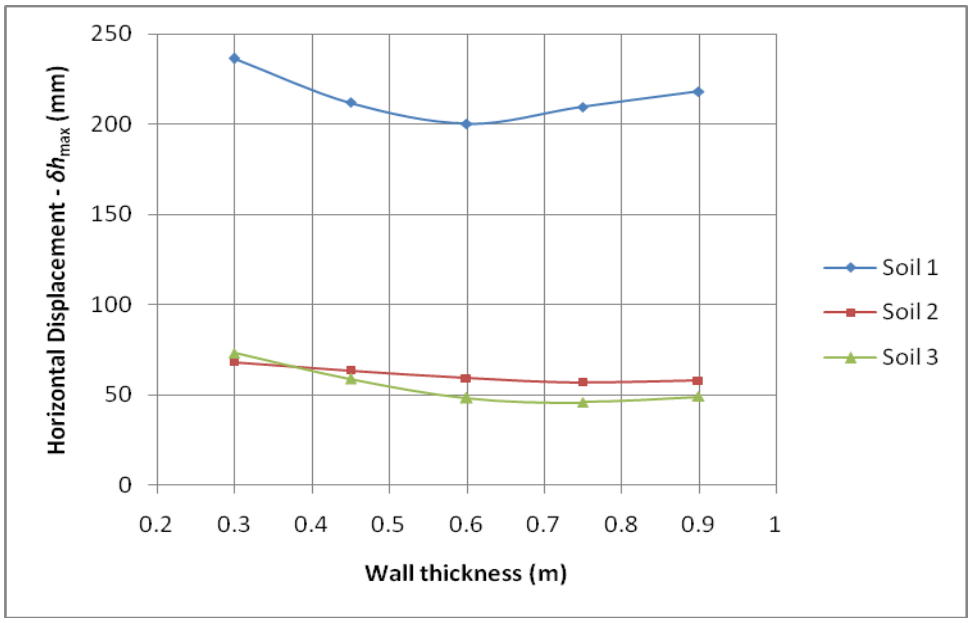

Figure 4. 26 Maximum horizontal displacement of the diaphragm wall with thickness of wall

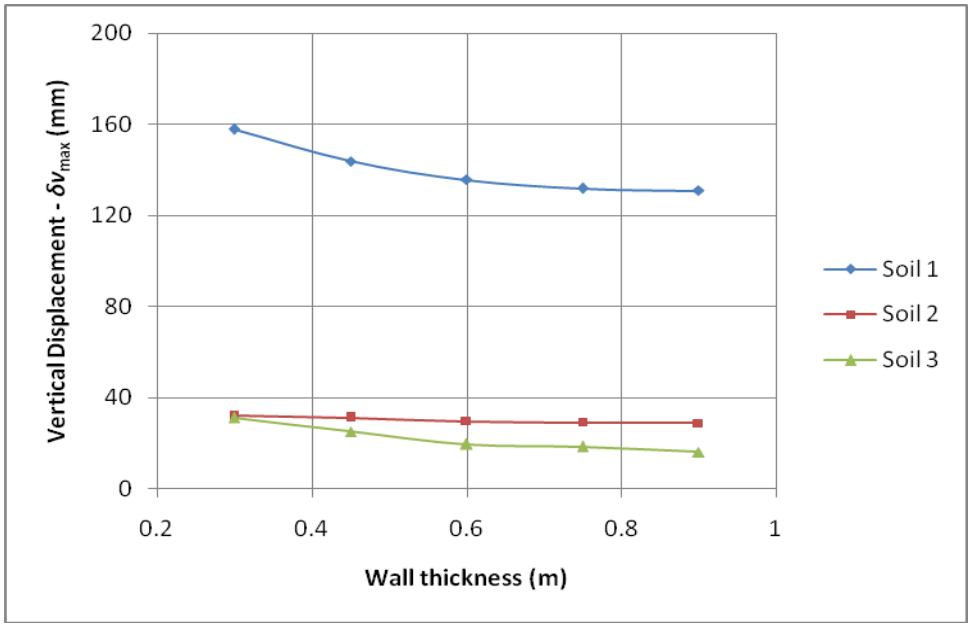

Figure 4. 27 Maximum ground settlement behind the diaphragm wall with thickness of wall

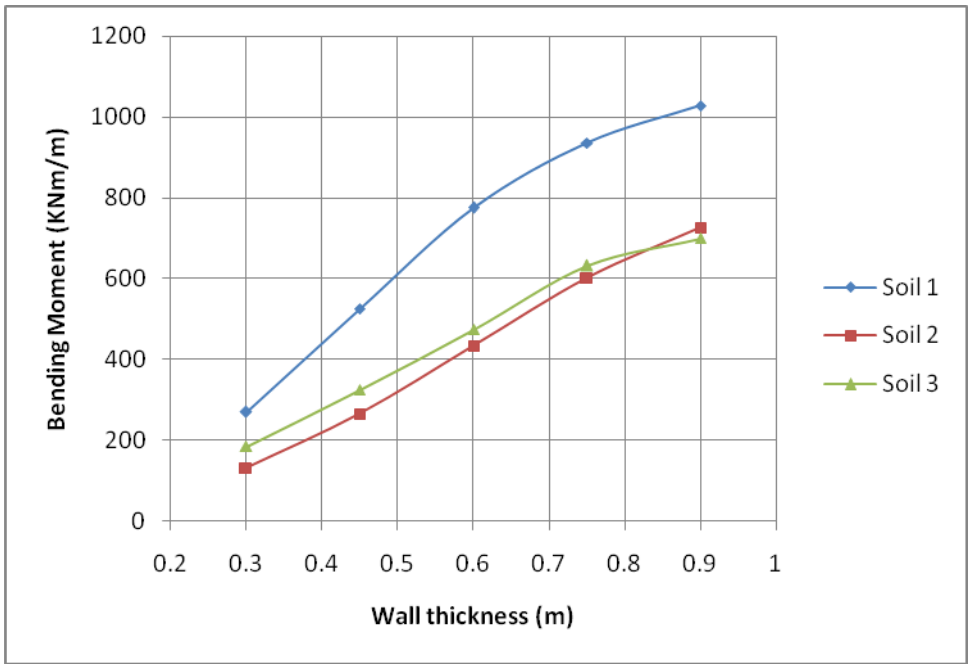

Figure 4. 28 Maximum bending moment in the diaphragm wall with thickness of wall

It can be seen from figures that the effect of change in thickness in diaphragm wall is not as prominent as the change in soil type, depth of excavation and depth wall embedment. It is interesting to note that the maximum bending moment in the diaphragm wall increases but the horizontal displacement of the diaphragm wall decreases when the thickness of diaphragm wall is increased. Clearly, a thicker diaphragm wall is able to resist horizontal deformation better but at the expense of induced greater bending moment. In other words, a stiffer diaphragm wall also needs greater bending strength. It is also worth noting that the horizontal displacement of the diaphragm wall does not reduce appreciably but the maximum bending moment continues to increase when the thickness of the diaphragm wall is increased. This implies that it is not useful to increase the stiffness of the diaphragm wall beyond a certain maximum value.

The horizontal displacement of the diaphragm wall and the ground settlement behind the diaphragm wall show contrasting trends with the change in thickness of the diaphragm wall. The horizontal displacement of the diaphragm wall decrease but the ground settlement behind the diaphragm wall increase as the thickness of the diaphragm wall is increased. In case of stiffer diaphragm wall, the ground is

prevented from spreading horizontally. The deformation of the ground, therefore, occurs mainly in the vertical direction, resulting in increase in ground settlement behind the diaphragm wall. In other words, the consolidation of the ground behind a stiff diaphragm wall is mainly one dimensional. For a relatively flexible diaphragm wall (smaller thickness), there is increase in horizontal displacement and decrease in ground settlement. In appendix 2, additional figures that show effect of change in diaphragm wall on the performance of deep excavation is presented.

5. Effect of Change in Strut Spacing

In this part of analysis, the effect of change in strut spacing on the performance of deep excavation is considered.

For all the analyses conducted in this section of parametric study, the following quantities or features were kept the same:

- All the parameters for the soil types, i.e. expansive clay, red silty clay and sandy soil.
- Thickness of diaphragm wall (t = 0.3 m)
- Depth of excavation (H = 16 m)
- Depth of embedment (D_{em} = 5 m)
- Construction sequences (as described at the end of section 4.2)

Figure 4.29 - Figure 4.31 show the effect of change in strut spacing on the maximum horizontal displacement of the diaphragm wall, maximum ground settlement behind the diaphragm wall and the maximum bending moment induced in the diaphragm wall due to deep excavations.

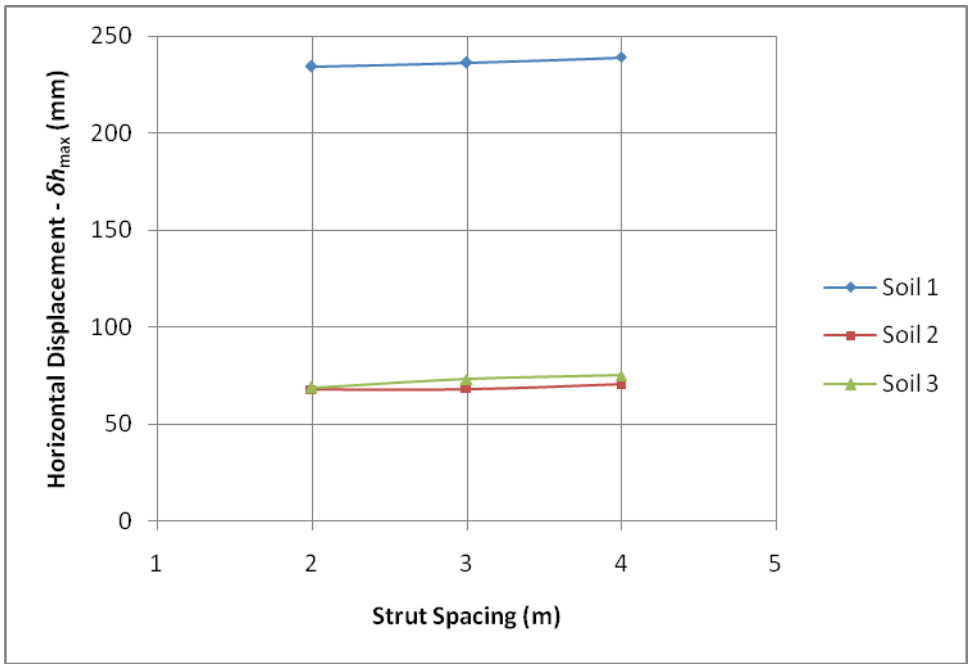

Figure 4. 29 Maximum horizontal displacement of the diaphragm wall with strut spacing

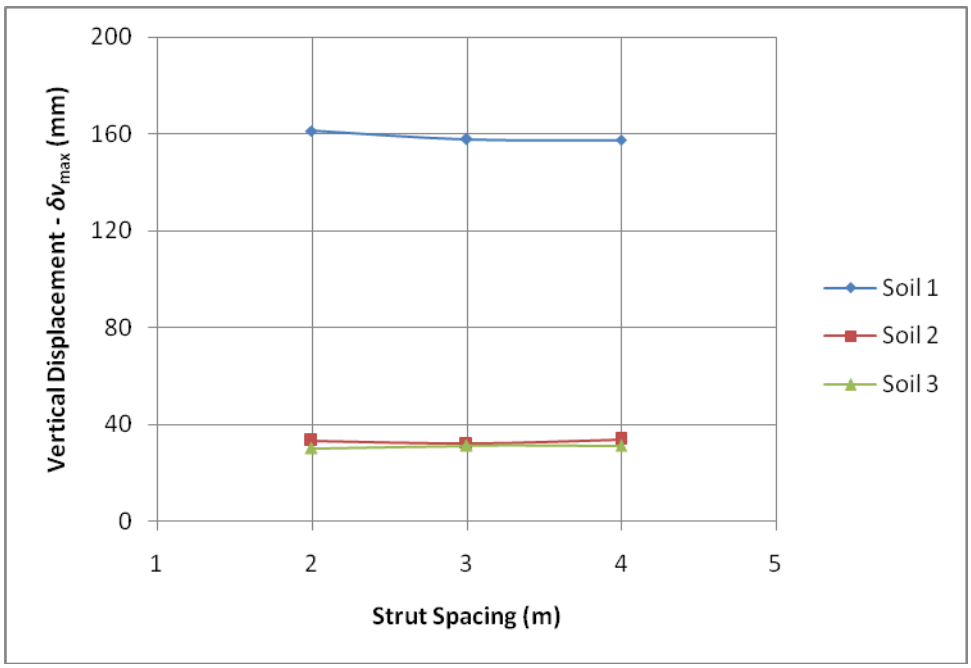

Figure 4. 30 Maximum ground settlement behind the diaphragm wall with strut spacing

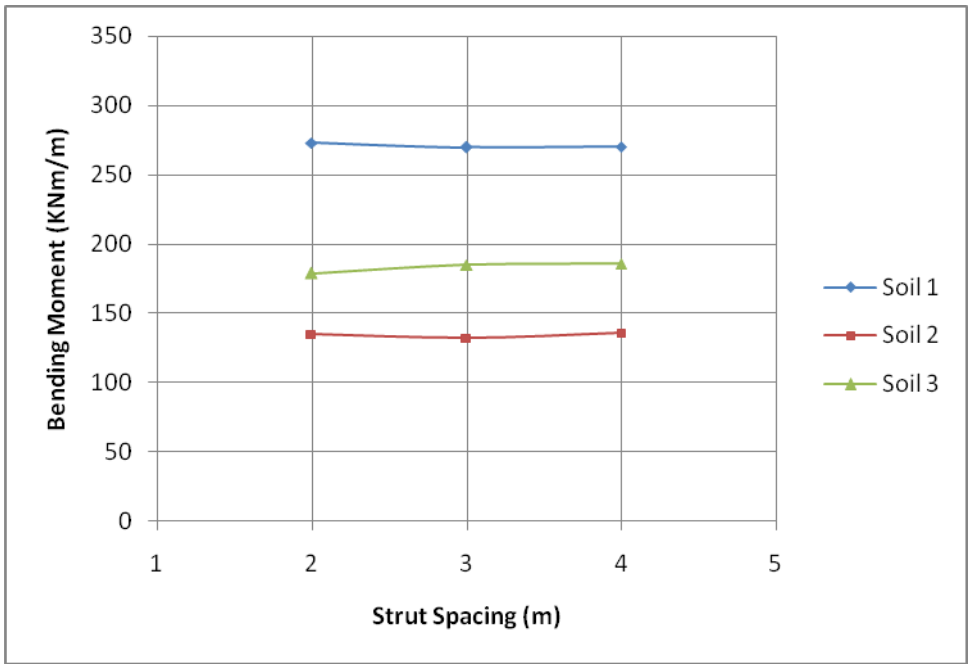

Figure 4. 31 Maximum bending moment in the diaphragm wall with strut spacing

A large ground deformation around the deep excavation is observed for expansive clay soil and a collapse of deep excavation after excavating 8m and 12m for red silty clay and sand respectively when tie back strut is not installed for less stiff, 0.3m thick, diaphragm wall.

For the change of no strut case to applying tie back strut at an interval of 4m, it is shown that a decrease in horizontal displacement from 410.08mm to 239.13mm, i.e. -417%, for expansive clay and from 70.36mm and 75.04mm to collapse of excavation for red silty clay and sand soil respectively. It is also worth noting that the horizontal displacement of the diaphragm wall does not reduce appreciably when the strut spacing change from 4m to 2m but applying struts change the performance of deep excavation radically.

This implies that it is not useful to decrease strut spacing beyond a certain value. In appendix 2, additional figures that show effect of change in tie back struts on the performance of deep excavation is presented.

5. Conclusion

Based on the study, the following conclusions are made:

1. The ground deformations around a deep excavation are significantly influenced by the type of soil. It is important, therefore, to obtain accurate estimates of soil parameters in order to obtain accurate estimates of ground deformation. Expansive soil shows more ground deformation than non-expansive soils.

2. The performance of deep excavation is dramatically affected by depth of excavation. Soil from Bole area, Arada area and the sandy soil show 122%, 204% and 319% increase in ground deformation respectively for 4m increase in depth of excavation. It is, therefore, important that care should be taken to existing structures nearby deep excavation before excavating to any appreciable depth.

3. Increasing wall embedment depth decreases ground deformations resulting from deep excavation by decreasing the span moment while increasing the fixity at the bottom. Soil from Bole area, Arada area and the sandy soil show 24%, 18% and 29% decrease in ground deformation respectively for 2.5m increase in depth of embedment.

4. A stiff diaphragm wall is required for controlling horizontal ground movements resulting from deep excavation. However, when choosing a support system for the deep excavation, it should be kept in mind that even the stiffest of diaphragm wall will result in some horizontal displacement of the ground. Therefore, selecting a stiff diaphragm wall alone does not eliminate all the horizontal ground movements.

5. Although the use of a stiff diaphragm wall results in a reduction in horizontal movement of the ground, it is virtually ineffective in reducing the settlement of the ground behind the diaphragm wall. In fact, it appears to increase the settlements. If the major concern is to limit the ground settlement behind the diaphragm wall, it might be better to use a slightly flexible diaphragm wall system.

6. Applying tie-back struts significantly reduces ground deformation around deep excavation, however decreasing strut spacing beyond some limit do not reduce ground deformation appreciably.

7. Using slightly flexible wall with tie-back supports is better in reducing ground deformation around deep excavation other than using stiffer diaphragm wall without tie-back supports.

6. Bibliography

1. Balasubramaniam, A., Bergado, D., & Sutabutr, T. (1994). Deformation analysis of deep excavation in Bangkok subsoils. *Proceedings of the Thirteen International Conference on Soil Mechanics and Foundation Engineering, 13(2)*, pp. 909-914.

2. Briaud, J., & Kim, B. (1998). Beam Column Method for Tieback Walls. (ASCE, Ed.) *Journal of Geotechnical and Geoenvironmental Engineering , 124* (1), 67–79.

3. Brinkgreve, R., Broere, W., & Waterman, D. (2004). *PLAXIS 2-D Professional Version 8.0 - User's Manual.* PLAXIS b.v., The Netherlands.

4. Clough, G., & O'Rourke, T. (1990). Construction induced movements of in-situ walls. *Proceeding of ASCE Special Conference on Design and Performance of Earth Retaining Structures,* (pp. 439-470). Cornell University, New York.

5. Clough, G., & Tsui, Y. (1974). Performance of Tied-Back Walls in Clay. (ASCE, Ed.) *Journal of Geotechnical Engineering Division , 10* (12), 1259-1273.

6. Garvin, R., & Boward, J. (1992). Using slurry walls to protect a historic building: a case study. *Slurry walls: Design, Construction, and Quality Control ASTM Special Topic Publication 1129* , 117-127.

7. Giffored, D., & Wheeler, J. (1992). Concrete slurry wall for Temporary and Permanent Foundation Wall at Gallery at Harborplace – Baltimore Maryland. *Slurry walls: Design, Construction, and Quality Control ASTM Special Topic Publication 1129* , 151-163.

8. Goh, A. (1990). Assessment of basal stability for braced excavation system using finite element method. *Computer and Geotechnics , 10* (4), 325-338.

9. Hashash, M. (1992). *Analysis of Deep Excavation in Clay.* MIT, Dept. of Civil Engineering. Cambridge, MA.

10. Hoe, N. H. (2007). *Numerical Modeling of Diaphragm Wall in Kuala Lumpur Limestone Formation.* MSc Thesis, Universiti Teknologi Malaysia, Civil Engineering, Kuala Lumpur.

11. Hsieh, P., & Ou, C. (1997). Use of the modified hyperbolic model in excavation analysis under undrained conditions. *Geotechnical Engineering Journal , 28* (2), 123-150.

12. Konstantakos, D., Whittle, A., Regalado, C., & Scharner, B. (2004). Control of ground movements for a multi-level-anchored, diaphragm wall during excavation. *Proceedings: Fifth International Conference on Case Histories in Geotechnical Engineering.* New York, NY.

13. Lings, M., Nash, D., Ng, C., & Boyce, M. (1991). Observed behavior of deep excavation in Gault Clay. A preliminary appraisal. *Proceedings of the Tenth European Conference on Soil Mechanics and Foundation Engineering, 10(2),* pp. 467-470.

14. Matlock, H., Bogard, D., & Lam, I. (1981). *BMCOL76: A Computer Program for the Analysis of Beam-columns under Static Axial and Lateral Loading.* University of Texas at Austin. Long Beach, CA: Ertec, Inc.

15. Ou, C., Hsieh, P., & Chion, D. (1993). Characteristics of ground surface settlement during excavation. *Canadian Geotechnical Journal , 30* (5), 758-767.

16. Peck, R. (1969). Deep excavations and tunneling in soft ground. *Proceedings of the 7th International Conference on Soil Mechanics*, (pp. 225-290).

17. Powrie, W., & Li, E. (1991). Finite element analysis of an in-situ wall propped at formation level. *Geotechnique , 41* (4), 499-514.

18. Raithel, M., Gebreselassie, B., Müller, S., & Pahl, F. (2005). Design and Numerical Investigations of a Deep Excavation for a Tunnel Entrance Pit. *16th International Conference on Soil Mechanics and Geotechnical Engineering.* Osaka, Japan.

19. Schoenwalf, D., Whiteman, R., Abbott, E., & Becker, J. (1992). Post office garage project – A case history of instrumented slurry wall performance. *Slurry wall: Design, Construction, and Quality Control ASTM STP 1129* , 361-376.

20. Teferra, A. (1992). *Foundation Engineering.* Addis Ababa: Addis Ababa University Press.

21. Teferra, A., & Leikun, M. (1999). *Soil Mechanics.* Addis Ababa: Addis Ababa University Press.

22. Terzaghi, C. (1943). *Theoritical Soil Mechanics.* John Willy and Sons.

23. Winter, E., Skep, N., & Tallard, G. (1992). Slurry wall performance Adjacent to Historic Church. *Slurry wall: Design, Construction, and Quality Control, ASTM STP 1129* , 164-171.

24. Wong, I., Poh, T., & Chuah, H. (1996). Analysis of case histories from construction of the Central Expressway in Singapore. *Canadian Geotechnical Journal , 33* (5), 732-746.

7. Appendices

Appendix 1 Soil Models

A.1.1 Mohr-Coulomb Model

The Mohr-Coulomb model coded in Plaxis version 8.0 is based on an elastic perfectly-plastic mode which is constitutive law with a fixed yield surface, i.e. a yield surface that is fully defined by model parameters and not affected by (plastic) straining. For stress state represented by points within the yield surface, the behavior is purely elastic and all strains are reversible.

There is no hardening or softening law required for the Mohr-Coulomb model as it is assumed to be perfectly plastic. A plastic yield function, *f*, is introduced as a function of stress and strain that can often be presented as a surface in principal stress space as shown in Figure below.

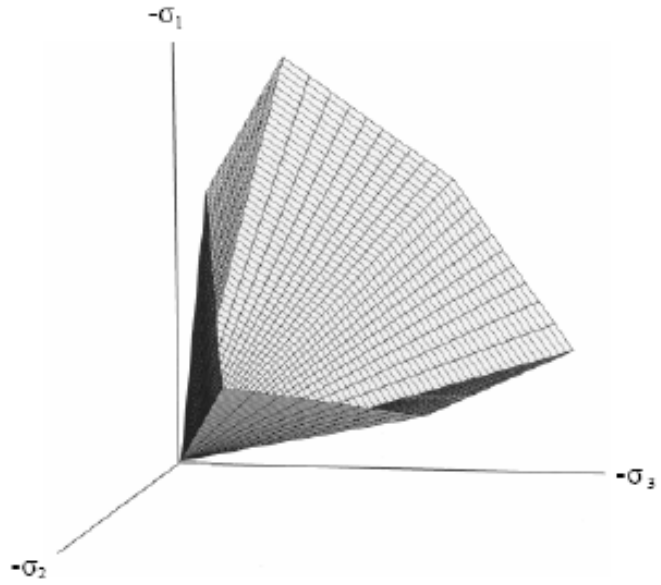

Figure A.1. 1 The Mohr-Coulomb yield surface in principal stress space (c = 0)

The strains and strain rates are decomposed into an elastic part and a plastic part in theory of elastoplasticity:

$$\underline{\varepsilon} = \underline{\varepsilon}^{e} + \underline{\varepsilon}^{p} \qquad \dot{\underline{\varepsilon}} = \dot{\underline{\varepsilon}}^{e} + \dot{\underline{\varepsilon}}^{p} \quad \ldots\ldots\ldots\ldots\ldots\ldots \qquad (A.1.1.1)$$

The Mohr-Coulomb model requires five parameters. Parameters related to elastic behavior are E and ν, whereas parameters related to plastic behavior are c and φ, and ψ, angle of dilatancy. These parameters with their standard units are listed below:

Table A.1. 1 Mohr Coulomb parameters with their standard units

PARAMETER		UNIT
E	Young's Modulus	[kN/m^2]
ν	Poisson's ratio	[-]
Φ	Friction angle	[°]
C	Cohesion	[kN/m^2]
ψ	Dilatancy angle	[°]

PLAXIS uses the Young's modulus as the basic stiffness modulus in the Mohr-Coulomb model. E_{ur} which tend to increase with the confining pressure is needed for unloading modeling such as in the case of excavations. This behavior in turn results in the deep soil layers tend to have greater stiffness than shallow layers. Hence, when using a constant stiffness modulus to represent soil behavior, a value that is consistent with the stress level and the stress path development should be chosen.

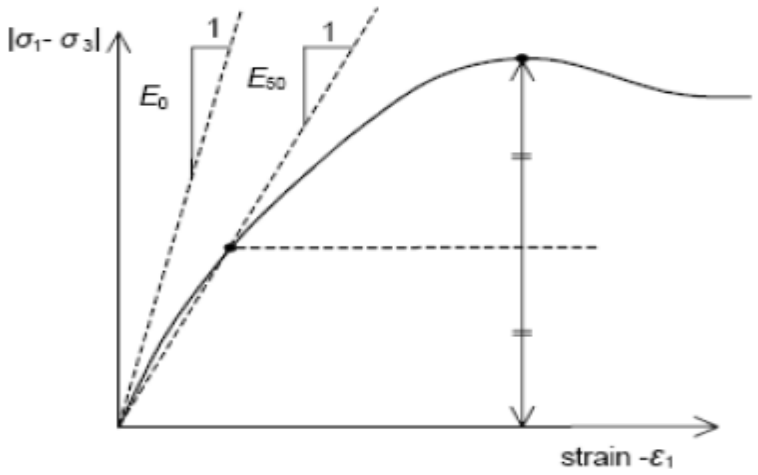

Figure A.1. 2 Definition of E_0 and E_{50} for standard drained triaxial test results

Although standard drained triaxial tests may yield a significant rate of volume decrease at the very beginning of axial loading, but PLAXIS recommended the use of a high value initial value of Poisson's ratio (ν_0) when using the Mohr-Coulomb model. In general, for unloading conditions, however, PLAXIS suggested to use values in the range between 0.15 and 0.25.

PLAXIS can handle cohesionless sands (c = 0), but some options will not perform well. To avoid complications, non-experienced users are advised to enter at least a small value (use c > 0.2 kPa). The friction angle, Φ, is entered in degrees. High friction angles, as sometimes obtained for dense sands, will substantially increase plastic computational effort.

PLAXIS suggested using this model as first analysis of the problem considered by approximating a constant average stiffness for each layer of soil to obtain a first impression of deformations.

A.1.2 Soil Hardening Model

Soil response to loading is highly nonlinear and highly dependent on the magnitude of stress. This behavior has a significant influence on the stresses and displacements developed within the reinforced structure. Nonlinear elastic (hyperbolic) model can be expected to provide acceptable prediction of the behavior of soil at relatively low shear stress levels. The soil stiffness modeled in this manner increases with increasing confining pressure and decreases with increasing stress level as shown in Figure below. A very low stiffness is assigned to elements with stress condition at failure.

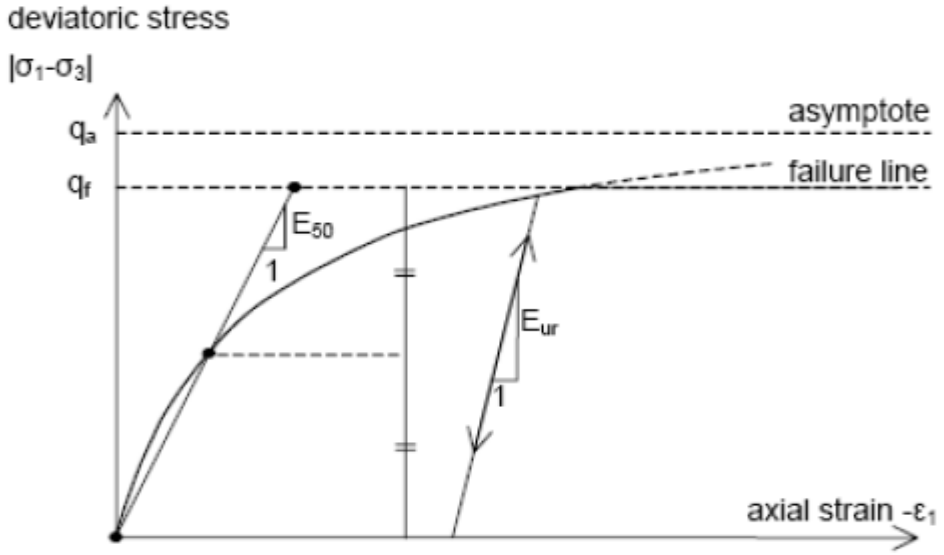

Figure A.1. 3 Hyperbolic stress-strain relation in primary loading for a standard drained triaxial test

The hyperbolic model is relatively simple, well validated and reliable to represent soil behavior.

Similar to the Mohr-Coulomb model, limiting states of stress in the HS model are described in terms of effective stress parameters, i.e. the friction angle, φ, the cohesion, c, and the dilatancy angle, ψ, or in terms of undrained shear strength of soil, S_u, by specifying zero values for φ and ψ and setting c equal to S_u. The soil stiffness, however, is described much more accurately in the HS model by using three different input stiffness values – the triaxial loading stiffness, E_{50}^{ref}, the triaxial unloading/reloading stiffness, E_{ur}^{ref}, and the odometer loading stiffness, E_{oed}^{ref}. Unlike the Mohr-Coulomb model, the HS model also accounts for stress-dependency of soil stiffness, i.e. the elastic stiffness values increase with confining stress in the HS model.

The HS model allows for plastic volume change (volumetric hardening) as well as plastic shearing due to deviatoric loading (shear hardening). Compared with the Mohr-Coulomb model, the unloading behavior of the soil is better taken into account in the HS model. The HS model may be used to calculate realistic pressure

distribution below raft foundations and behind soil retaining structures (Brinkgreve et al. 2004).

The HS model does not account for softening in which the modulus decreases with strain whereas strain hardening model for which the modulus increase with strain. The use of the HS model generally results in longer calculation time than the Mohr-Coulomb model since the material stiffness matrix is formed and decomposed in each calculation step.

Some parameters required in the strain hardening model are the (Effective) cohesion [c, kN/m2], (effective) angle of internal friction [Φ, °] and the angle of dilatancy [ψ, °]. The basic parameters for soil stiffness in soil hardening model are the secant stiffness in standard drained triaxial test [E_{ref}^{50}, KN/m^2], the tangent stiffness for primary odometer loading [E_{ref}^{oed}, kN/m^2] and power for stress-level dependency of stiffness [m]. Table below shows the parameters used in the soil hardening model with their respective unit.

Table A.1. 2 Advanced parameters with their standard units and default setting for Hardening Soil Model

SOIL PARAMETER AND RESPECTIVE DEFAULT SETTING		UNIT
E_{ref}^{50}	Secant stiffness in standard drained triaxial test	$[KN/M^2]$
E_{oed}^{ref}	Tangent stiffness for primary oedometer loading (default $E_{oed}^{ref} = E_{50}^{ref}$)	$[KN/M^2]$
m	Power for stress-level dependency of stiffness	[-]
E_{ur}^{ref}	Unloading/reloading stiffness (default $E_{ur}^{ref}=3\ E_{50}^{ref}$)	$[KN/M^2]$
v_{ur}	Poisson's ratio for unloading-reloading (default $V_{ur}=0.2$)	[-]
P^{ref}	Reference stress for stiffness (default $P^{ref}=100$ stress units)	$[KN/M^2]$
K_o^{nc}	K_0-value for normal consolidation (default $K_o^{nc} = 1 - \sin\phi$)	[-]
R_f	Failure ratio q_f/q_a (default $R_f=0.9$)	[-]
$\sigma_{tension}$	Tensile strength (default $\sigma_{tension} = 0$ stress units)	$[KN/M^2]$
$\sigma_{increment}$	As in Mohr-Coulomb model (default $\sigma_{increment} = 0$)	$[KN/M^2]$

Appendix 2 Test Results

In this section, additional relevant figures are incorporated to show how change in stiffness of diaphragm wall and spacing of struts affect the performance of deep excavations.

I. In this section, the paper concentrates on how change in stiffness of diaphragm wall affects the performance of deep excavations supported by diaphragm wall for each soil types. Figure A.2.1 – Figure A.2.6 are presented for each soil for deep excavation with the following constant parametrs.

   a. Depth of excavation = 16m
   b. Depth of embedment = 5m
   c. Strut Spacing = 3m

1. Expansive clay

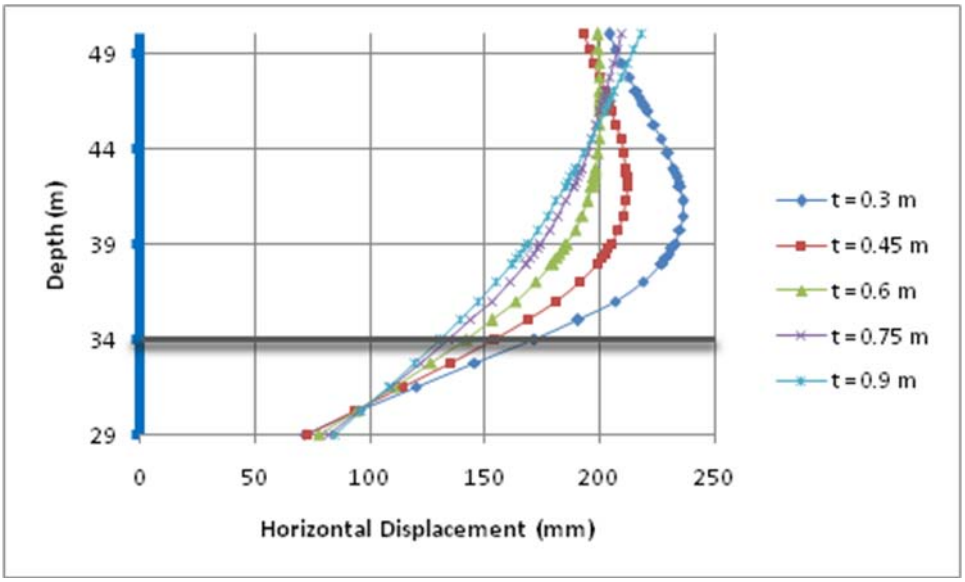

Figure A.2. 1 Horizontal Displacement on a diaphragm wall due to deep excavation when stiffness of a diaphragm wall is varied.

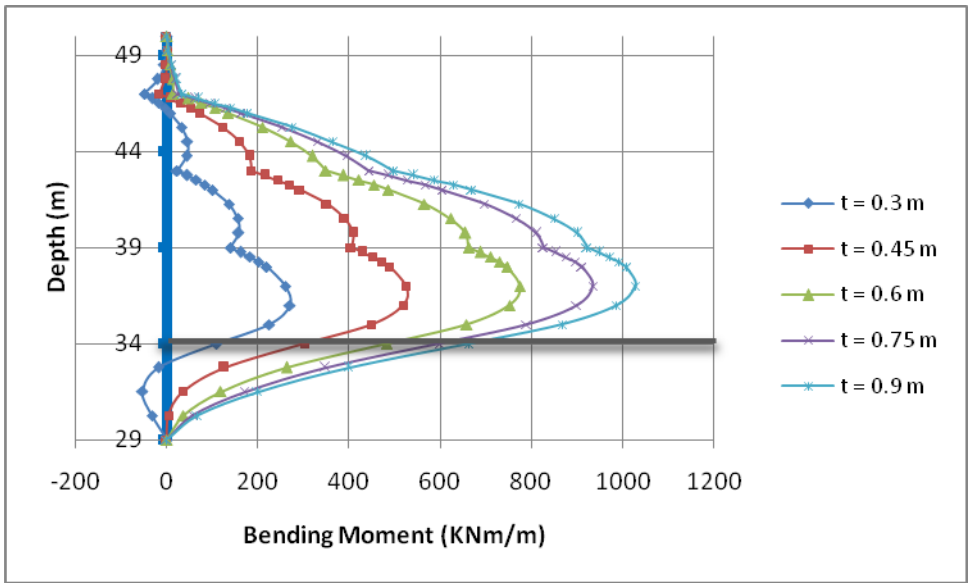

Figure A.2. 2 Bending moment on a diaphragm wall due to deep excavation when stiffness of a diaphragm wall is varied.

2. Red silty clay

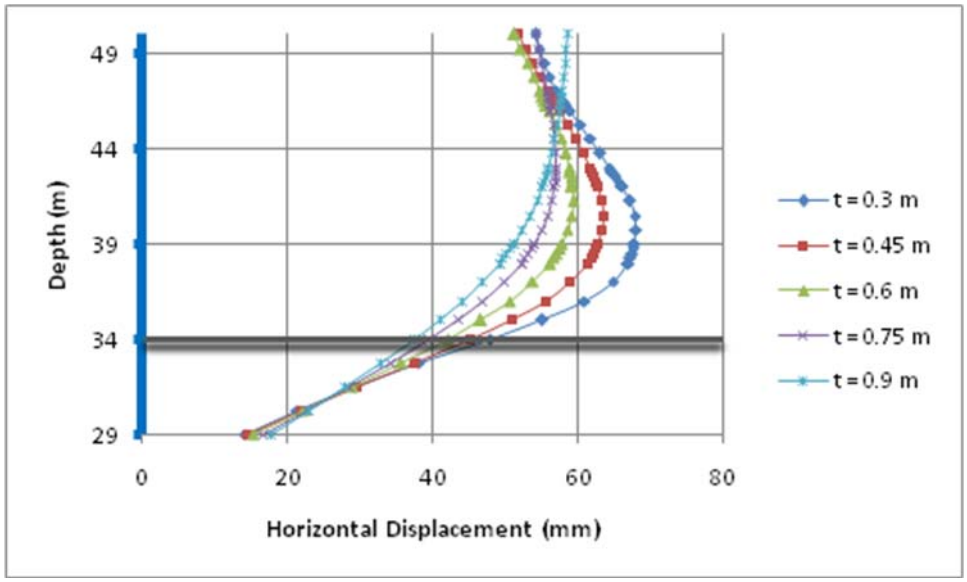

Figure A.2. 3 Horizontal Displacement on a diaphragm wall due to deep excavation when stiffness of a diaphragm wall is varied for red silty clay

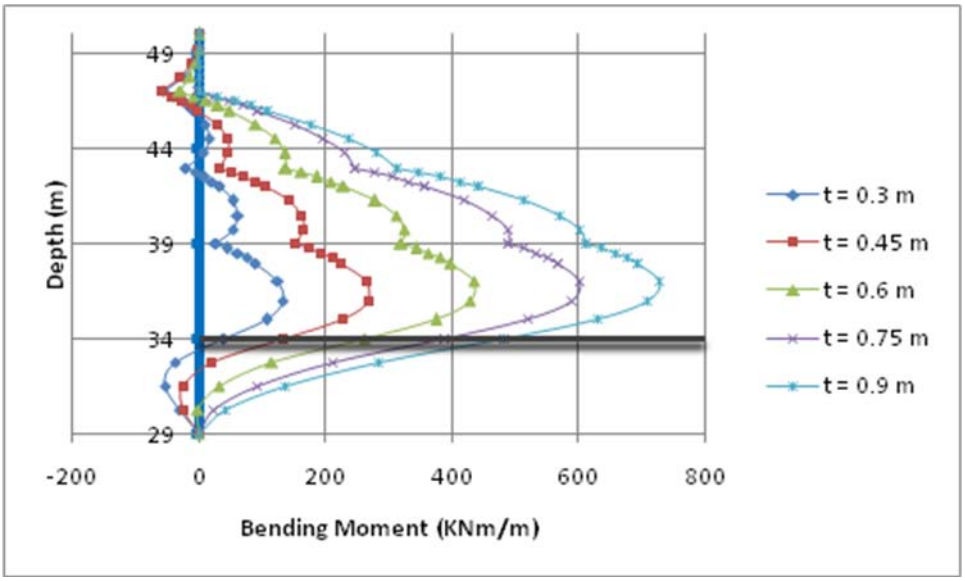

Figure A.2. 4 Bending moment on a diaphragm wall due to deep excavation when stiffness of a diaphragm wall is varied.

3. Sand

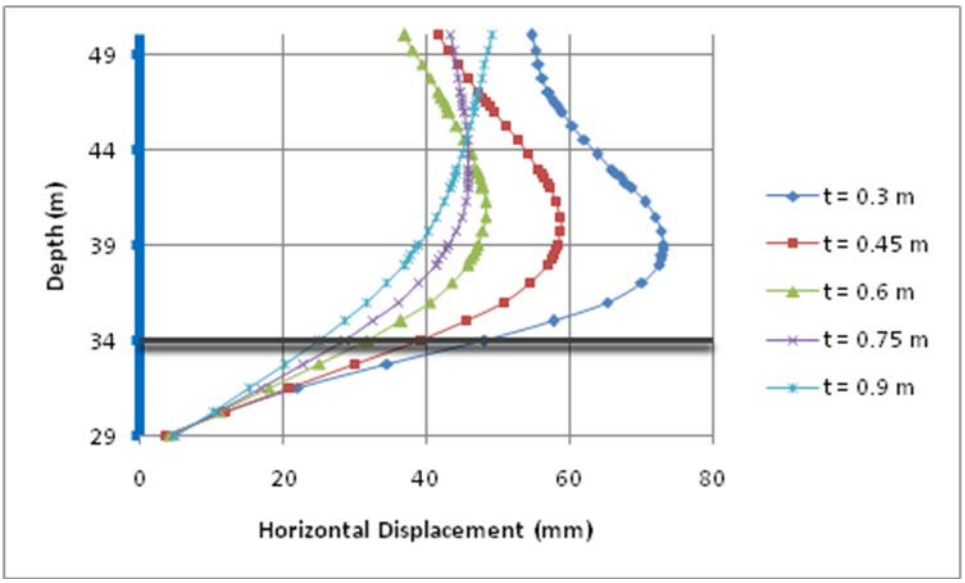

Figure A.2. 5 Horizontal Displacement on a diaphragm wall due to deep excavation when stiffness of a diaphragm wall is varied.

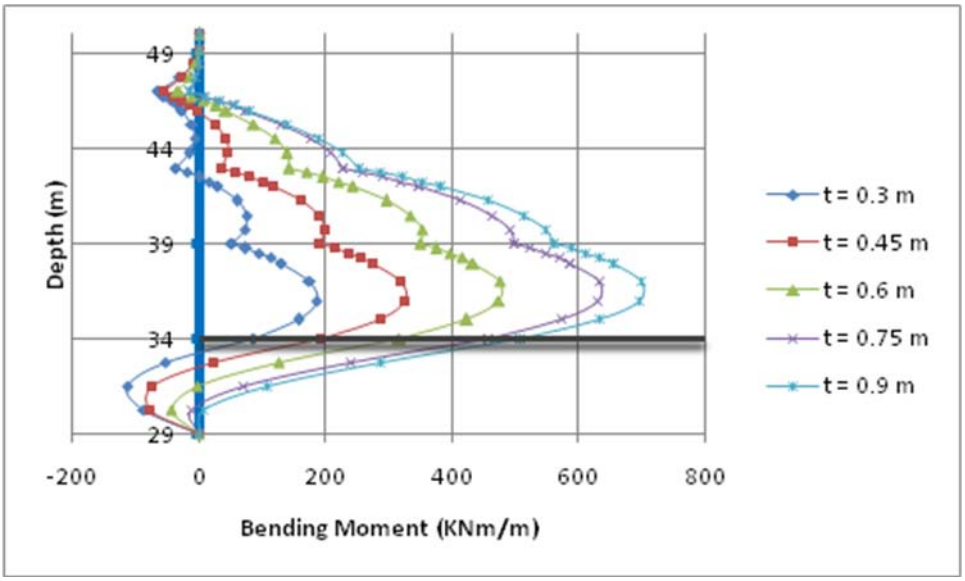

Figure A.2. 6 Bending moment on a diaphragm wall due to deep excavation when stiffness of a diaphragm wall is varied.

II. In this section, the paper concentrates on how change in spacing of struts affect the performance of deep excavations supported by diaphragm wall for each soil types. Figure A.2.1 – Figure A.2.6 are presented for each soil for deep excavation with the following constant parametrs.

a. Depth of excavation = 16m
b. Depth of embedment = 5m
c. Diaphragm wall thickness = 0.3m

1. **Expansive clay**

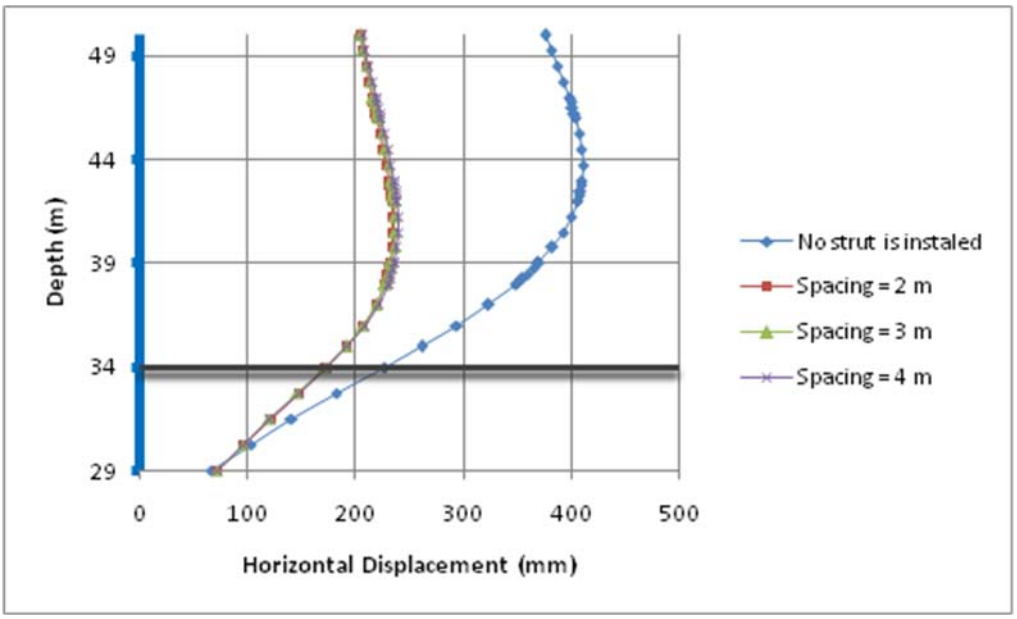

Figure A.2. 7 Horizontal displacement of a diaphragm wall due to deep excavation when spacing of struts is varied.

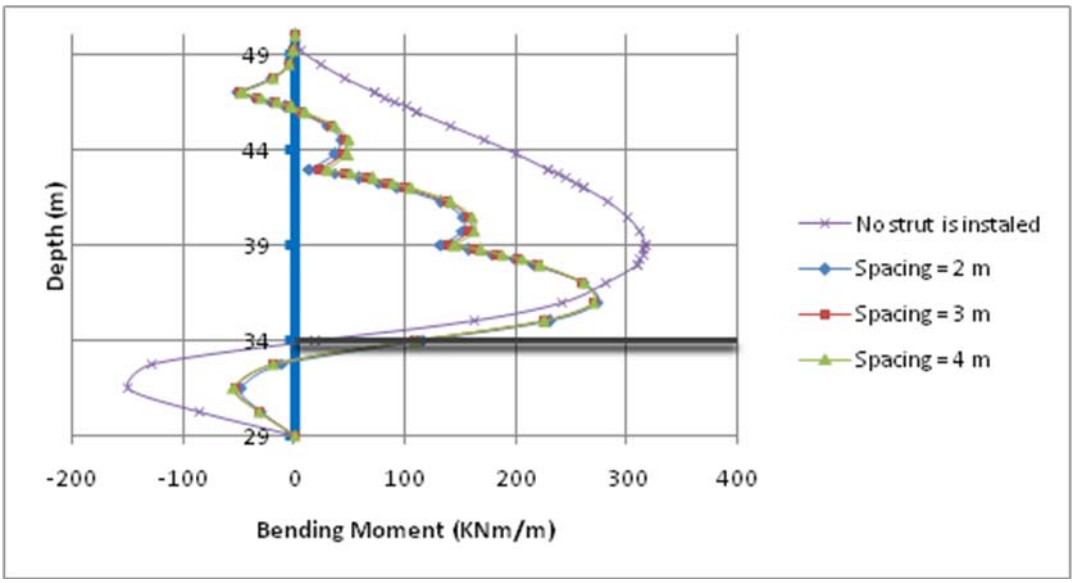

Figure A.2. 8 Bending moment on a diaphragm wall due to deep excavation when spacing of struts is varied.

2. Red silty clay

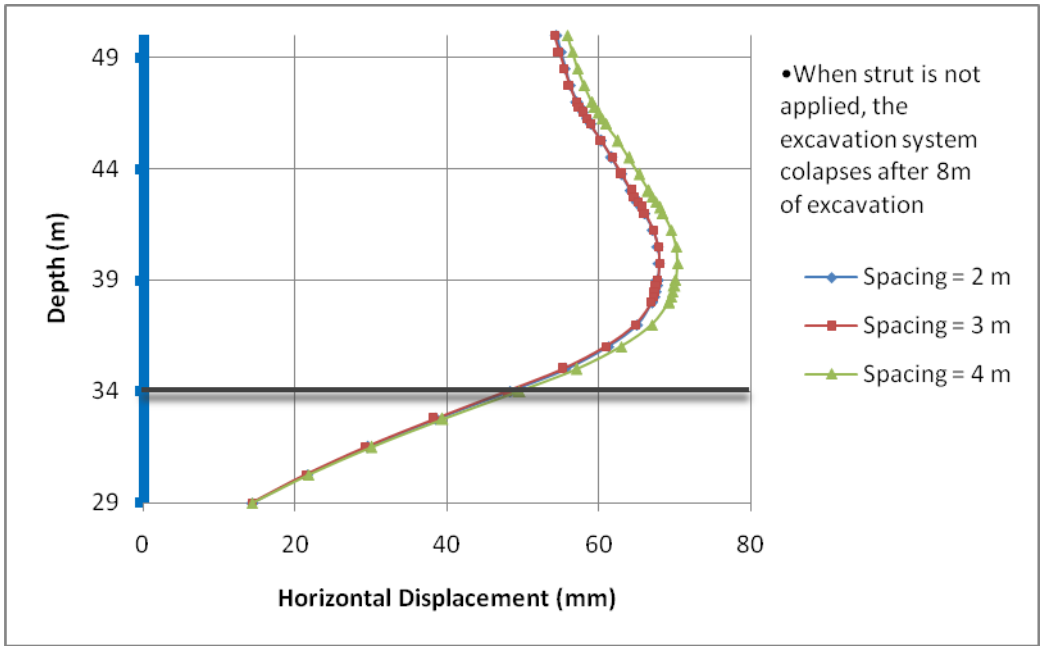

Figure A.2. 9 Horizontal displacement of a diaphragm wall due to deep excavation when spacing of struts is varied.

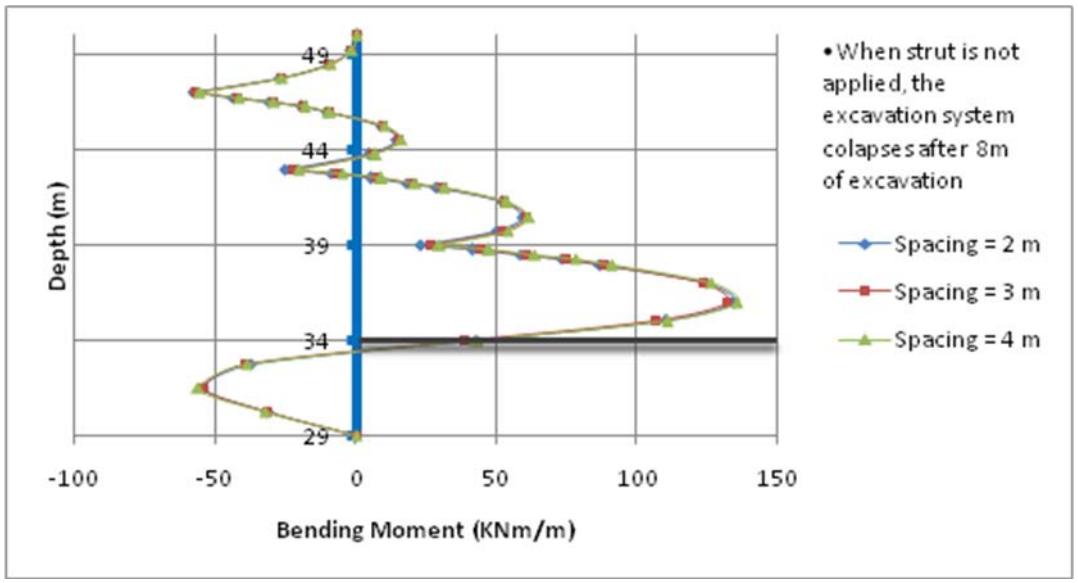

Figure A.2. 10 Bending moment on a diaphragm wall due to deep excavation when spacing of struts is varied.

3. Sand

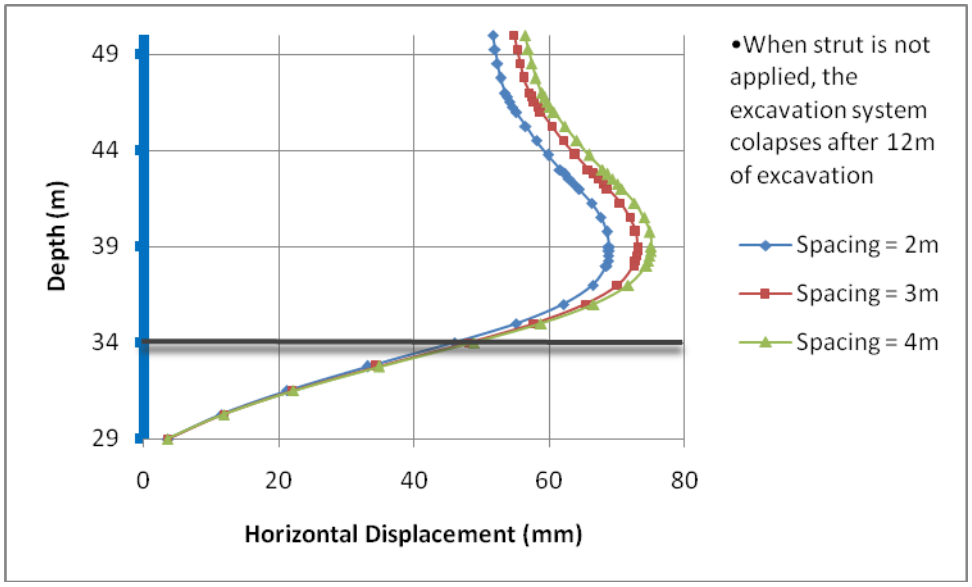

Figure A.2. 11 Horizontal displacement of a diaphragm wall due to deep excavation when spacing of struts is varied.

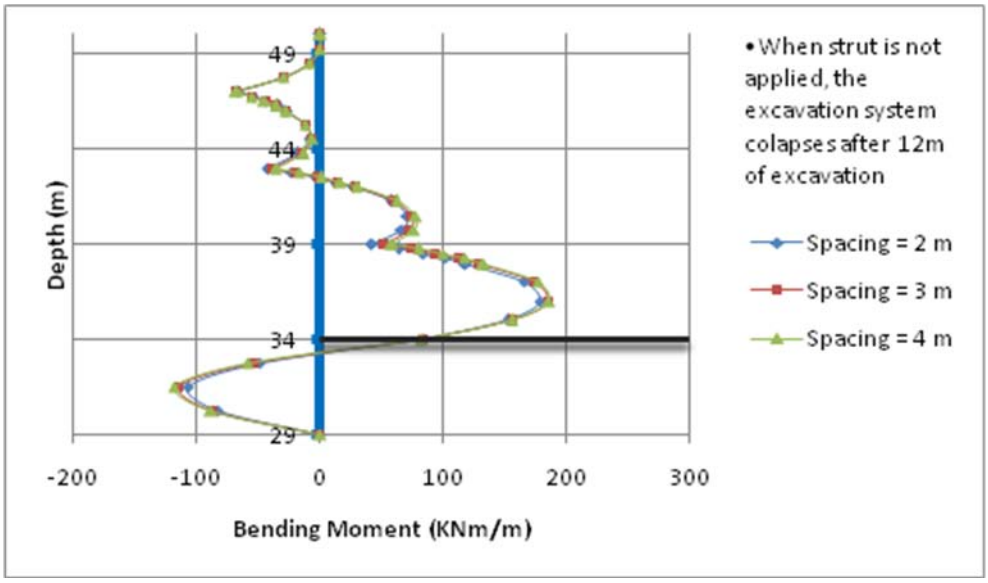

Figure A.2. 12 Bending moment on a diaphragm wall due to deep excavation when spacing of struts is varied.

III. In this section, the paper concentrates on how drained and undrained material model affect the performance of deep excavations supported by diaphragm wall.

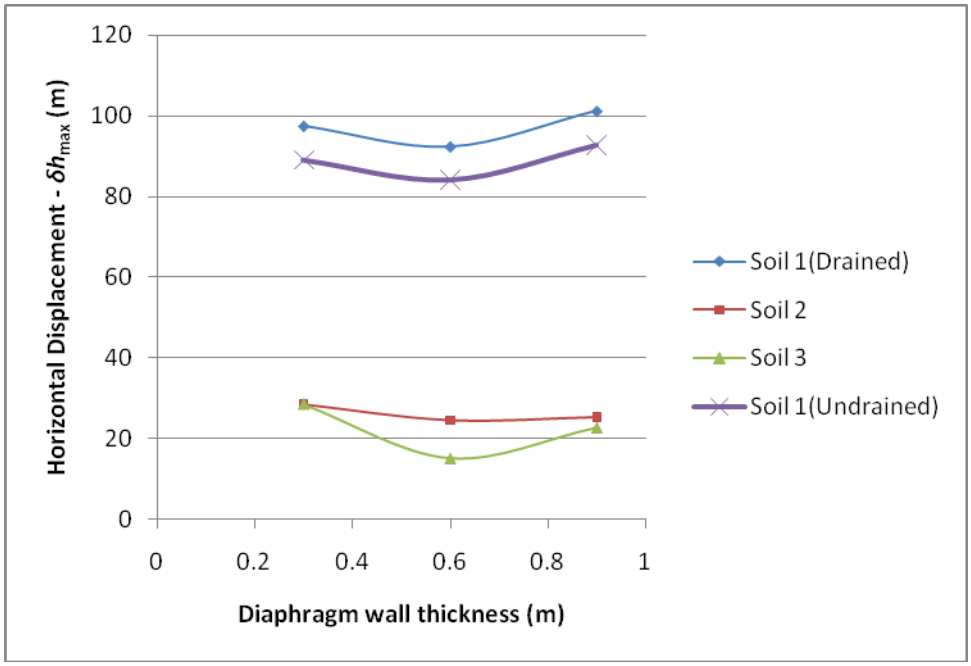

Figure A.2. 13 Maximum horizontal displacement of the diaphragm wall with diaphragm wall thickness(8m depth of excavation)

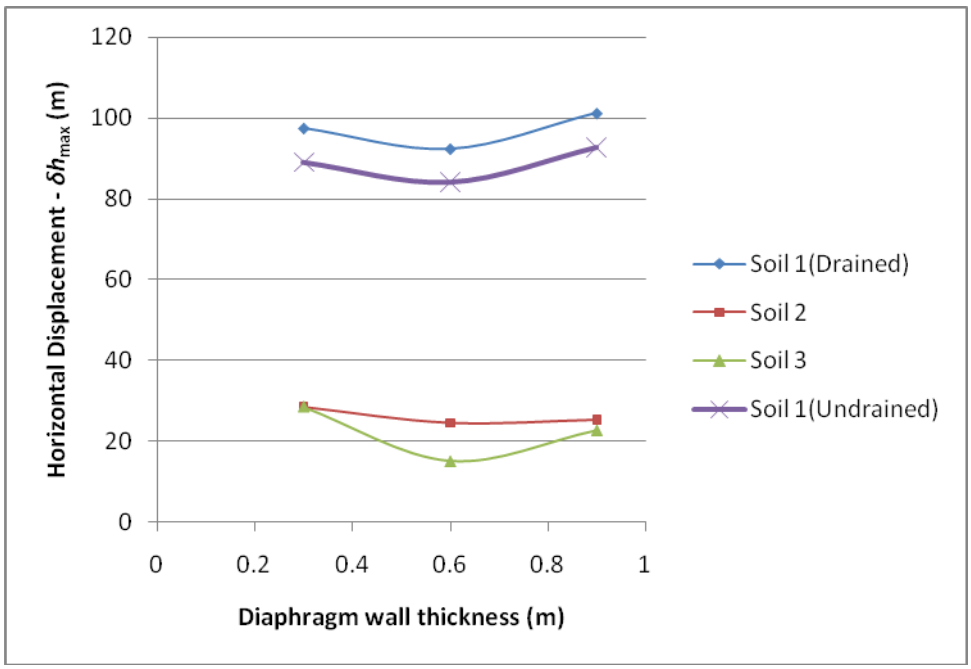

Figure A.2. 14 Maximum horizontal displacement of the diaphragm wall with diaphragm wall thickness(12m depth of excavation)

Appendix 3 Parametric Combinations

The different parametric combinations for the parametric study are as shown below. For the description of names given below, Table 4.2 – Table 4.6 can be referred.

Soil S1	Soil S2	Soil S3
Dpgm3	Dpgm3	Dpgm3
St1	St1	St1
$D_{ex}1$	$D_{ex}1$	$D_{ex}1$
$D_{em}1$	$D_{em}1$	$D_{em}1$

Soil S1	Soil S2	Soil S3
Dpgm3	Dpgm3	Dpgm3
St1	St1	St1
$D_{ex}3$	$D_{ex}3$	$D_{ex}3$
$D_{em}1$	$D_{em}1$	$D_{em}1$

Soil S1	Soil S1	Soil S1
Dpgm3	Dpgm5	Dpgm1
St3	St3	St3
$D_{ex}1$	$D_{ex}1$	$D_{ex}1$
$D_{em}1$	$D_{em}1$	$D_{em}1$

Soil S3	Soil S3	Soil S3
Dpgm5	Dpgm5	Dpgm5
St1	St2	St3
$D_{ex}1$	$D_{ex}1$	$D_{ex}1$
$D_{em}1$	$D_{em}1$	$D_{em}1$

Soil S1	Soil S2	Soil S3
Dpgm5	Dpgm5	Dpgm5
St1	St1	St1
$D_{ex}1$	$D_{ex}1$	$D_{ex}1$
$D_{em}1$	$D_{em}1$	$D_{em}1$

Soil S1	Soil S2	Soil S3
Dpgm5	Dpgm5	Dpgm5
St1	St1	St1
$D_{ex}3$	$D_{ex}3$	$D_{ex}3$
$D_{em}1$	$D_{em}1$	$D_{em}1$

Soil S2	Soil S2	Soil S2
Dpgm3	Dpgm5	Dpgm1
St3	St3	St3
$D_{ex}1$	$D_{ex}1$	$D_{ex}1$
$D_{em}1$	$D_{em}1$	$D_{em}1$

Soil S2	Soil S2	Soil S2
Dpgm5	Dpgm5	Dpgm5
St1	St2	St3
$D_{ex}1$	$D_{ex}1$	$D_{ex}1$
$D_{em}1$	$D_{em}1$	$D_{em}1$

Soil S1	Soil S2	Soil S3
Dpgm1	Dpgm1	Dpgm1
St1	St1	St1
$D_{ex}1$	$D_{ex}1$	$D_{ex}1$
$D_{em}1$	$D_{em}1$	$D_{em}1$

Soil S1	Soil S2	Soil S3
Dpgm1	Dpgm1	Dpgm1
St1	St1	St1
$D_{ex}3$	$D_{ex}3$	$D_{ex}3$
$D_{em}1$	$D_{em}1$	$D_{em}1$

Soil S3	Soil S3	Soil S3
Dpgm3	Dpgm5	Dpgm1
St3	St3	St3
$D_{ex}1$	$D_{ex}1$	$D_{ex}1$
$D_{em}1$	$D_{em}1$	$D_{em}1$

Soil S2	Soil S2	Soil S2
Dpgm1	Dpgm1	Dpgm1
St1	St2	St3
$D_{ex}1$	$D_{ex}1$	$D_{ex}1$
$D_{em}1$	$D_{em}1$	$D_{em}1$

Soil S1	Soil S2	Soil S3
Dpgm3	Dpgm3	Dpgm3
St2	St2	St2
$D_{ex}1$	$D_{ex}1$	$D_{ex}1$
$D_{em}1$	$D_{em}1$	$D_{em}1$

Soil S1	Soil S2	Soil S3
Dpgm3	Dpgm3	Dpgm3
St1	St1	St1
$D_{ex}1$	$D_{ex}1$	$D_{ex}1$
$D_{em}2$	$D_{em}2$	$D_{em}2$

Soil S1	Soil S1	Soil S1
Dpgm3	Dpgm5	Dpgm1
St1	St1	St1
$D_{ex}2$	$D_{ex}2$	$D_{ex}2$
$D_{em}1$	$D_{em}1$	$D_{em}1$

Soil S3	Soil S3	Soil S3
Dpgm5	Dpgm5	Dpgm5
St1	St2	St3
$D_{ex}1$	$D_{ex}1$	$D_{ex}1$
$D_{em}1$	$D_{em}1$	$D_{em}1$

Soil S1	Soil S2	Soil S3
Dpgm3	Dpgm3	Dpgm3
St3	St3	St3
$D_{ex}1$	$D_{ex}1$	$D_{ex}1$
$D_{em}1$	$D_{em}1$	$D_{em}1$

Soil S1	Soil S2	Soil S3
Dpgm3	Dpgm3	Dpgm3
St1	St1	St1
$D_{ex}1$	$D_{ex}1$	$D_{ex}1$
$D_{em}3$	$D_{em}3$	$D_{em}3$

Soil S1	Soil S1	Soil S1
Dpgm3	Dpgm5	Dpgm1
St1	St1	St1
$D_{ex}3$	$D_{ex}3$	$D_{ex}3$
$D_{em}1$	$D_{em}1$	$D_{em}1$

Soil S1	Soil S1	Soil S1
Dpgm5	Dpgm5	Dpgm5
St2	St2	St2
$D_{ex}1$	$D_{ex}1$	$D_{ex}1$
$D_{em}1$	$D_{em}1$	$D_{em}1$

Soil S1	Soil S2	Soil S3
Dpgm3	Dpgm5	Dpgm1
St1	St2	St3
$D_{ex}1$	$D_{ex}2$	$D_{ex}3$
$D_{em}1$	$D_{em}1$	$D_{em}1$

Soil S1	Soil S2	Soil S3
Dpgm5	Dpgm3	Dpgm1
St1	St2	St3
$D_{ex}2$	$D_{ex}1$	$D_{ex}1$
$D_{em}1$	$D_{em}1$	$D_{em}1$

Soil S1	Soil S1	Soil S1
Dpgm3	Dpgm5	Dpgm1
St1	St1	St1
$D_{ex}1$	$D_{ex}1$	$D_{ex}1$
$D_{em}3$	$D_{em}3$	$D_{em}3$

Soil S2	Soil S2	Soil S2
Dpgm5	Dpgm5	Dpgm5
St2	St2	St2
$D_{ex}1$	$D_{ex}2$	$D_{ex}3$
$D_{em}1$	$D_{em}1$	$D_{em}1$

Soil S1	Soil S2	Soil S3
Dpgm1	Dpgm1	Dpgm1
St1	St1	St1
$D_{ex}2$	$D_{ex}2$	$D_{ex}2$
$D_{em}1$	$D_{em}1$	$D_{em}1$

Soil S3	Soil S3	Soil S3
Dpgm3	Dpgm5	Dpgm1
St2	St2	St2
$D_{ex}1$	$D_{ex}1$	$D_{ex}1$
$D_{em}1$	$D_{em}1$	$D_{em}1$

Soil S2	Soil S2	Soil S2
Dpgm5	Dpgm5	Dpgm5
St1	St2	St3
$D_{ex}1$	$D_{ex}1$	$D_{ex}1$
$D_{em}1$	$D_{em}1$	$D_{em}1$

Soil S3	Soil S3	Soil S3
Dpgm5	Dpgm5	Dpgm5
St2	St2	St2
$D_{ex}1$	$D_{ex}2$	$D_{ex}3$
$D_{em}1$	$D_{em}1$	$D_{em}1$

Soil S2	Soil S2	Soil S2
Dpgm3	Dpgm3	Dpgm3
St2	St2	St2
$D_{ex}1$	$D_{ex}2$	$D_{ex}3$
$D_{em}1$	$D_{em}1$	$D_{em}1$

Soil S3	Soil S3	Soil S3
Dpgm5	Dpgm5	Dpgm5
St2	St2	St2
$D_{ex}2$	$D_{ex}2$	$D_{ex}2$
$D_{em}1$	$D_{em}2$	$D_{em}3$

Soil S2	Soil S2	Soil S2
Dpgm5	Dpgm5	Dpgm5
St2	St2	St2
$D_{ex}3$	$D_{ex}3$	$D_{ex}3$
$D_{em}1$	$D_{em}2$	$D_{em}3$

Soil S1	Soil S2	Soil S3
Dpgm2	Dpgm2	Dpgm2
St2	St2	St2
$D_{ex}3$	$D_{ex}3$	$D_{ex}3$
$D_{em}1$	$D_{em}1$	$D_{em}1$

Soil S2	Soil S2	Soil S2
Dpgm5	Dpgm5	Dpgm5
St2	St2	St2
$D_{ex}1$	$D_{ex}2$	$D_{ex}3$
$D_{em}1$	$D_{em}1$	$D_{em}1$

Soil S1	Soil S1	Soil S1
Dpgm5	Dpgm5	Dpgm5
St2	St2	St2
$D_{ex}1$	$D_{ex}1$	$D_{ex}1$
$D_{em}1$	$D_{em}2$	$D_{em}3$

Soil S3	Soil S3	Soil S3
Dpgm5	Dpgm5	Dpgm5
St2	St2	St2
$D_{ex}3$	$D_{ex}3$	$D_{ex}3$
$D_{em}1$	$D_{em}2$	$D_{em}3$

Soil S1	Soil S2	Soil S3
Dpgm4	Dpgm4	Dpgm4
St2	St2	St2
$D_{ex}3$	$D_{ex}3$	$D_{ex}3$
$D_{em}1$	$D_{em}1$	$D_{em}1$

Soil S2	Soil S2	Soil S2
Dpgm1	Dpgm1	Dpgm1
St2	St2	St2
$D_{ex}1$	$D_{ex}2$	$D_{ex}3$
$D_{em}1$	$D_{em}1$	$D_{em}1$

Soil S2	Soil S2	Soil S2
Dpgm5	Dpgm5	Dpgm5
St2	St2	St2
$D_{ex}1$	$D_{ex}1$	$D_{ex}1$
$D_{em}1$	$D_{em}2$	$D_{em}3$

Soil S1	Soil S1	Soil S1
Dpgm1	Dpgm1	Dpgm1
St2	St2	St2
$D_{ex}2$	$D_{ex}2$	$D_{ex}2$
$D_{em}1$	$D_{em}2$	$D_{em}3$

Soil S1	Soil S1	Soil S1
Dpgm3	Dpgm3	Dpgm3
St2	St2	St2
$D_{ex}3$	$D_{ex}3$	$D_{ex}3$
$D_{em}1$	$D_{em}2$	$D_{em}3$

Soil S2	Soil S2	Soil S2
Dpgm5	Dpgm5	Dpgm5
St2	St2	St2
$D_{ex}1$	$D_{ex}2$	$D_{ex}3$
$D_{em}1$	$D_{em}1$	$D_{em}1$

Soil S3	Soil S3	Soil S3
Dpgm5	Dpgm5	Dpgm5
St2	St2	St2
$D_{ex}1$	$D_{ex}1$	$D_{ex}1$
$D_{em}1$	$D_{em}2$	$D_{em}3$

Soil S2	Soil S2	Soil S2
Dpgm1	Dpgm1	Dpgm1
St2	St2	St2
$D_{ex}2$	$D_{ex}2$	$D_{ex}2$
$D_{em}1$	$D_{em}2$	$D_{em}3$

Soil S2	Soil S2	Soil S2
Dpgm3	Dpgm3	Dpgm3
St2	St2	St2
$D_{ex}3$	$D_{ex}3$	$D_{ex}3$
$D_{em}1$	$D_{em}2$	$D_{em}3$

Soil S2	Soil S2	Soil S2
Dpgm5	Dpgm5	Dpgm5
St2	St2	St2
$D_{ex}1$	$D_{ex}2$	$D_{ex}3$
$D_{em}2$	$D_{em}2$	$D_{em}2$

Soil S1	Soil S1	Soil S1
Dpgm5	Dpgm5	Dpgm5
St2	St2	St2
$D_{ex}2$	$D_{ex}2$	$D_{ex}2$
$D_{em}1$	$D_{em}2$	$D_{em}3$

Soil S3	Soil S3	Soil S3
Dpgm1	Dpgm1	Dpgm1
St2	St2	St2
$D_{ex}2$	$D_{ex}2$	$D_{ex}2$
$D_{em}1$	$D_{em}2$	$D_{em}3$

Soil S2	Soil S2	Soil S2
Dpgm5	Dpgm5	Dpgm5
St2	St2	St2
$D_{ex}1$	$D_{ex}2$	$D_{ex}3$
$D_{em}3$	$D_{em}3$	$D_{em}3$

Soil S2	Soil S2	Soil S2
Dpgm5	Dpgm5	Dpgm5
St2	St2	St2
$D_{ex}2$	$D_{ex}2$	$D_{ex}2$
$D_{em}1$	$D_{em}2$	$D_{em}3$

Soil S1	Soil S1	Soil S1
Dpgm1	Dpgm1	Dpgm1
St2	St2	St2
$D_{ex}3$	$D_{ex}3$	$D_{ex}3$
$D_{em}1$	$D_{em}2$	$D_{em}3$

Soil S1	Soil S1	Soil S1
Dpgm5	Dpgm5	Dpgm5
St2	St2	St2
$D_{ex}2$	$D_{ex}2$	$D_{ex}2$
$D_{em}1$	$D_{em}2$	$D_{em}3$

Soil S3	Soil S3	Soil S3
Dpgm5	Dpgm5	Dpgm5
St2	St2	St2
$D_{ex}2$	$D_{ex}2$	$D_{ex}2$
$D_{em}1$	$D_{em}2$	$D_{em}3$

Soil S2	Soil S2	Soil S2
Dpgm1	Dpgm1	Dpgm1
St2	St2	St2
$D_{ex}3$	$D_{ex}3$	$D_{ex}3$
$D_{em}1$	$D_{em}2$	$D_{em}3$

Soil S1	Soil S1	Soil S1
Dpgm5	Dpgm5	Dpgm5
St2	St2	St2
$D_{ex}2$	$D_{ex}2$	$D_{ex}2$
$D_{em}1$	$D_{em}2$	$D_{em}3$

Soil S3	Soil S3	Soil S3
Dpgm1	Dpgm1	Dpgm1
St2	St2	St2
$D_{ex}3$	$D_{ex}3$	$D_{ex}3$
$D_{em}1$	$D_{em}2$	$D_{em}3$